

Rydberg atoms: excitation, interactions, trapping

Mark Saffman

I: Coherent excitation of Rydberg states

II: Rydberg atom interactions

III: Coherence properties of ground and
Rydberg atom traps

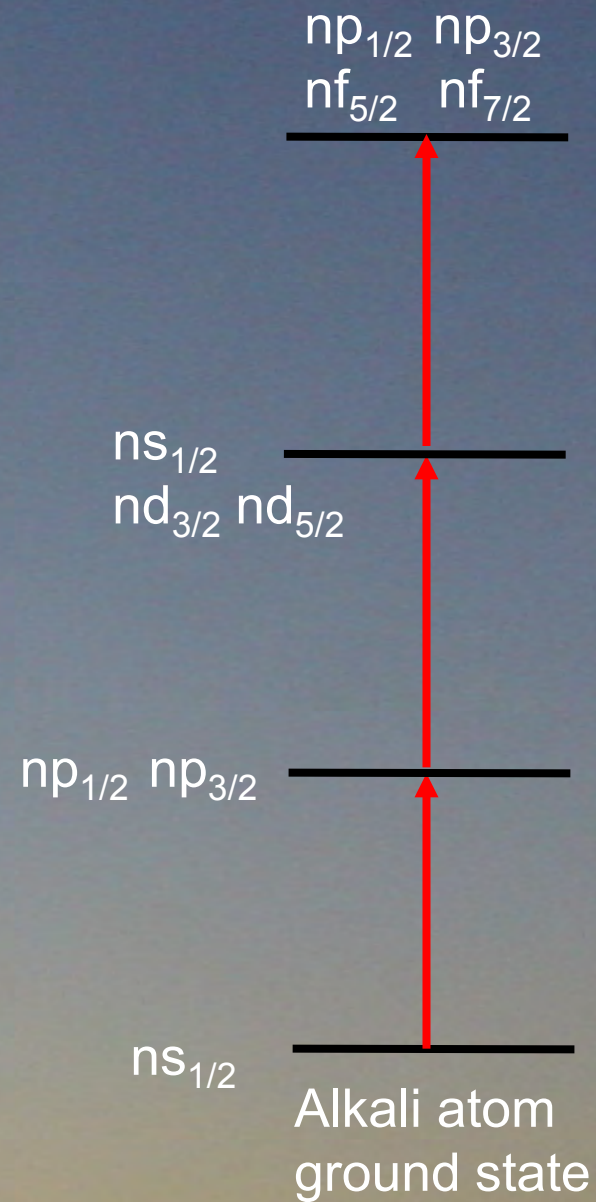
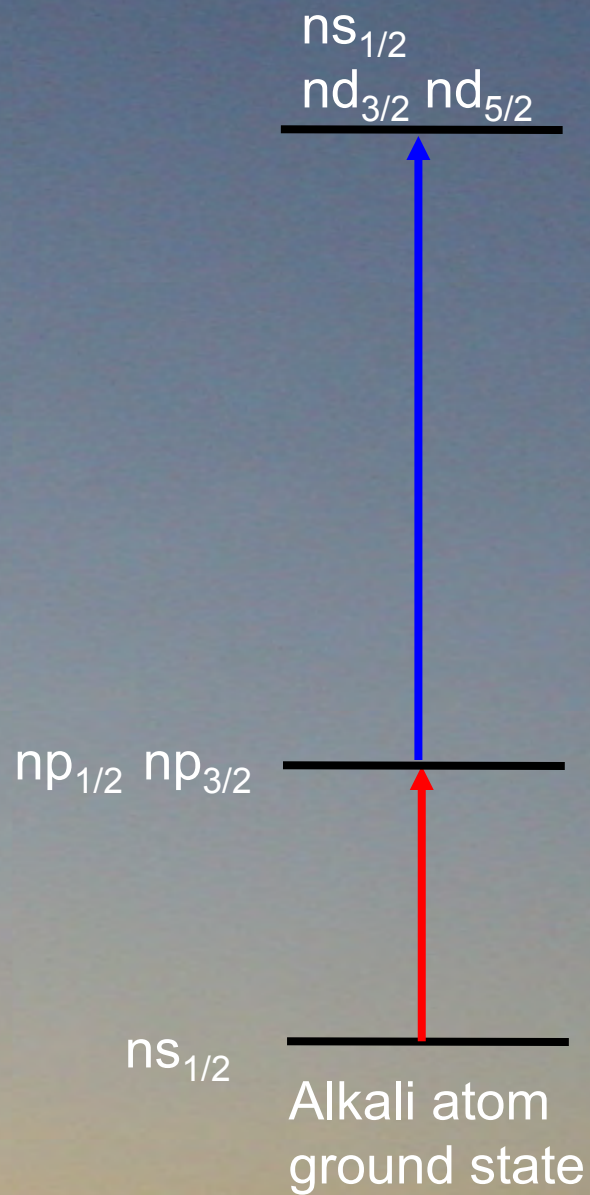
1: Coherent excitation of Rydberg states

- overview
- calculation of rates
- 1 photon methods
- 2 photon methods, Doppler, AC Stark shifts
- 3 photon methods
- experiments, coherent oscillations

Overview

- Experiments that use Rydberg atoms require excitation of Rydberg states
- 1,2 and 3 photon techniques can be used to access low L Rydberg states (high L (circular) states involve special techniques)
- For applications involving Quantum information it is generally necessary for the excitation to be fast, coherent and state selective
- With modern laser systems coherent excitation is relatively straightforward

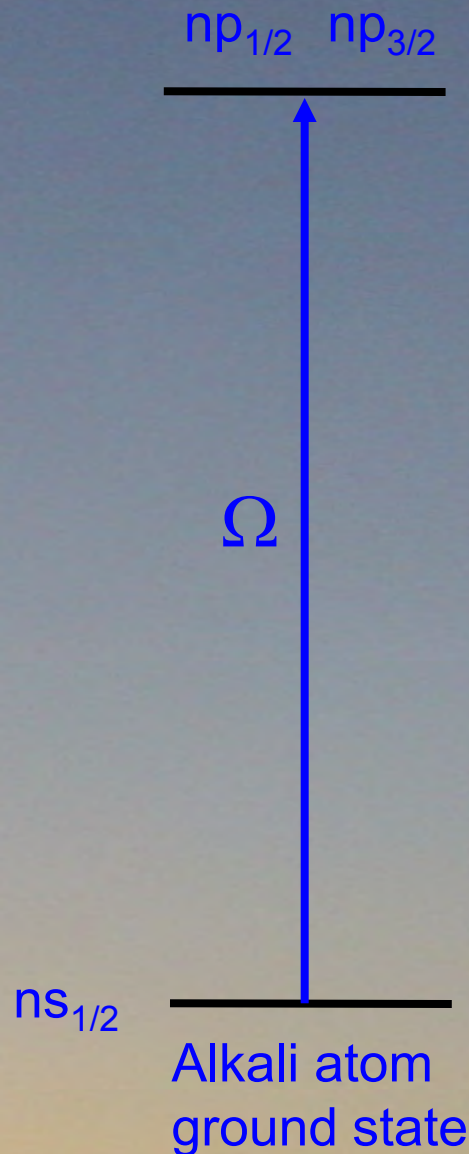
Few photon excitation



1: Coherent excitation of Rydberg states

- overview
- calculation of rates
- 1 photon methods
- 2 photon methods, Doppler, AC Stark shifts
- 3 photon methods
- experiments, coherent oscillations

One photon excitation rate



Intensity $I(\mathbf{r}) = \frac{\epsilon_0 c}{2} |\mathcal{E}(\mathbf{r})|^2$

Rabi frequency $\Omega(\mathbf{r}) = \frac{d\mathcal{E}(\mathbf{r})}{\hbar}$

Transition matrix element $d = e\langle r | r_q | g \rangle$

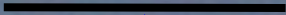
$$r_0 = z, \quad r_+ = -\frac{1}{\sqrt{2}}(x + iy), \quad r_- = \frac{1}{\sqrt{2}}(x - iy)$$

Wigner-Eckart theorem $\langle \beta j' m' | r_q | \alpha j m \rangle = \frac{\langle \beta j' || r || \alpha j \rangle}{\sqrt{2j'+1}} C_{jm1q}^{j'm'}$

Additional complication mixed representations
hyperfine – fine structure states

Radial matrix element

$np_{1/2}$ $np_{3/2}$



Ω



Alkali atom ground state

reduced matrix element $\langle \beta j' || r || \alpha j \rangle$

$$\langle n' L' S; J' I' F' || r || n L S; J I F \rangle = (-1)^{(1+I+J'+F)} \sqrt{(2F+1)(2F'+1)} \begin{Bmatrix} J & I & F \\ F' & 1 & J' \end{Bmatrix} \langle n' L' S; J' || r || n L S; J \rangle$$

$$\langle n'; L' S J' || r || n; L S J \rangle = (-1)^{(1+S+L'+J)} \sqrt{(2J+1)(2J'+1)} \begin{Bmatrix} L & S & J \\ J' & 1 & L' \end{Bmatrix} \langle n'; L' || r || n; L \rangle$$

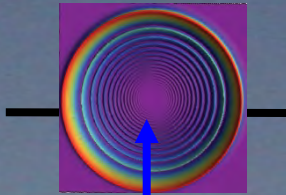
$$\langle n' L' || r || n L \rangle = (-1)^{L'+(1+L+L')/2} \sqrt{\max(L, L')} R_{n' L', n L}$$

$$R_{n' L', n L} = \int_0^\infty dr r^3 R_{n' L'} R_{n L}$$

Apart the many angular factors we need to calculate radial integrals.

Scaling of radial integrals

$np_{1/2}$
 $np_{3/2}$



$$R_{n'L',nL} = \int_0^\infty dr r^3 R_{n'L'} R_{nL}$$

Estimate integral in the limit $n \gg 1$:

Integrand vanishes away from the origin.

Assume Rydberg state ns , $|R_{ns}(0)|^2 \sim 1/n^3$

$$\text{Integral} \sim a_0/n^{3/2}$$

Scaling is valid for any low angular momentum Rydberg state. This says optical power $P \sim n^3$ at constant Ω

Calculation methods:

Semi-classical (WKB)

(my favorite Kaulakys, J. Phys. B, 28, 4963 (1995))

Coulomb wave functions

(q.d. theory, Seaton)

Model potentials

$ns_{1/2}$



Alkali atom
ground state

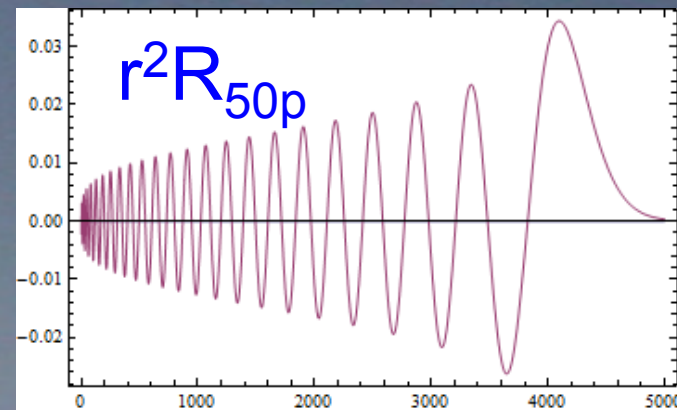
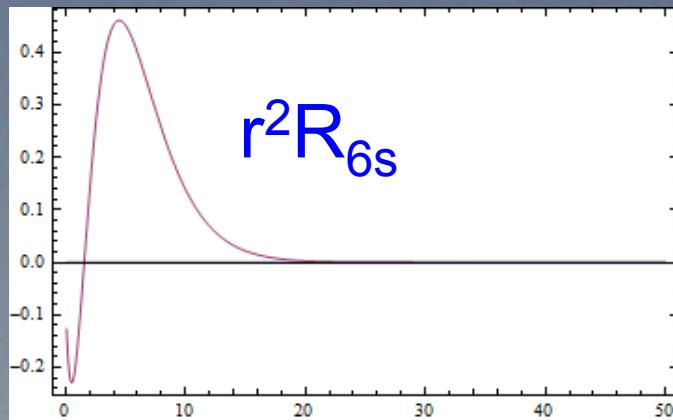
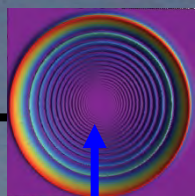
Review: D.P. Dewangan, Physics Reports 511 (2012) 1-142

Radial integral numerics

$$R_{n'L',nL} = \int_0^\infty dr r^3 R_{n'L'} R_{nL}$$

Cs wavefunctions

$np_{1/2}$
 $np_{3/2}$

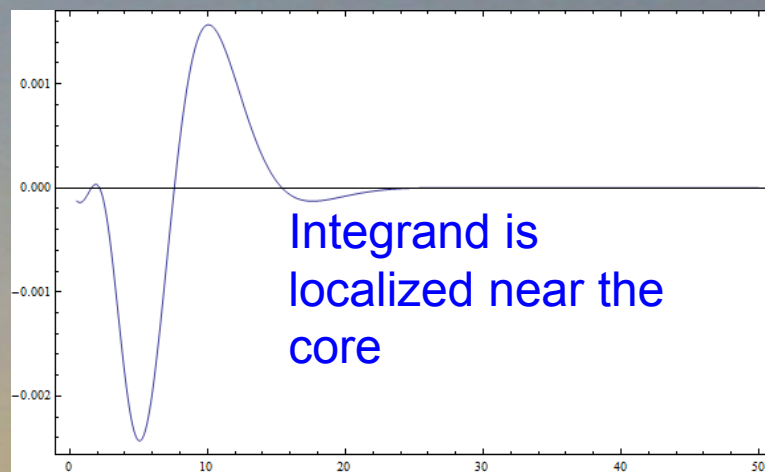


$50 a_0$

$5000 a_0$

$ns_{1/2}$

Alkali atom
ground state



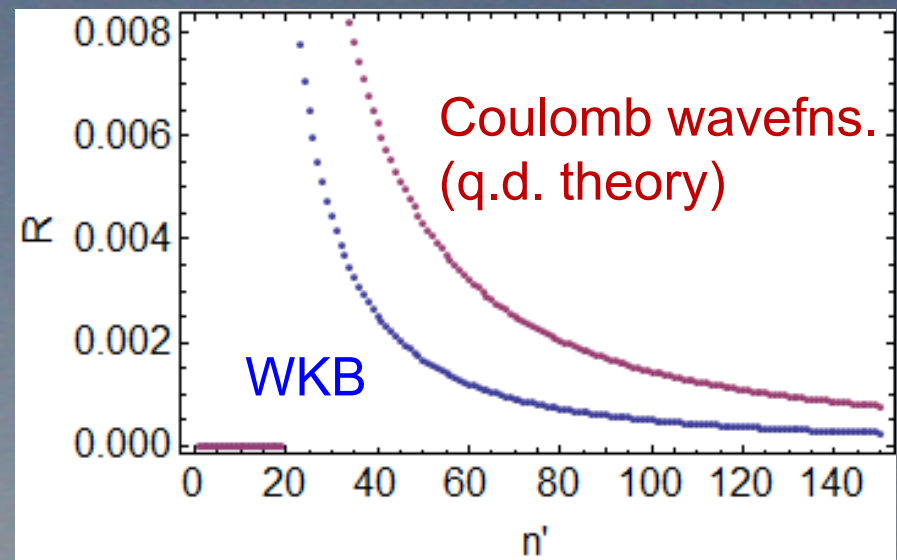
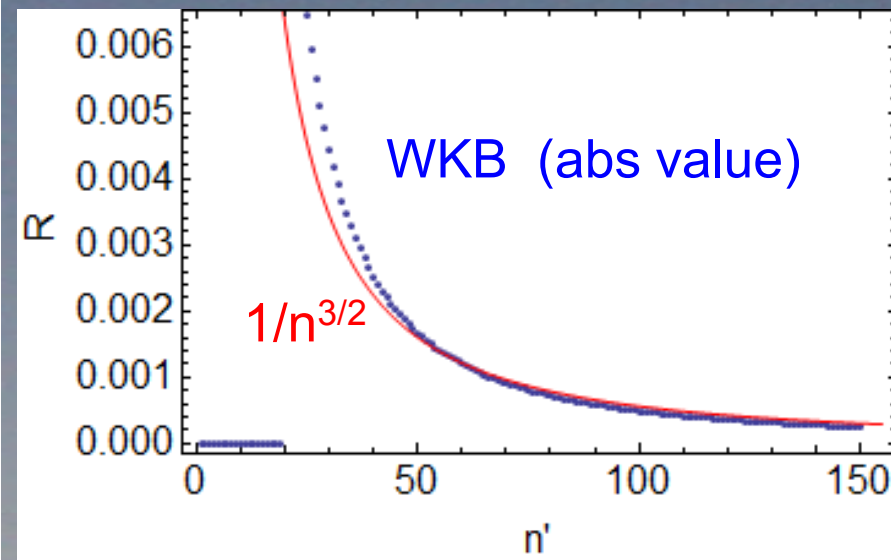
Integrand is
localized near the
core

$50 a_0$

Radial integral numerics

Cs 6s – np_{1/2}

$$R_{n'L',nL} = \int_0^\infty dr r^3 R_{n'L'} R_{nL}$$



- Asymptotic scaling is very good for $n > 50$
- WKB approximation about 2x too small.
- WKB works much better for n, n' both large (lecture 2)

1: Coherent excitation of Rydberg states

- overview
- calculation of rates
- 1 photon methods
- 2 photon methods, Doppler, AC Stark shifts
- 3 photon methods
- experiments, coherent oscillations

Single photon excitation



For high lying Rydberg levels wavelength is 297 nm for Rb, 319 nm for Cs.

Not commonly done.

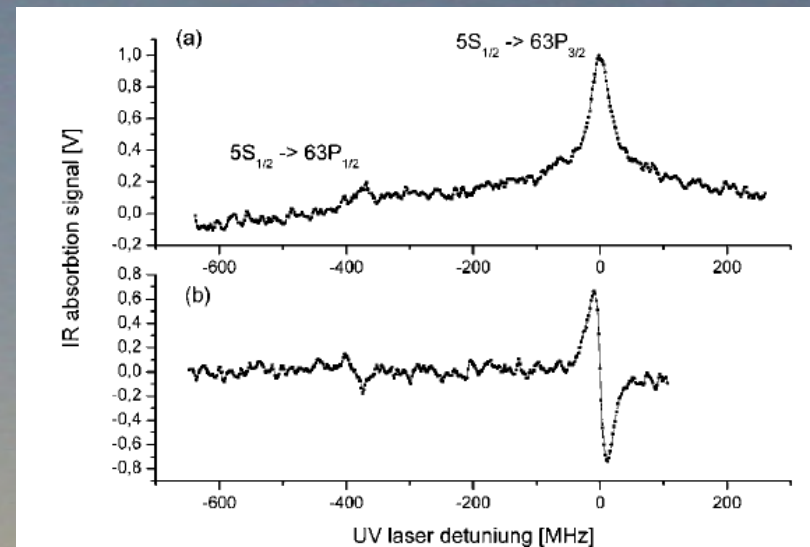
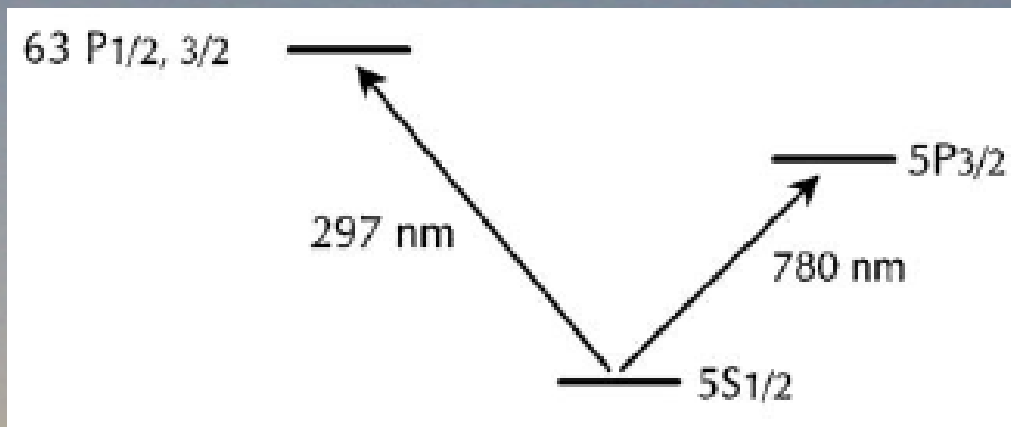
Also strong Doppler sensitivity, we will come back to this.

1 photon excitation

June 1, 2009 / Vol. 34, No. 11 / OPTICS LETTERS

Optical spectroscopy of rubidium Rydberg atoms with a 297 nm frequency-doubled dye laser

P. Thoumany, T. Hänsch, G. Stania, L. Urbonas, and Th. Becker*



Quantum interference in V system used to observe subDoppler linewidths

1: Coherent excitation of Rydberg states

- overview
- calculation of rates
- 1 photon methods
- 2 photon methods, Doppler, AC Stark shifts
- 3 photon methods
- experiments, coherent oscillations

Two photon excitation

With two photon scheme can use longer wavelengths.

Less Doppler if we use counterpropagation.

Drawback spontaneous emission from intermediate level.

For large detuning from $|p\rangle$ the two-photon Rabi frequency is

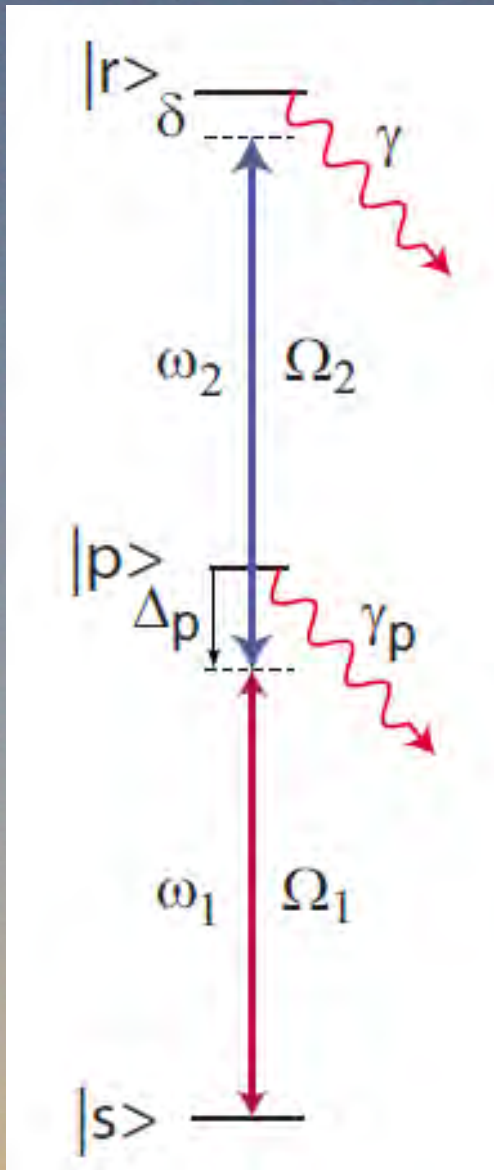
$$\Omega = \frac{\Omega_1 \Omega_2}{2\Delta_p}$$

Spontaneous emission in π pulse

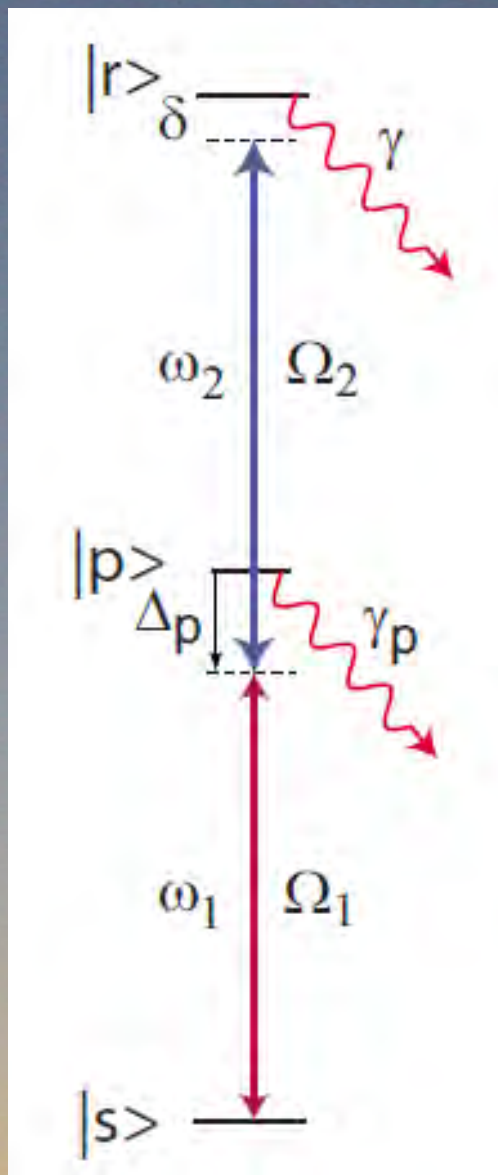
$$P_{se} = \frac{\pi\gamma_p}{4|\Delta_p|} (q + 1/q), \quad q = |\Omega_2/\Omega_1|$$

Putting $q=1$

$$\Omega = \frac{P_{se} |\Omega_2|^2}{\pi \gamma_p}$$



Two photon excitation



We found

$$\Omega = \frac{P_{se}}{\pi} \frac{|\Omega_2|^2}{\gamma_p}$$

Thus

$$\Omega \sim \frac{P_{se} P_2}{\gamma_p}$$

If we have enough optical power we can have fast Rabi frequency with small spontaneous emission.

Common wavelengths:

Rb: $5p_{3/2}$: 780 nm, 480 nm
 $6p_{3/2}$: 420 nm, 1015 nm

Cs: $6p_{3/2}$: 852 nm, 510 nm
 $7p_{3/2}$: 459 nm, 1038 nm

Second resonance levels have smaller γ_p .

Two photon excitation – design example for Rb

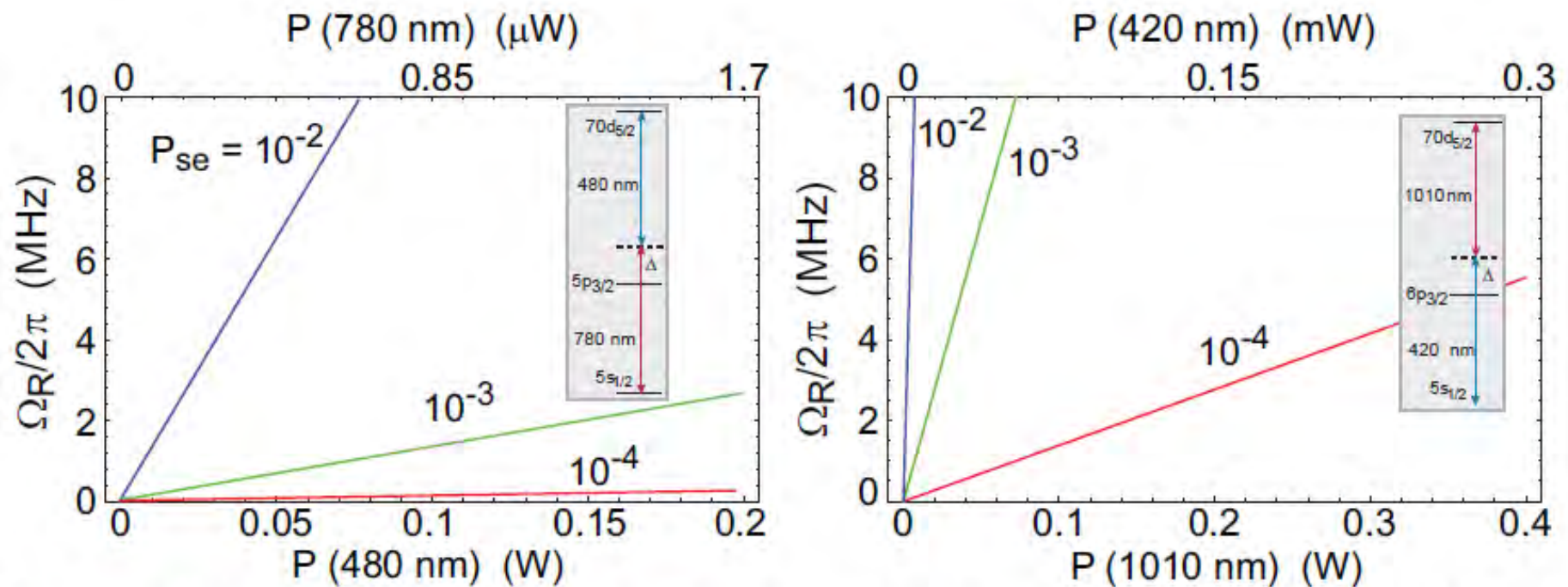


Figure 8: Rabi frequency for excitation of the $70d_{5/2}$ level for $P_{se} = 10^{-2}, 10^{-3}, 10^{-4}$. The 780 nm, 480 nm approach via $5p_{3/2}$ is shown on the left and the 420 nm, 1010 nm approach via $6p_{3/2}$ is shown on the right. The power requirements are calculated for our current experimental beam size of $w = 4 \mu\text{m}$.

M. Saffman 2006

Second resonance excitation of Rb has been implemented here in Pisa.

PRL 107, 060402 (2011)

Two photon excitation - headaches

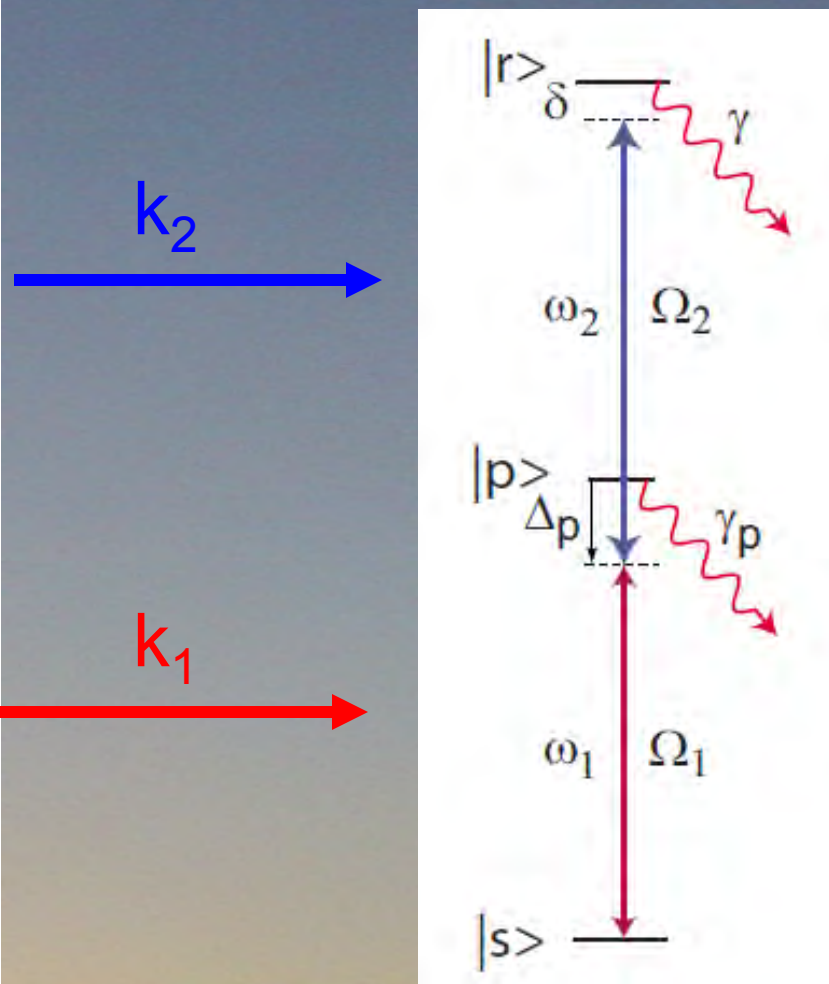
Doppler broadening:

Copropagation:

$$\delta\omega = \mathbf{v} \cdot (\mathbf{k}_1 + \mathbf{k}_2)$$

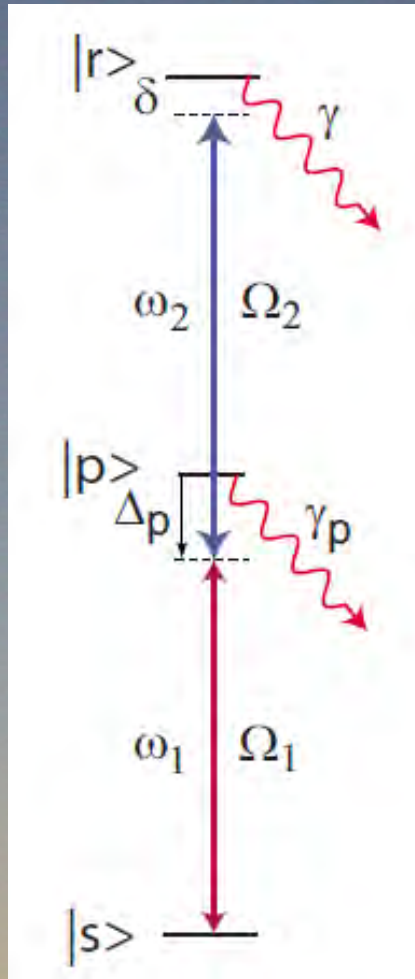
Take $v=10$ cm/s, $\lambda_1=780$ nm, $\lambda_2=480$ nm

$$\delta\omega/2\pi = 0.34 \text{ MHz}$$



Doppler broadening example

Doppler broadening:



Copropagation:

$$\delta\omega = \mathbf{v} \cdot (\mathbf{k}_1 + \mathbf{k}_2)$$

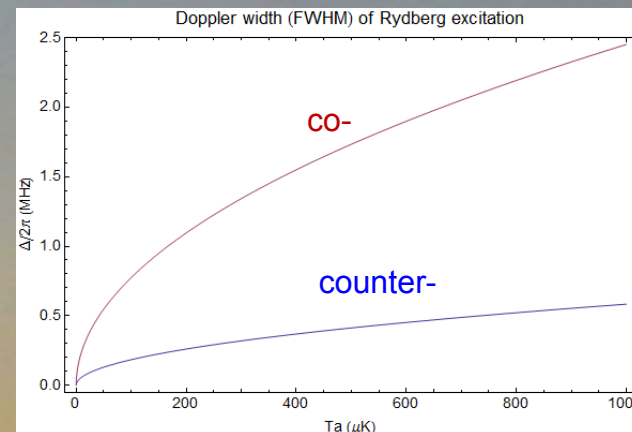
Take $v=10$ cm/s, $\lambda_1=780$ nm, $\lambda_2=480$ nm

$$\delta\omega/2\pi = 0.34 \text{ MHz}$$

Counterpropagation:

$$\delta\omega = \mathbf{v} \cdot (\mathbf{k}_1 - \mathbf{k}_2)$$

$$\delta\omega/2\pi = 0.08 \text{ MHz}$$

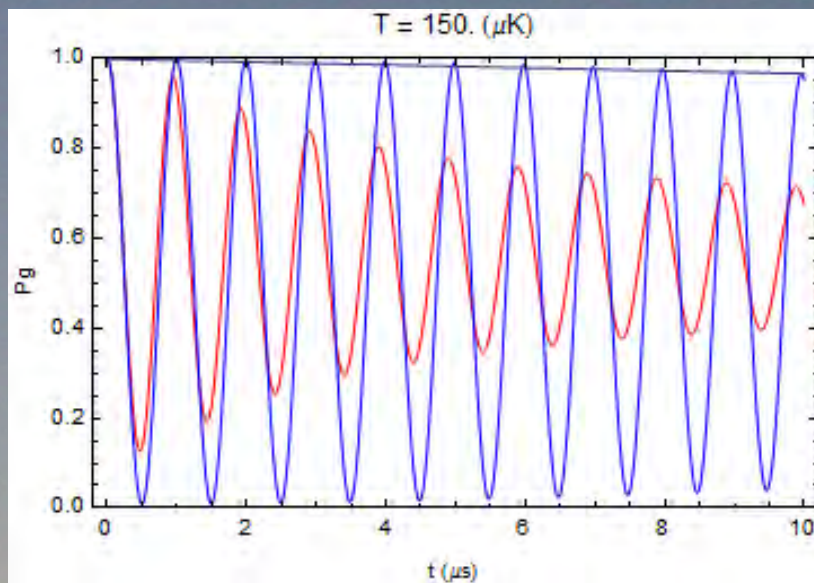


Doppler broadening – time domain

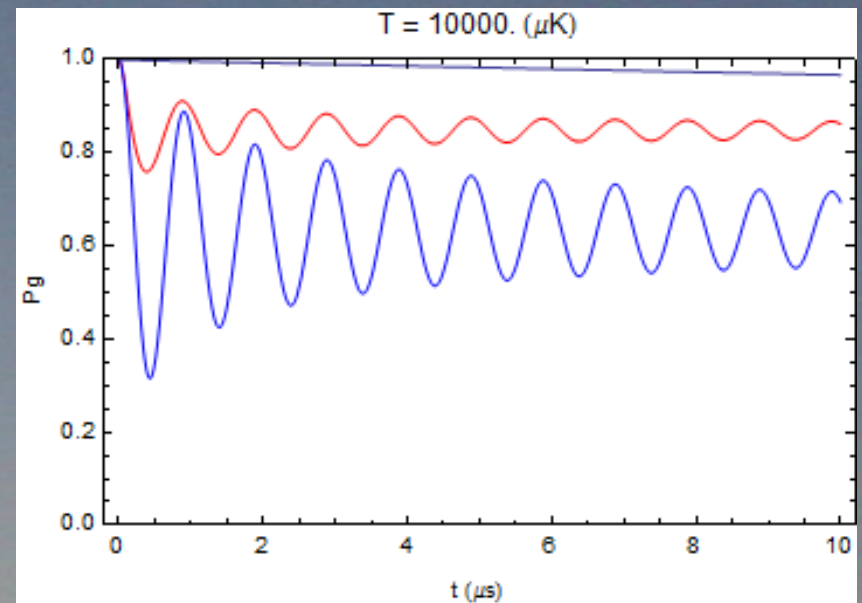
Rb 780+480 nm excitation, $\Omega/2\pi=1$ MHz

Integrate under Doppler curve.

150 μK



$T=10$ mK

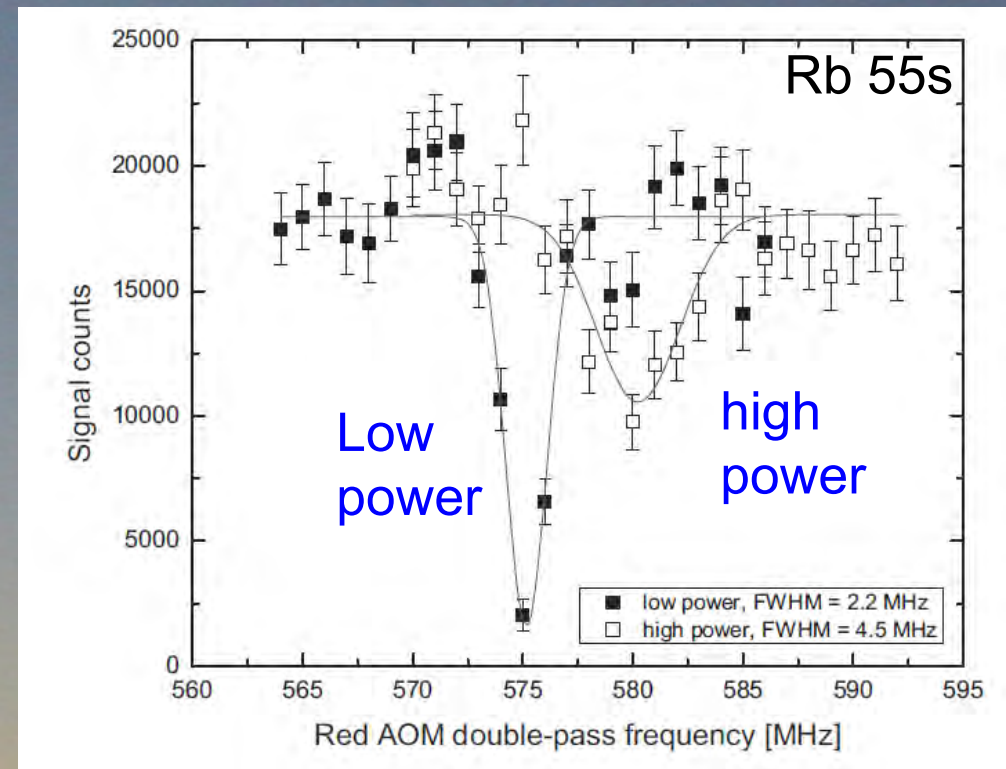
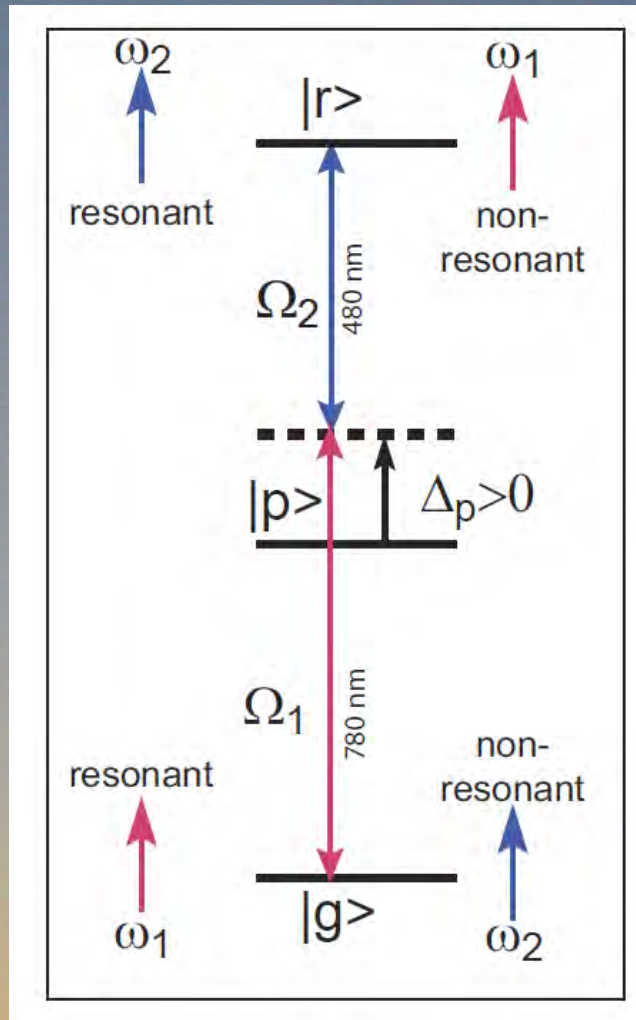


Copropagating/counterpropagating

Upper gray line is spontaneous emission limit with Rydberg lifetime $300 \mu\text{s}$, $n \sim 90$

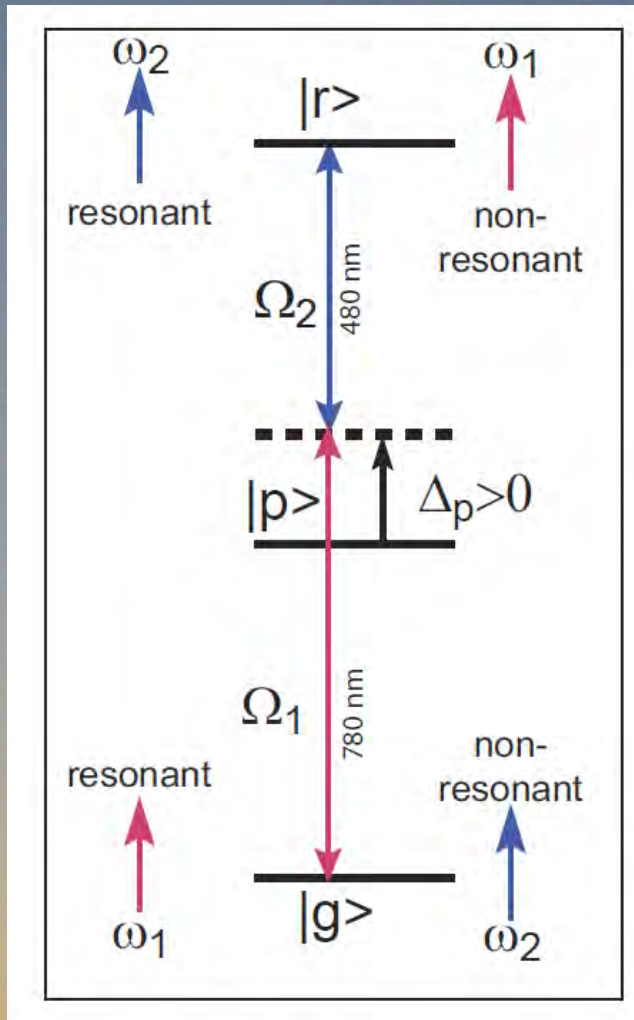
AC Stark shifts

The two-photon transition is AC Stark shifted by the excitation beams. This gives sensitivity to intensity noise on lasers, atomic position under envelope of beam intensity.



AC Stark shifts

The two-photon transition is AC Stark shifted by the excitation beams. This gives sensitivity to intensity noise on lasers, atomic position under envelope of beam intensity.



Main contribution is 1st beam on ground state and 2nd beam on Rydberg state, i.e. near resonant interactions

$$\Delta_{ac} = \frac{|\Omega_2|^2 - |\Omega_1|^2}{4\Delta_p}$$

Choose $\Omega_1 = \Omega_2$ to cancel.

Doppler and AC Stark cancellation

The Doppler shifts depend on velocity. The AC Stark shifts depend on detuning from $|p\rangle$, which also depends on velocity.

It is possible to make these two effects cancel each other.

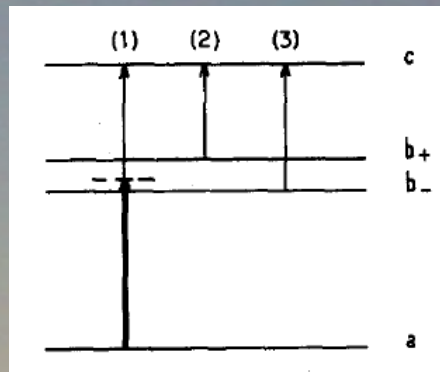
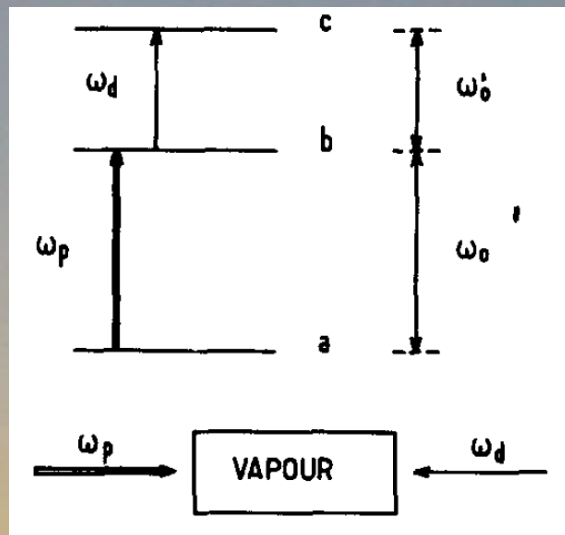
Volume 42, number 1

OPTICS COMMUNICATIONS

1 June 1982

COMPENSATION OF DOPPLER BROADENING BY LIGHT SHIFTS IN TWO PHOTON ABSORPTION

S. REYNAUD, M. HIMBERT, J. DALIBARD, J. DUPONT-ROC and C. COHEN-TANNOUJJI



$$\frac{\Omega_1^2}{\Omega_1^2 + 2\delta^2} = \frac{\omega_0 - \omega'_0}{\omega_0}$$

Interesting, but not that useful for coherent experiments since it requires tuning close to intermediate level

1: Coherent excitation of Rydberg states

- overview
- calculation of rates
- 1 photon methods
- 2 photon methods, Doppler, AC Stark shifts
- 3 photon methods
- experiments, coherent oscillations

Three photon excitation

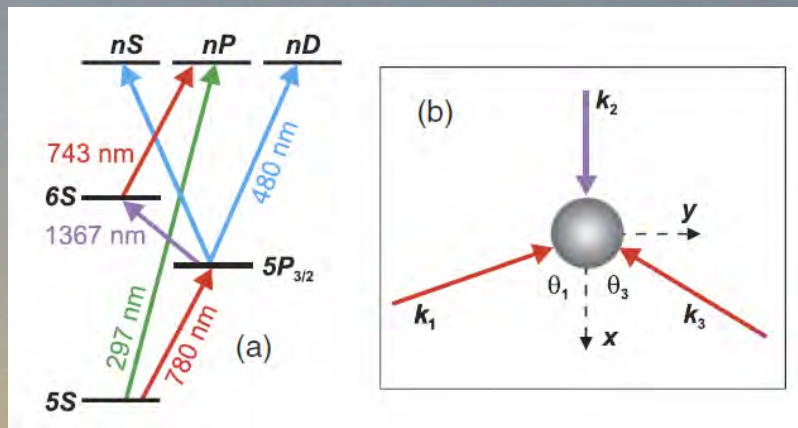
Gives access to np and nf, final states

Can choose levels so all wavelengths can be derived from IR laser diodes.

Can choose directions of k_1, k_2, k_3 to cancel Doppler broadening.



PHYSICAL REVIEW A **84**, 053409 (2011)
Doppler- and recoil-free laser excitation of Rydberg states via three-photon transitions
 I. I. Ryabtsev, * I. I. Beterov, D. B. Tretyakov, V. M. Entin, and E. A. Yakshina



$$\mathbf{k}_1 + \mathbf{k}_2 + \mathbf{k}_3 = 0$$

Coplanar solution

$$\cos \theta_1 = (k_1^2 + k_2^2 - k_3^2) / (2k_1k_2),$$

$$\cos \theta_3 = (-k_1^2 + k_2^2 + k_3^2) / (2k_2k_3).$$

Doppler broadening comparison

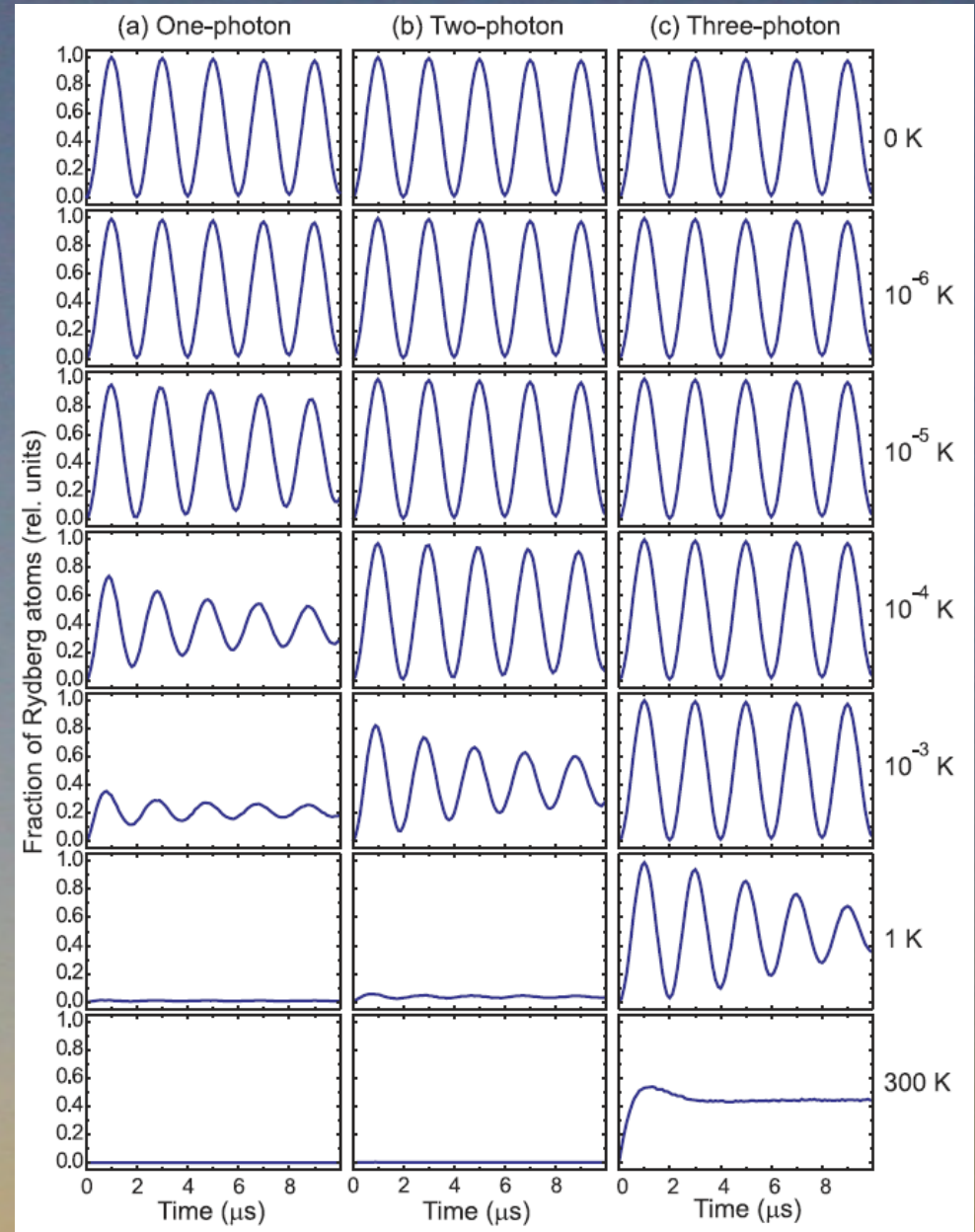
PHYSICAL REVIEW A 84, 053409 (2011)

Doppler- and recoil-free laser excitation of Rydberg states via three-photon transitions

I. I. Ryabtsev,* I. I. Beterov, D. B. Tretyakov, V. M. Entin, and E. A. Yakshina

Rb, $\Omega/2\pi=0.5$ MHz

Three photon scheme gives substantial Rydberg excitation even at room temperature



3 photon excitation

Pillet group

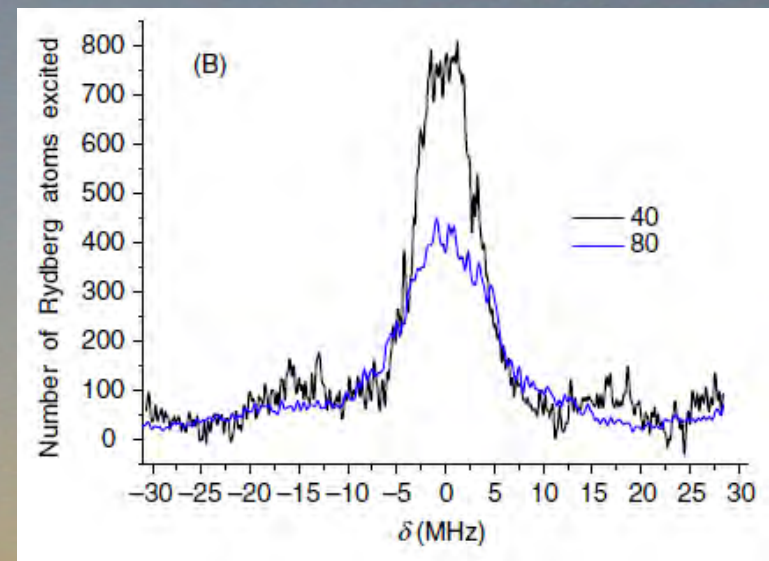
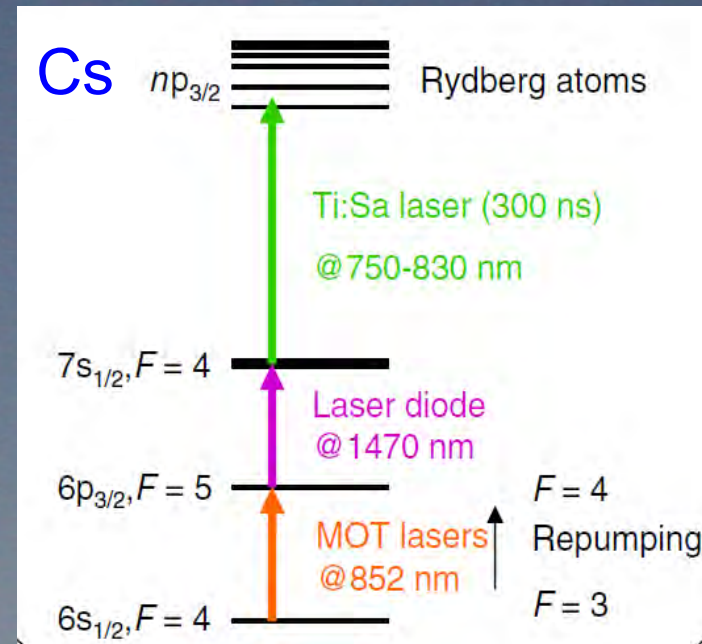
Diode lasers or Ti:Sa

About 10 MHz linewidth,
may also be broadened
by interactions

Kinetic Monte Carlo modeling of dipole blockade in Rydberg excitation experiment

Amodsen Chotia¹, Matthieu Viteau, Thibault Vogt,
Daniel Comparat and Pierre Pillet

New Journal of Physics **10** (2008) 045031



3 photon excitation with 2 photon degeneracy

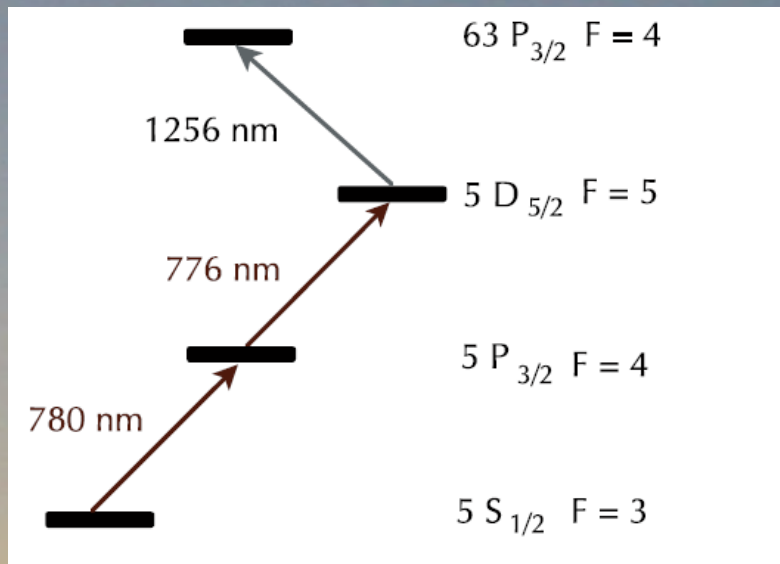
Journal of Modern Optics

Vol. 56, Nos. 18–19, 20 October–10 November 2009, 2055–2060



Spectroscopy of rubidium Rydberg states with three diode lasers

P. Thoumany, Th. Germann, T. Hänsch, G. Stania, L. Urbonas and Th. Becker*



780 and 776 counterpropagating
780 and 1256 copropagating

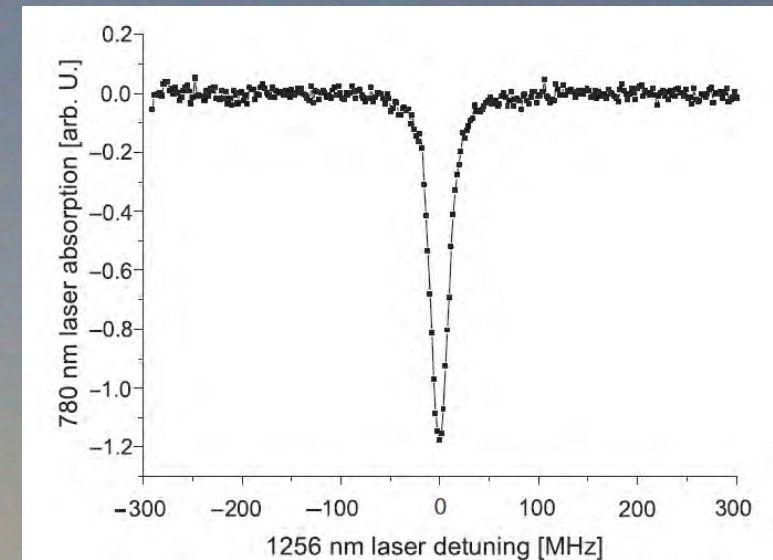


Figure 6. Absorption signal from the 63P_{3/2} Rydberg state in a room-temperature gas cell obtained with a three diode laser cascade setup. The 1256 nm laser is applied copropagating with the 780 nm laser.

1: Coherent excitation of Rydberg states

- overview
- calculation of rates
- 1 photon methods
- 2 photon methods, Doppler, AC Stark shifts
- 3 photon methods
- experiments, coherent oscillations

Experiments

First experiments were in 1970s, 1980s, for a review see

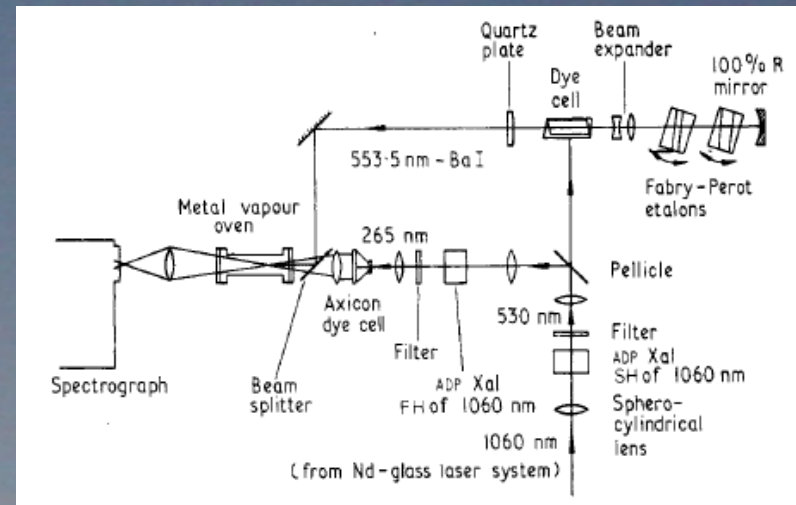
J. Phys. B: Atom. Molec. Phys., Vol. 6, August 1973.

Excited state absorption spectroscopy of alkaline earths selectively pumped by tunable dye lasers

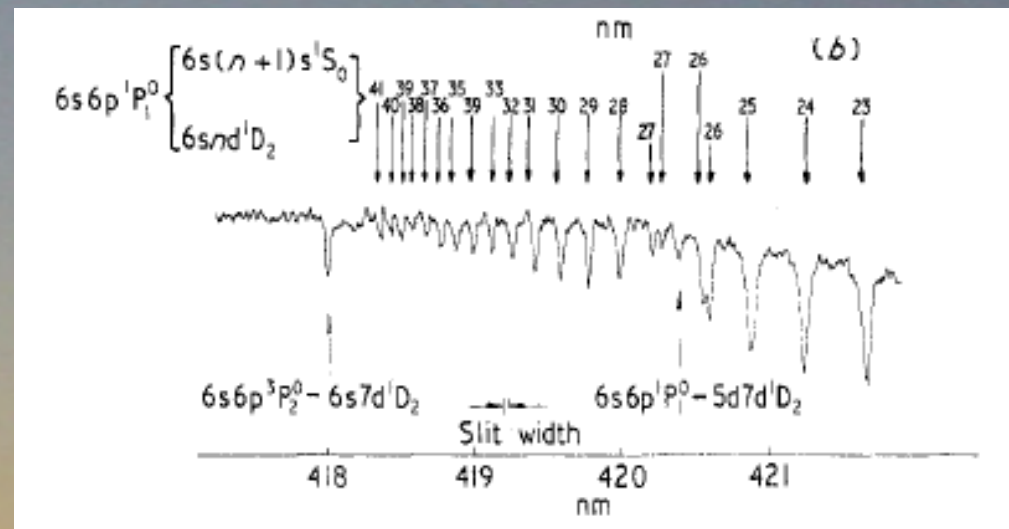
I. Barium arc spectra

D J Bradley, P Ewart, J V Nicholas and J R D Shaw
 Department of Pure and Applied Physics, The Queen's University of Belfast
 Belfast BT7 1NN, Northern Ireland

Fabre, C., and S. Haroche, 1983, in *Rydberg States of Atoms and Molecules*, edited by R. F. Stebbings and F. B. Dunning Cambridge University Press, Cambridge, Chap. 4, p. 117.



1973 data,
 resolution about
 0.1 nm



Stark structure of the Rydberg states of alkali-metal atoms

Myron L. Zimmerman, Michael G. Littman, Michael M. Kash, and Daniel Kleppner

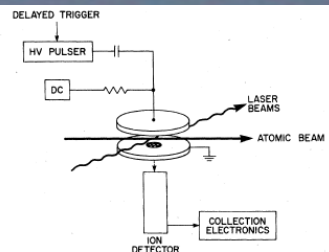


FIG. 2. Experimental arrangement.

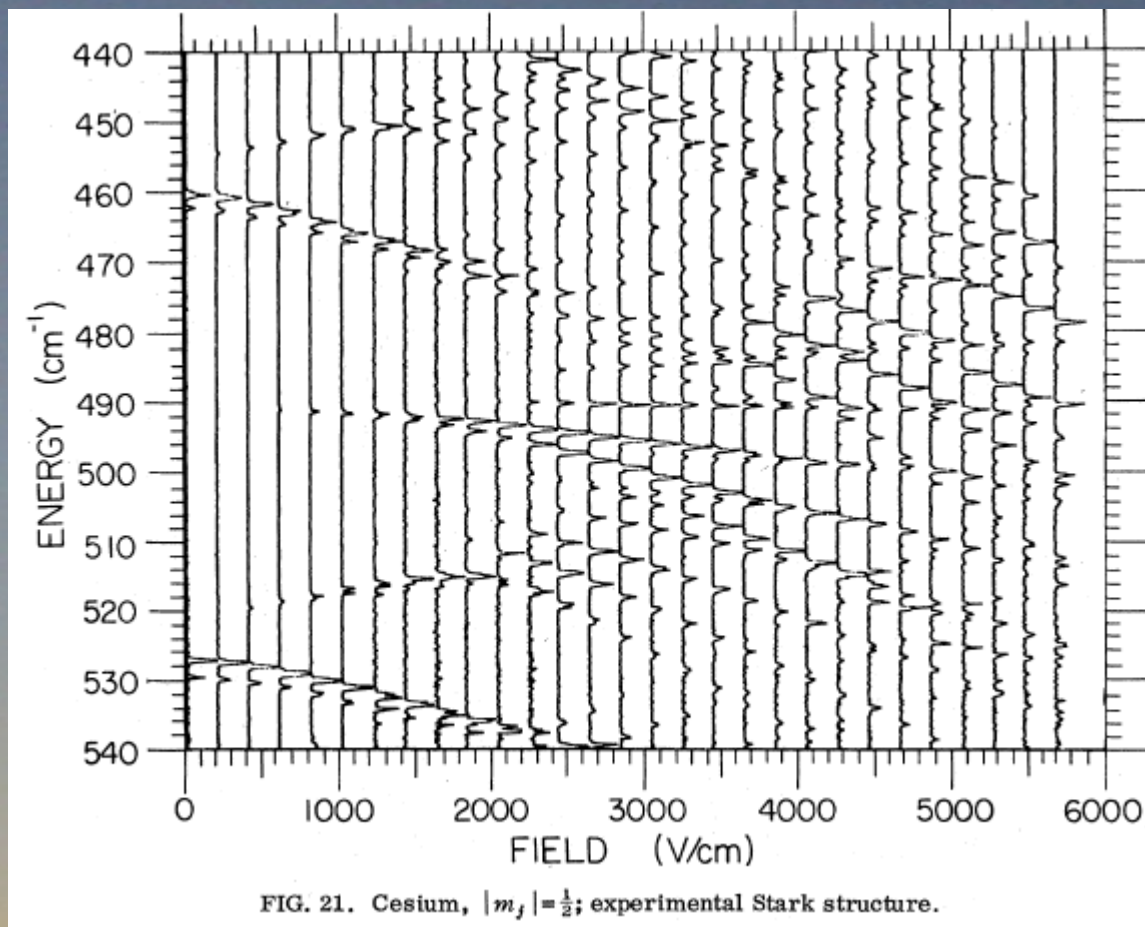
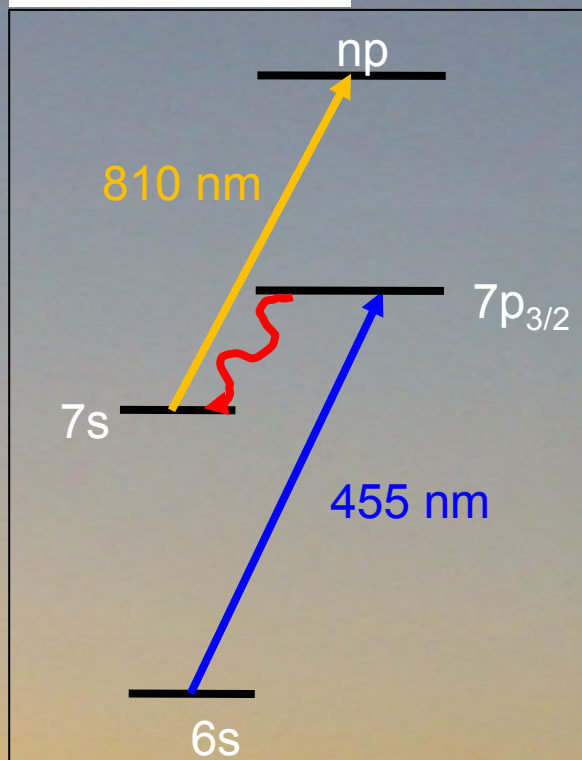


FIG. 21. Cesium, $|m_j| = \frac{1}{2}$; experimental Stark structure.

1979 data,
resolution about 10 GHz

2 photon excitation – Autler Townes splitting

PHYSICAL REVIEW A 68, 053407 (2003)

Autler-Townes spectroscopy of the $5S_{1/2}$ - $5P_{3/2}$ - $44D$ cascade of cold ^{85}Rb atoms

B. K. Teo, D. Feldbaum, T. Cubel, J. R. Guest, P. R. Berman, and G. Raithel

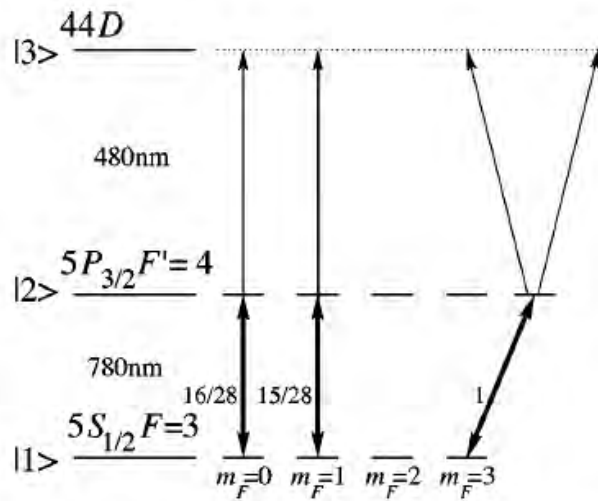
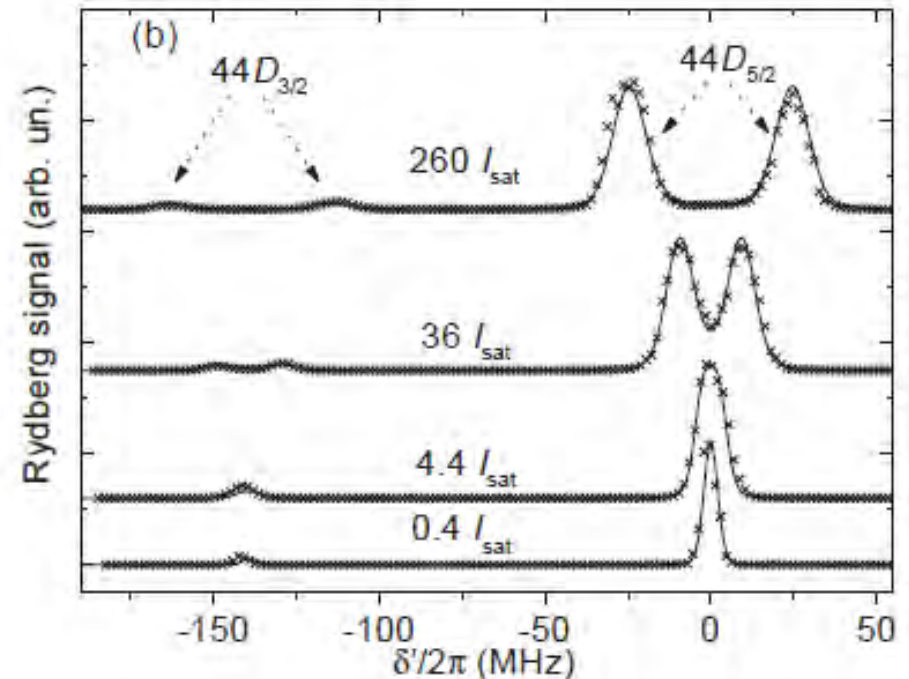


FIG. 1. Excitation scheme of ^{85}Rb from the $5S_{1/2}$ ground state to the $44D$ Rydberg states using linear and σ^+ pump fields. The squares of the Clebsch-Gordan coefficients associated with the transitions are indicated next to the lower arrows. The probe field is linearly polarized in direction parallel to the linear pump field.



2003 data, resolution few MHz,
Note, Rabi frequency depends on ground quantum state.

2 photon excitation – Rabi oscillations

PRL 100, 253001 (2008)

PHYSICAL REVIEW LETTERS

week ending
27 JUNE 2008

Rabi Oscillations and Excitation Trapping in the Coherent Excitation of a Mesoscopic Frozen Rydberg Gas

M. Reetz-Lamour, T. Amthor, J. Deiglmayr, and M. Weidemüller*

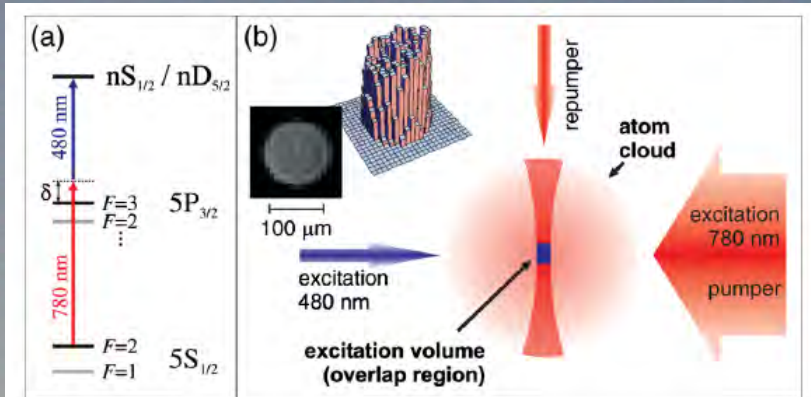


FIG. 1 (color online). (a) Relevant level scheme for two-photon excitation of rubidium. (b) Preparation of a mesoscopic subensemble. All atoms are pumped to the $F = 1$ hyperfine component of the ground state. Only a tight tube of atoms is pumped to $F = 2$ whence the excitation originates. Within this tube, a mesoscopic subensemble containing about 100 atoms is excited to Rydberg states with two counterpropagating laser beams at 780 and 480 nm. The latter has a flattop intensity profile shown in the inset, to ensure a constant Rabi frequency.

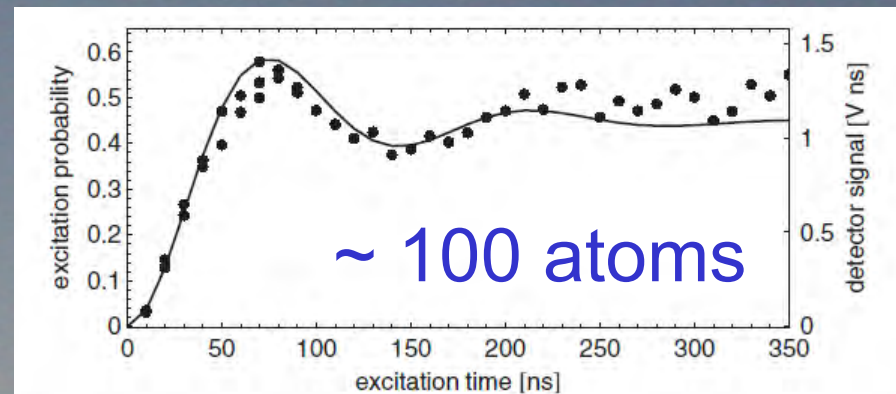


FIG. 2. Rabi oscillations between the $5S_{1/2}$ and $31D_{5/2}$ states of ^{87}Rb . Each dot is an average of measurements over 28 experimental repetition cycles. The solid line shows the simulated excitation probability taking the measured intensity distribution, the residual $5P_{3/2}$ admixture, and our finite laser linewidth into account. The scaling between the detector signal and simulated excitation probability is a free parameter that represents the detector efficiency.

Rabi oscillations in hot vapor cells

PRL 107, 243001 (2011)

PHYSICAL REVIEW LETTERS

week ending
9 DECEMBER 2011

GHz Rabi Flopping to Rydberg States in Hot Atomic Vapor Cells

B. Huber, T. Baluktian, M. Schlagmüller, A. Kölle, H. Kübler, R. Löw, and T. Pfau

Oscillations on nsec time scale !

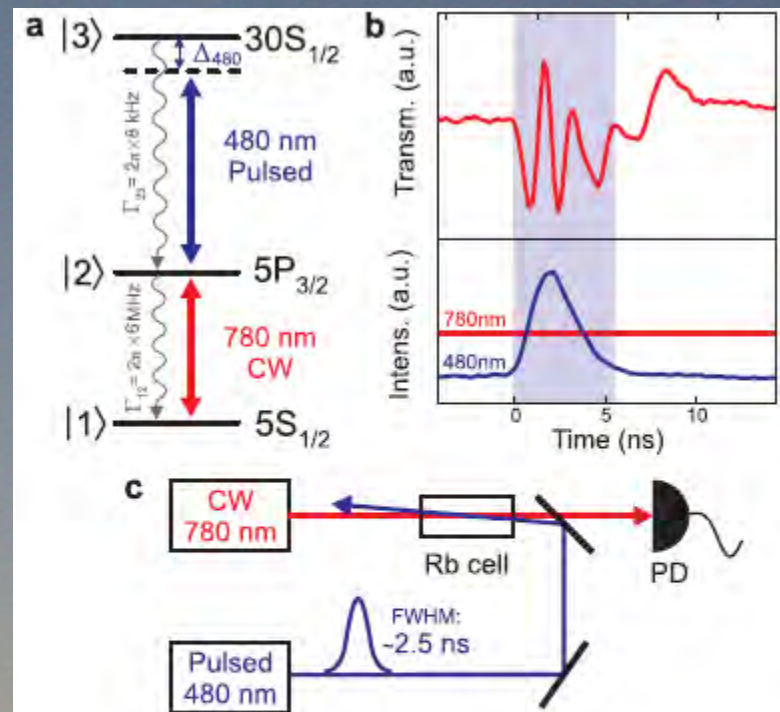


FIG. 1 (color online). Schema of the experiment. (a) The Rydberg state is addressed with a two-photon transition via an intermediate state. The laser for the upper transition is pulsed. (b) Transmission signal of the 780 nm laser (upper half) and corresponding laser intensities (lower half) as a function of time. (c) Simplified schematic of the optical setup.

Single atom Rabi oscillations

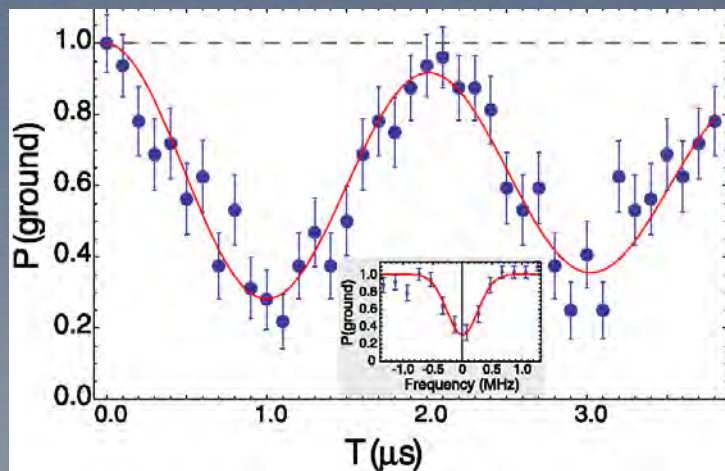
PRL 100, 113003 (2008)

PHYSICAL REVIEW LETTERS

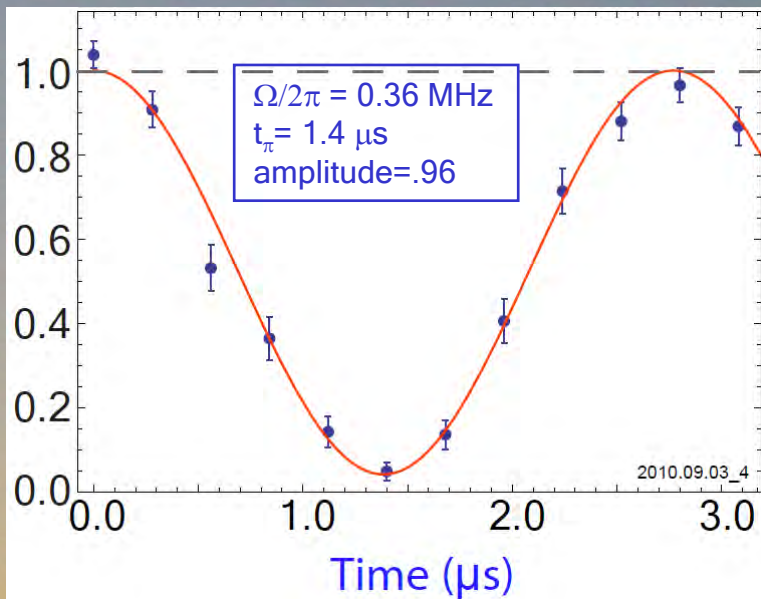
week ending
21 MARCH 2008

Rabi Oscillations between Ground and Rydberg States with Dipole-Dipole Atomic Interactions

T. A. Johnson, E. Urban, T. Henage, L. Isenhower, D. D. Yavuz, T. G. Walker, and M. Saffman



Ground State Probability



PHYSICAL REVIEW A 82, 013405 (2010)

Coherent excitation of a single atom to a Rydberg state

Y. Miroshnychenko,¹ A. Gaëtan,¹ C. Evellin,¹ P. Grangier,¹ D. Comparat,² P. Pillet,³ T. Wilk,¹ and A. Browaeys¹

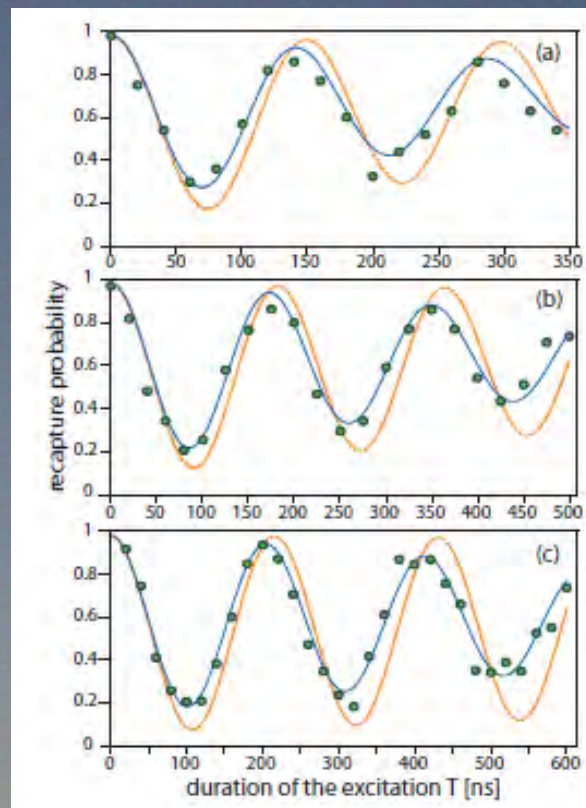
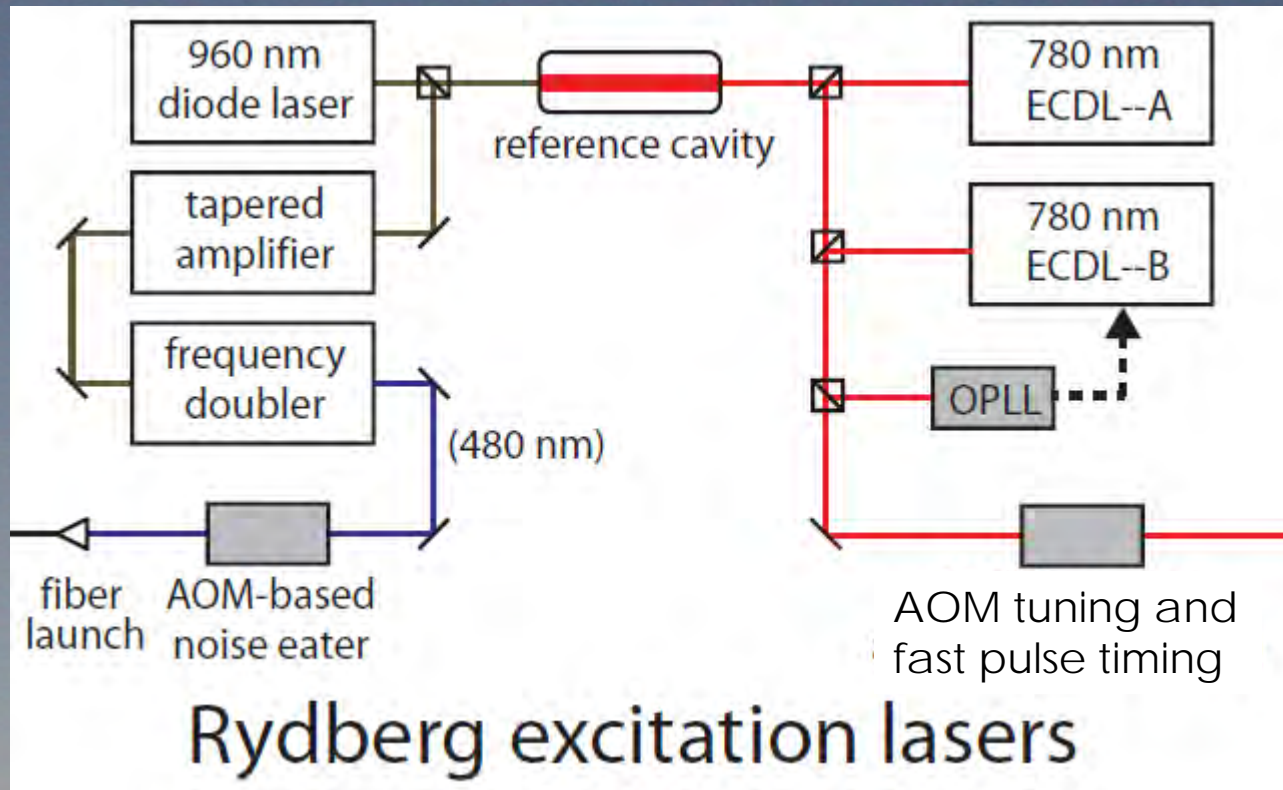


FIG. 4. (Color online) Coherent Rydberg excitation of a single atom to the level $|58d_{3/2}, F=3, m_F=3\rangle$ for different experimental parameters: (a) $(\Omega_R, \Omega_B, \Delta)/2\pi = (255, 24, 400)$ MHz, (b) $(\Omega_R, \Omega_B, \Delta)/2\pi = (250, 28, 600)$ MHz, and (c) $(\Omega_R, \Omega_B, \Delta)/2\pi = (80, 70, 600)$ MHz. Each point corresponds to 100 repetitions of the experiment. The blue line is the result of a Monte Carlo simulation of the dynamics of a five-level system, which includes a decay from the intermediate state, fluctuations of the power and of the frequency of the lasers, and imperfection of the optical pumping. The dotted orange line shows for comparison the results of simulations with the same parameters of Ω_R , Ω_B , and Δ but without fluctuations.

Experimental approach - UW Madison



Reference cavity is 5 kHz linewidth, ULE spacer Fabry-Perot in temperature stabilized vacuum can.
This gives long term stability < 100 kHz and ~200 Hz linewidths.
Verified by beating two lasers together.

State preparation and selection

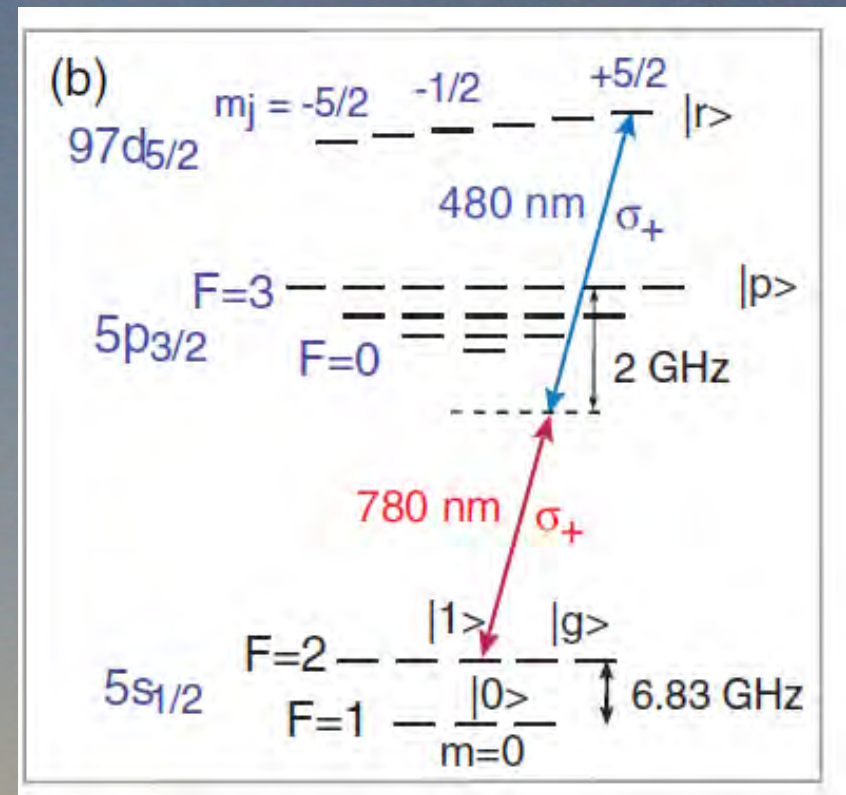
High fidelity oscillations require optical pumping to a single initial state and Rydberg state selection.

We start by pumping into $f=2, m_f=0$.

This hyperfine state is a superposition of electron spin up and spin down.

The hyperfine interaction is negligible at $n=100$. With two σ_+ photons we can excite $97d_{5/2}$ $m_j=3/2$ or $m_j=5/2$.

The Rabi frequency is different for these two end states which leads to non-sinusoidal oscillations.



State preparation and selection

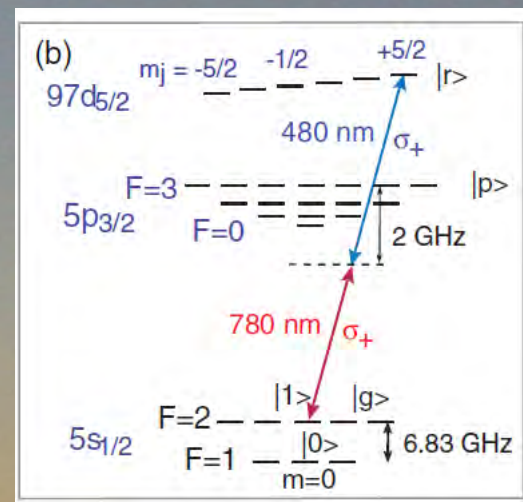
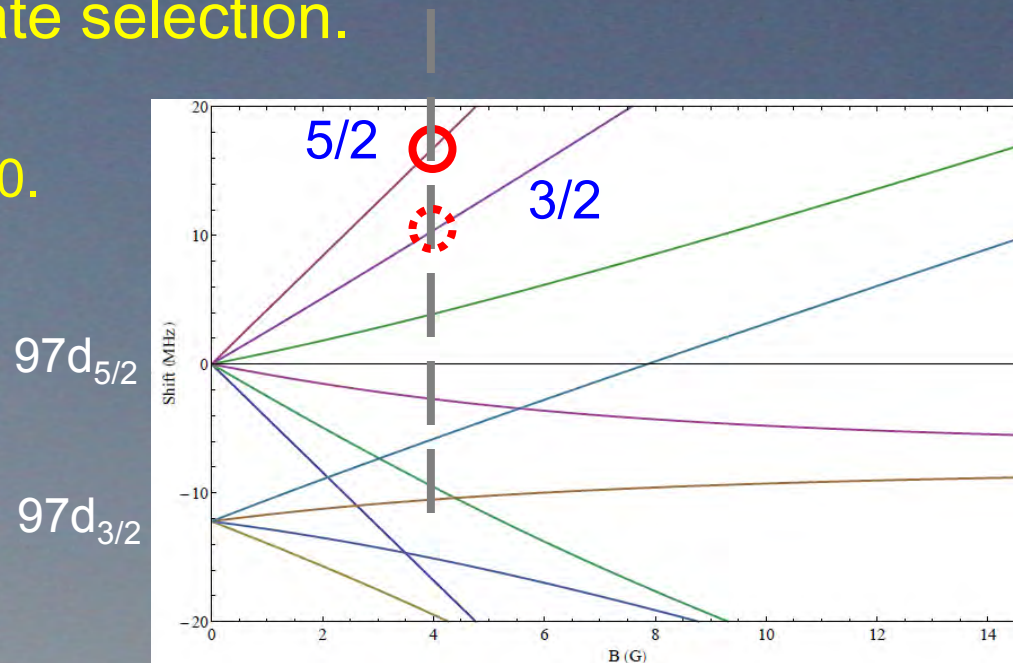
High fidelity oscillations require optical pumping to a single initial state and Rydberg state selection.

We start by pumping into $f=2, m_f=0$.

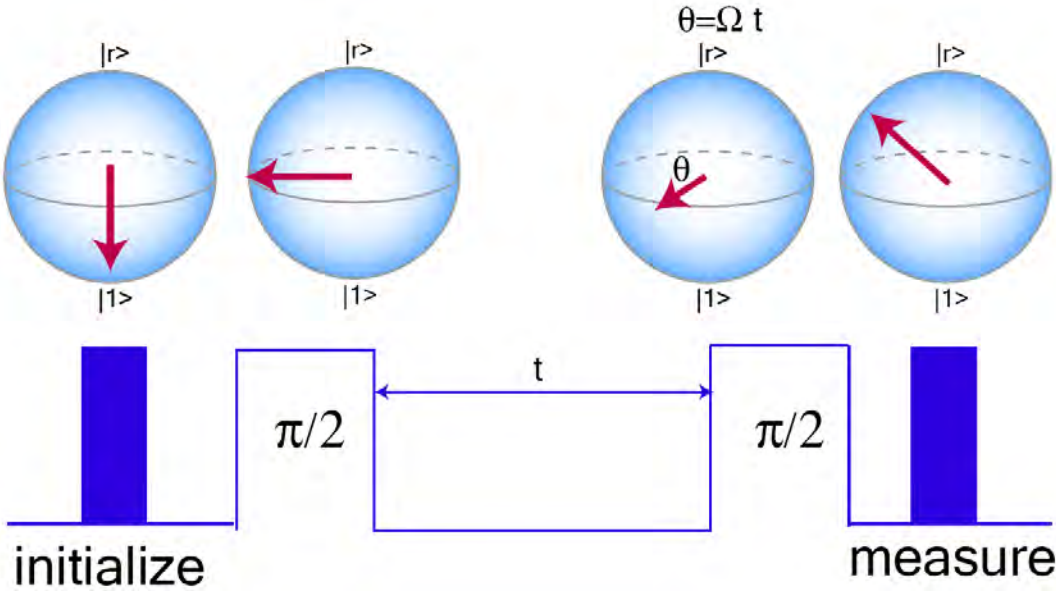
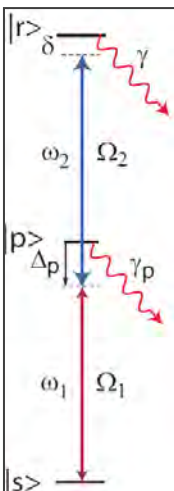
This hyperfine state is a superposition of electron spin up and spin down.

The hyperfine interaction is negligible at $n=100$. With two σ_+ photons we can excite $97d_{5/2}$ $m_j=3/2$ or $m_j=5/2$.

The Rabi frequency is different for these two end states which leads to non-sinusoidal oscillations.

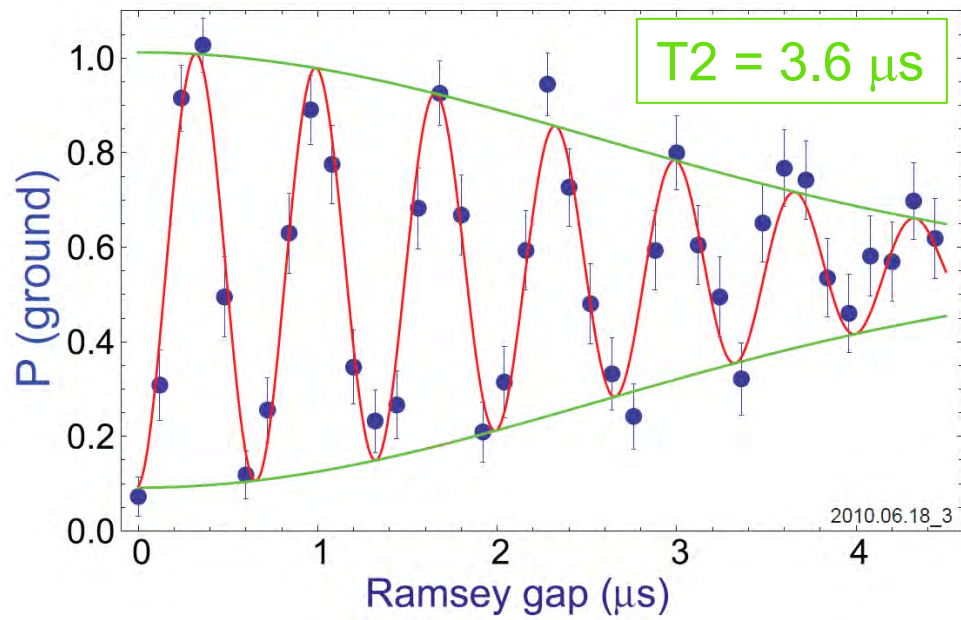
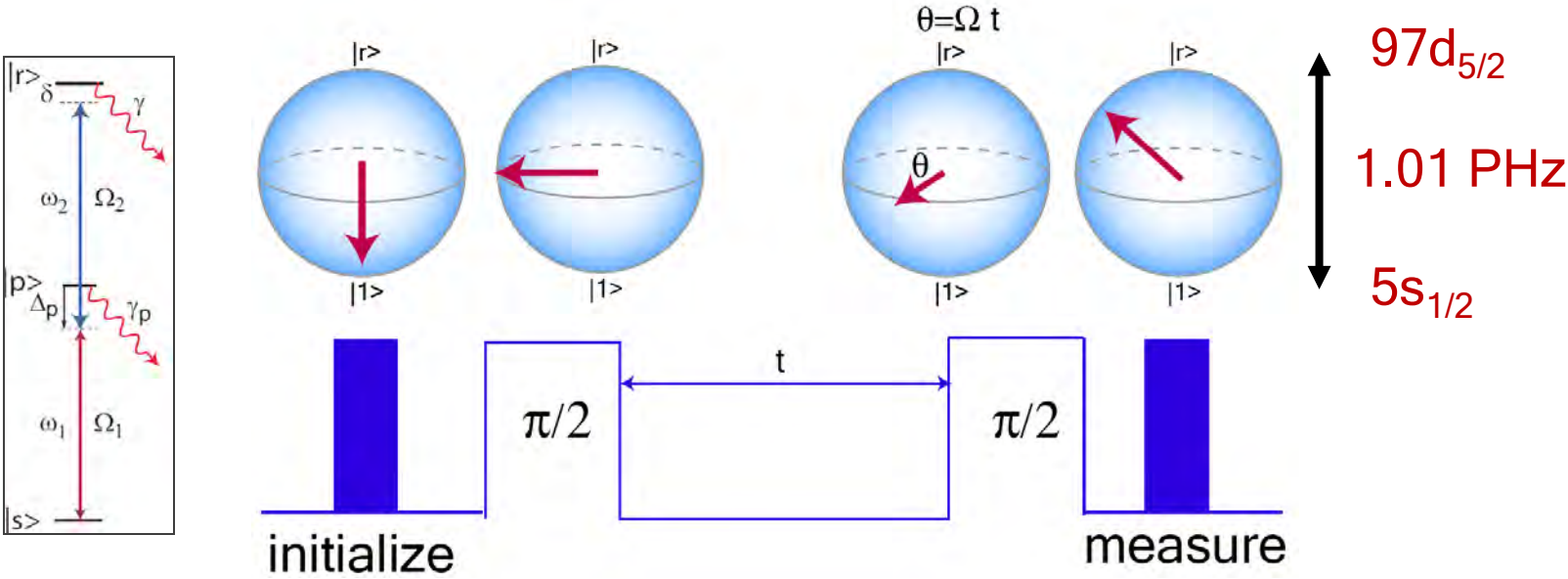


Coherence of Rydberg excitation

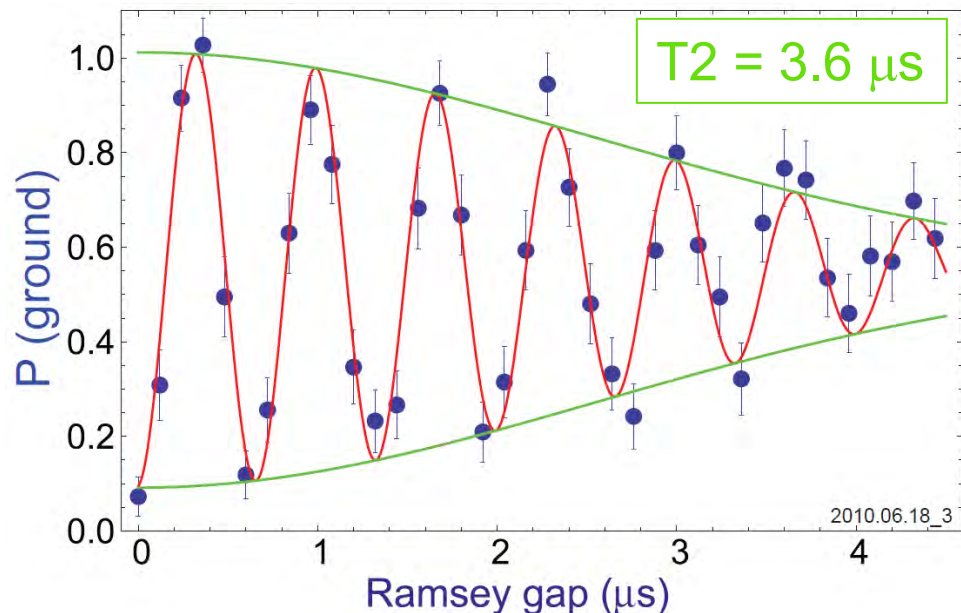
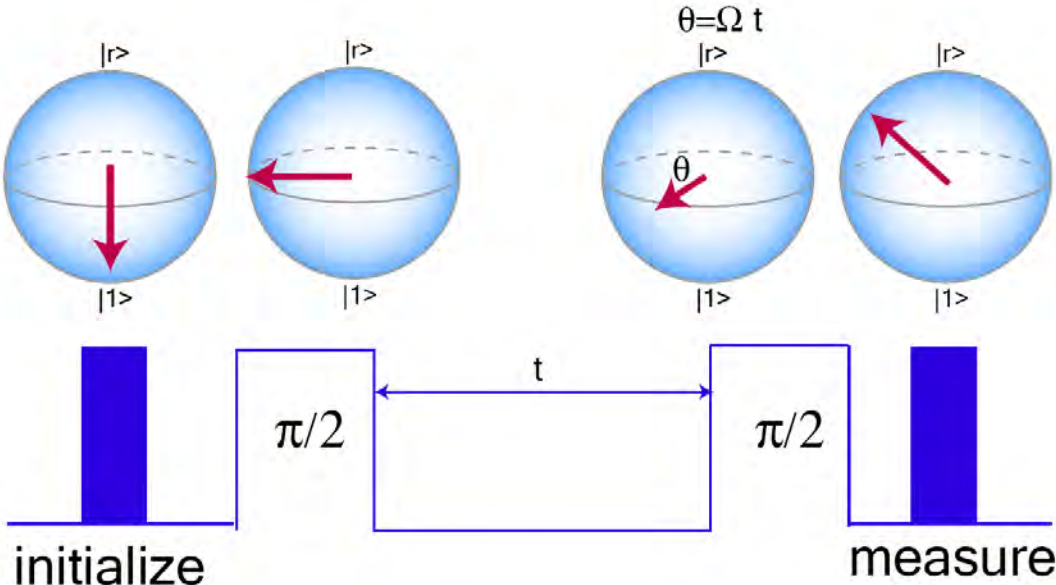
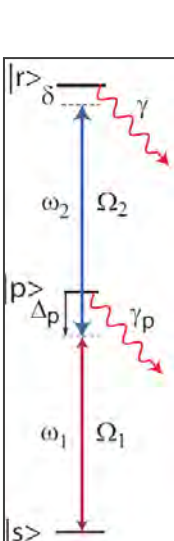


$97d_{5/2}$
 1.01 PHz
 $5s_{1/2}$

Coherence of Rydberg excitation



Coherence of Rydberg excitation



Signal decays as

$$e^{-t^2 / T_2^2}$$

$$T_2 = \frac{T_{2,B} T_{2,D}}{(T_{2,B}^2 + T_{2,D}^2)^{1/2}}$$

$T_{2,\text{magnetic}} = 6.8 \mu\text{s}$

$$T_{2,B} = \frac{2^{3/2} \pi \hbar}{|g_R m_{jR} - g_g m_{fg}| \mu_B \sigma}$$

$T_{2,\text{Doppler}} = 4.2 \mu\text{s}$

$$T_{2,D} = \left(\frac{2m}{k_B T} \right)^{1/2} \frac{1}{k_{2\nu}}$$

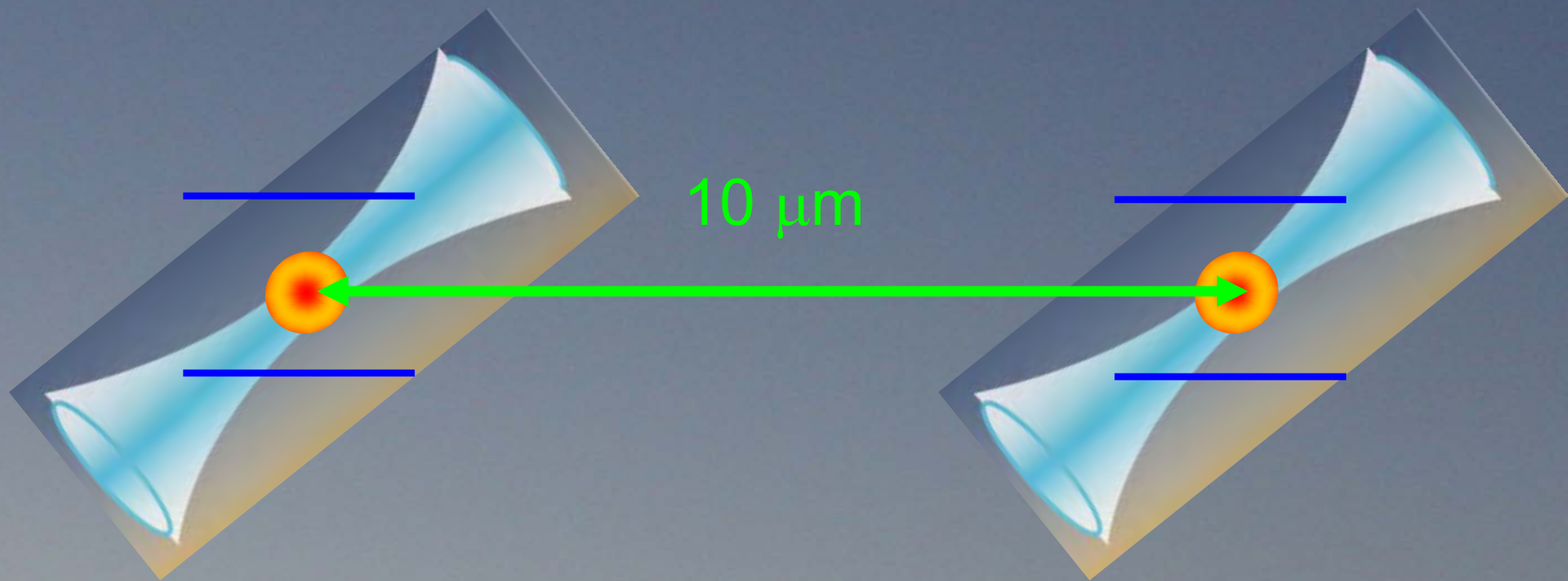
Summary

- Excitation of Rydberg states can be performed coherently with modern, stabilized laser sources.
- I have concentrated on the simplest case of constant in time, linear excitation of non-interacting atomic samples.
- With interactions blockade plays an important role, leading also to a $N^{1/2}$ speedup.
- Quantum interference effects can be exploited to achieve large optical nonlinearities (C. Adams lectures)
- Temporally modulated pulse sequences such as STIRAP can lead to novel quantum states in interacting samples (K. Mølmer lectures)

II: Rydberg atom interactions

- orders of magnitude
- dipole-dipole interactions: resonant limit, van der Waals limit
- angular dependence
- Ground – Rydberg interaction
- ground state dressing

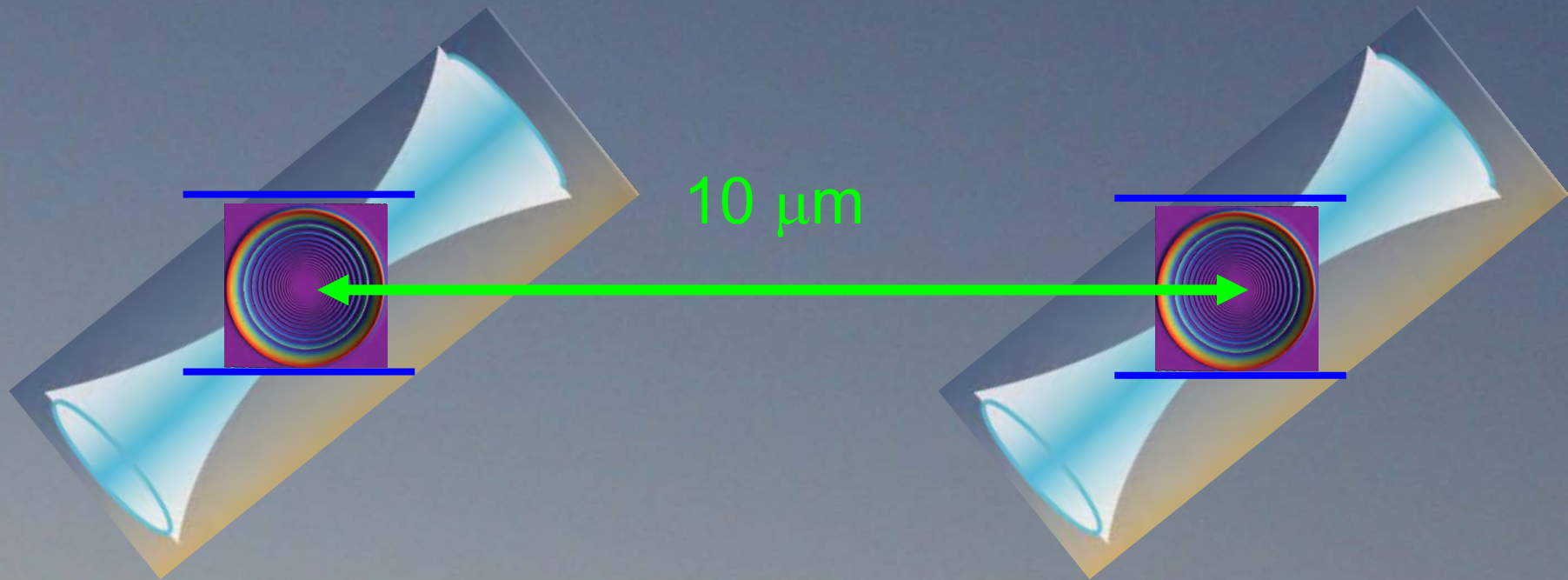
Long range interactions



Rb-Rb ground state
magnetostatic interaction

$$\Delta E \sim 100 \mu\text{Hz}$$

Long range interactions



Rb-Rb ground state
magnetostatic interaction

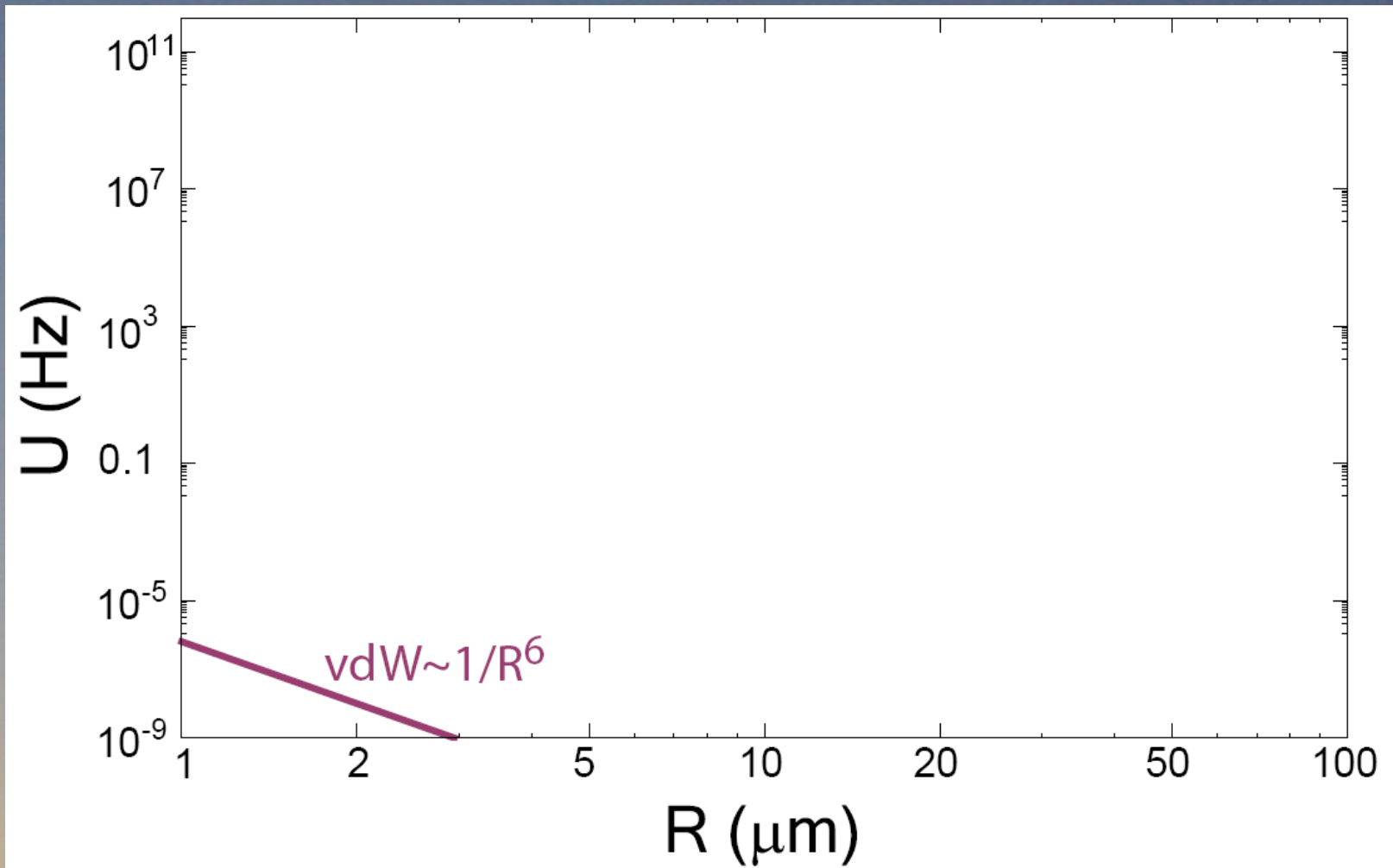
$$\Delta E \sim 100 \mu\text{Hz}$$

Rydberg $n=100$
van der Waals interaction

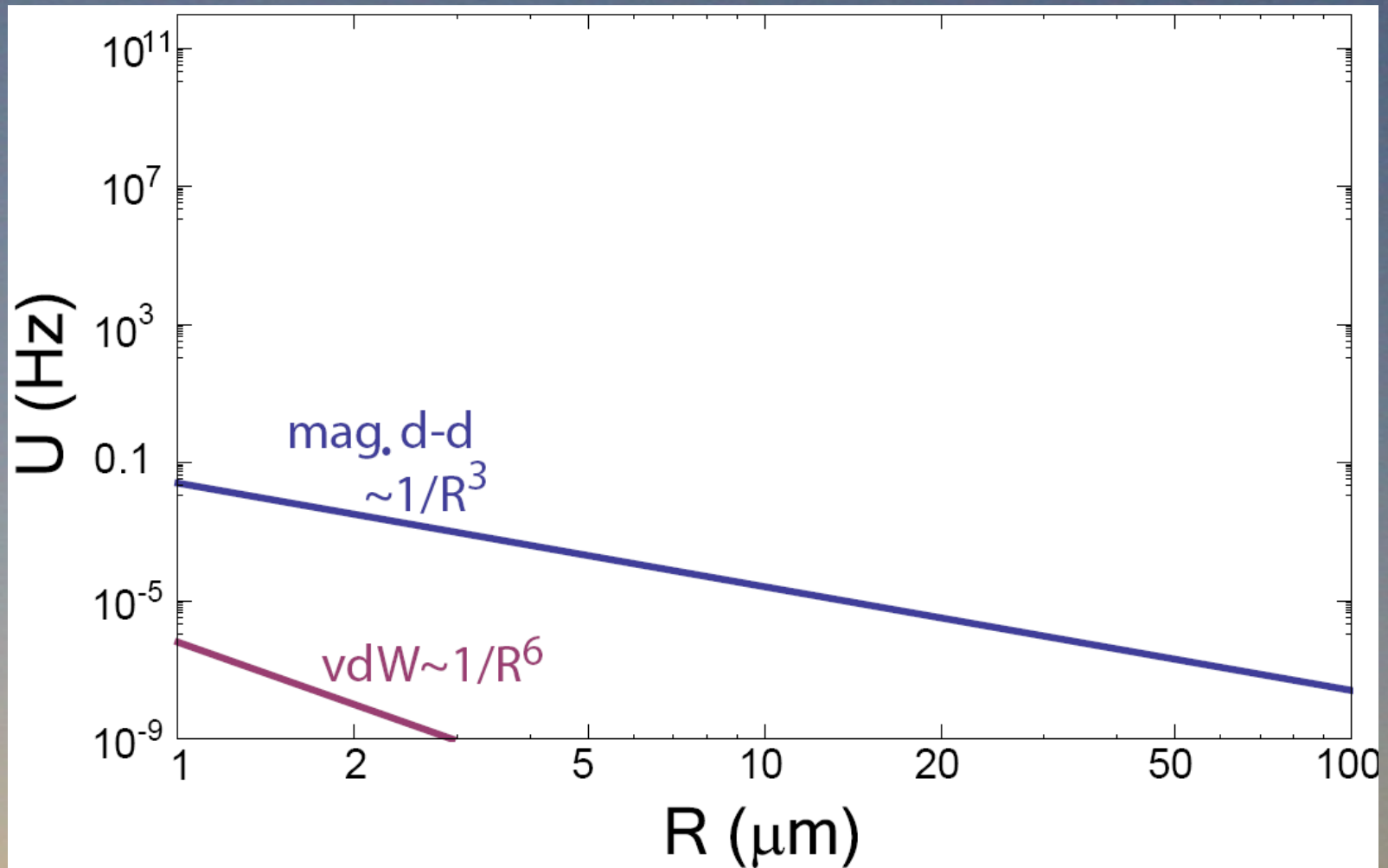
$$\Delta E \sim 100 \text{ MHz}$$

12 orders of magnitude!

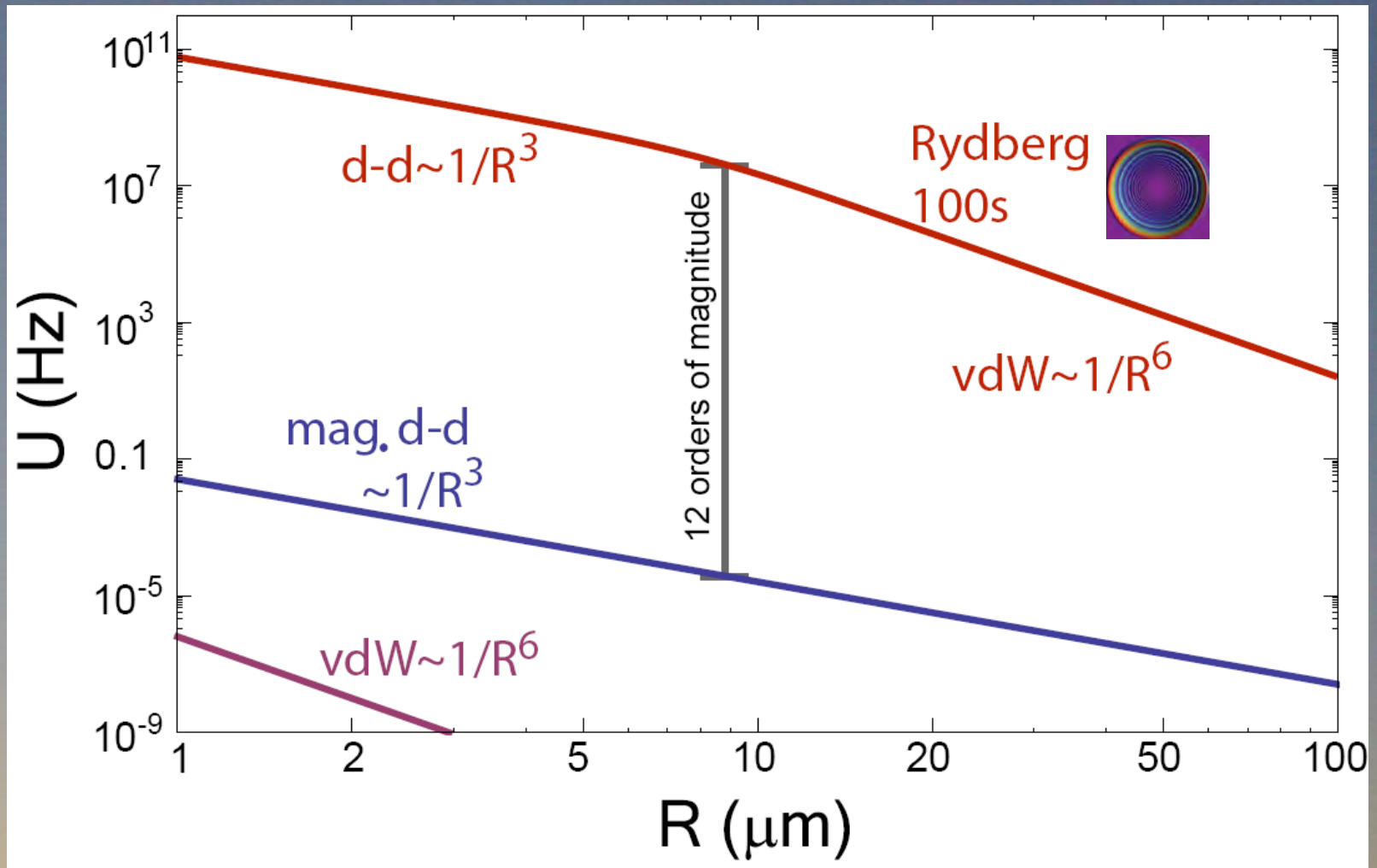
Rydberg interactions: strong and controllable



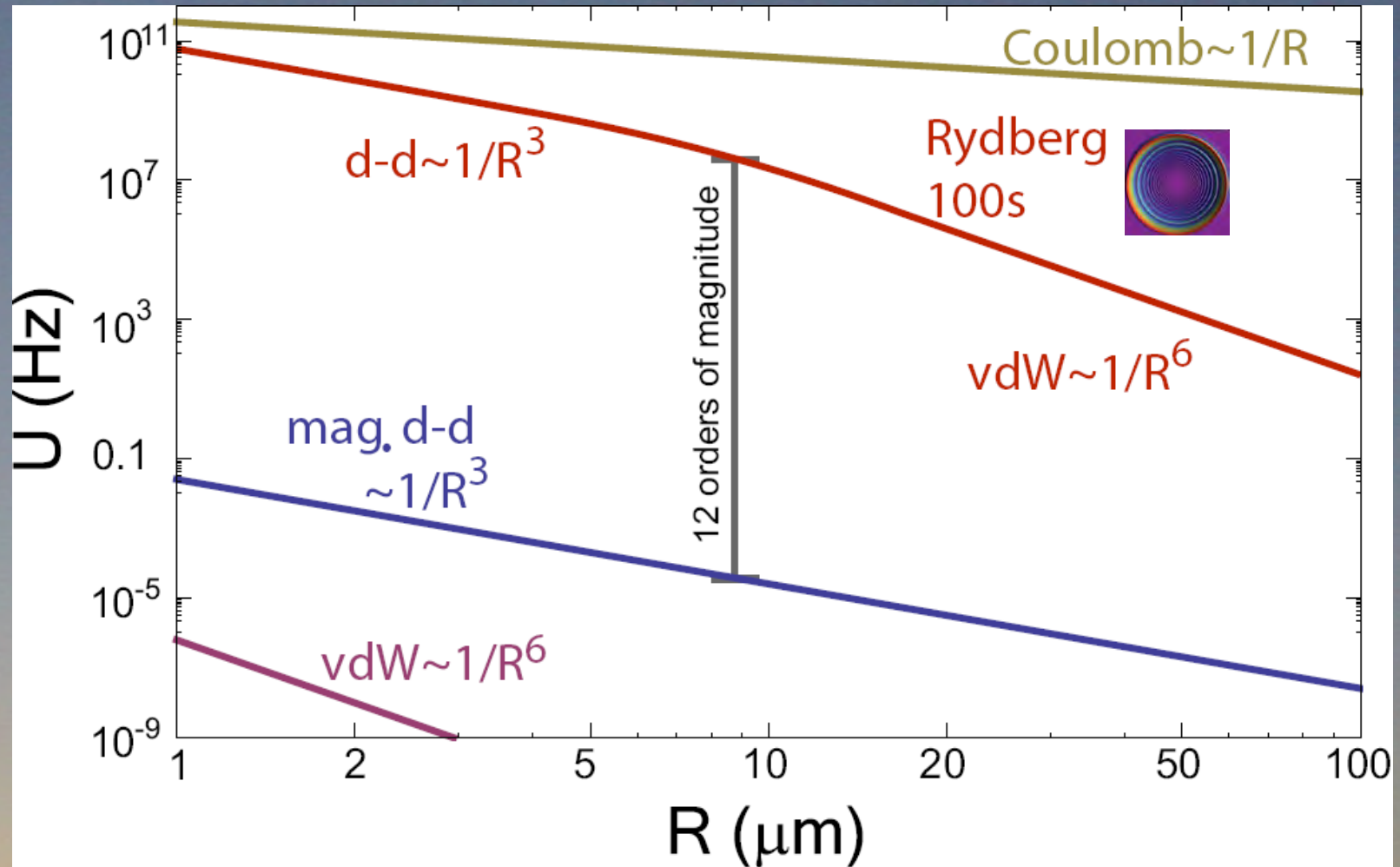
Rydberg interactions: strong and controllable



Rydberg interactions: strong and controllable

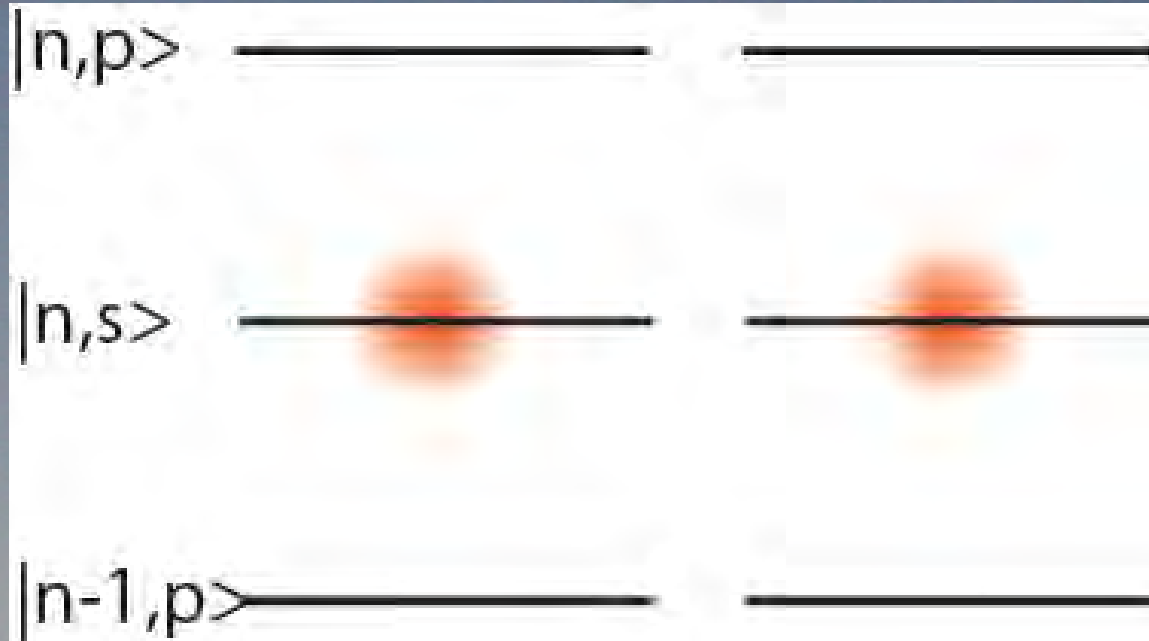


Rydberg interactions: strong and controllable



Rydberg - Rydberg interaction

Förster resonance



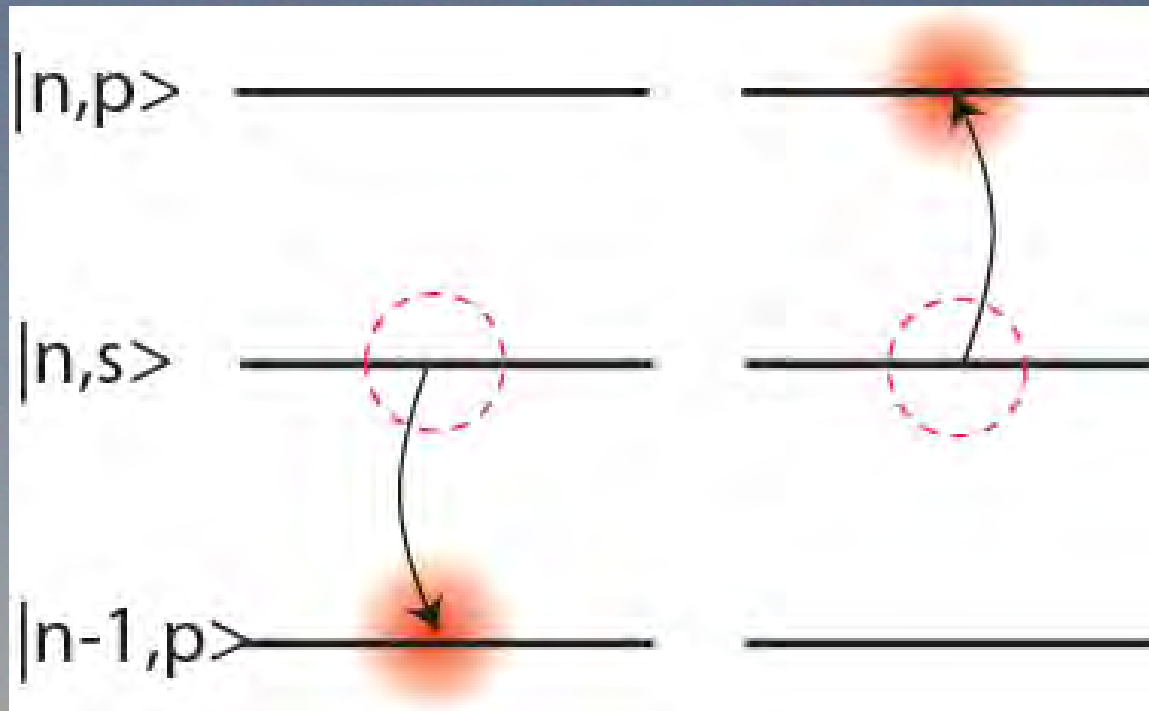
Th. Förster,
Zwischenmolekulare energiewanderung
und fluoreszenz,
Annalen der Physik **2**, 55 (1948).

Rydberg theory:

Protsenko, Reymond, Schlosser, Grangier PRA 2002
Walker & MS, JPB 2005, PRA 2008
Li, Tanner, Gallagher PRL 2005

Rydberg - Rydberg interaction

Förster resonance



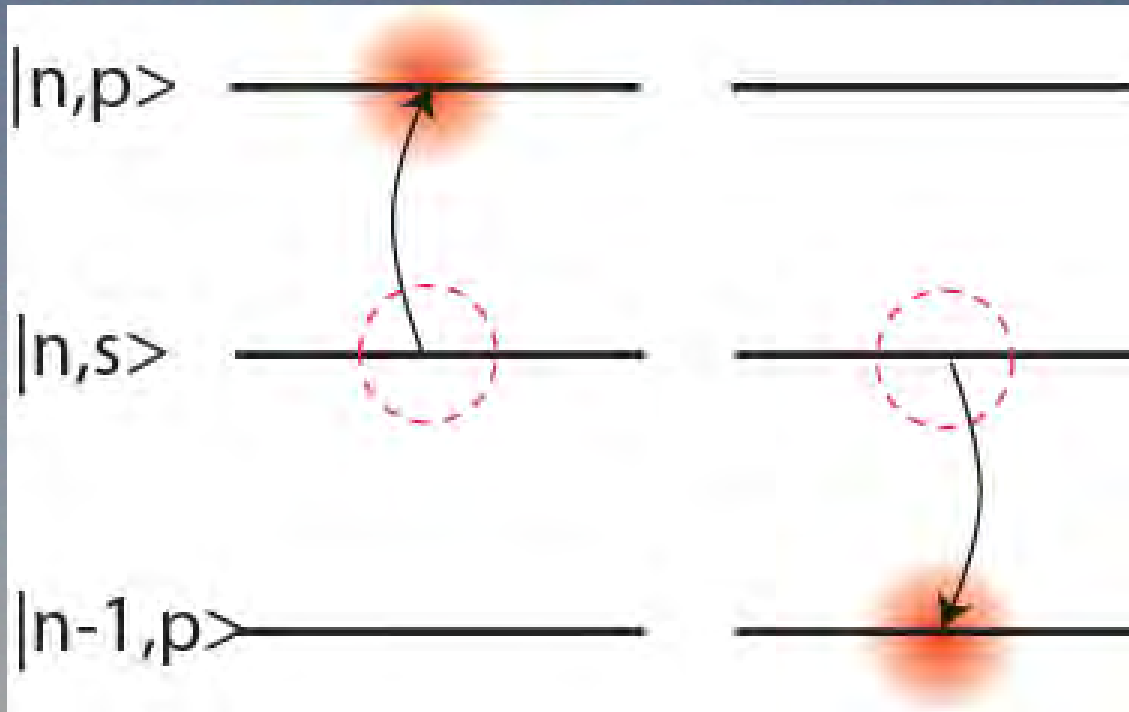
Th. Förster,
Zwischenmolekulare energiewanderung
und fluoreszenz,
Annalen der Physik **2**, 55 (1948).

Rydberg theory:

Protsenko, Reymond, Schlosser, Grangier PRA 2002
Walker & MS, JPB 2005, PRA 2008
Li, Tanner, Gallagher PRL 2005

Rydberg - Rydberg interaction

Förster resonance



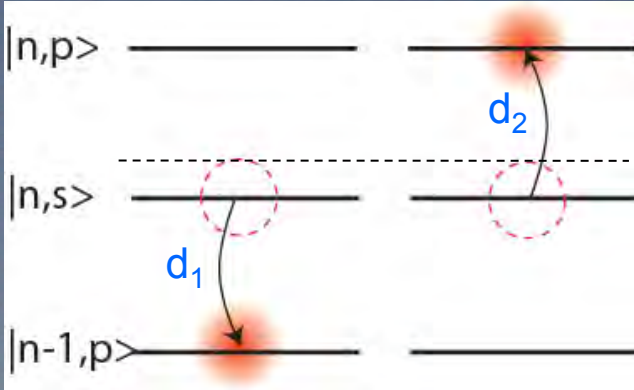
Th. Förster,
Zwischenmolekulare energiewanderung
und fluoreszenz,
Annalen der Physik **2**, 55 (1948).

Rydberg theory:

Protsenko, Reymond, Schlosser, Grangier PRA 2002
Walker & MS, JPB 2005, PRA 2008
Li, Tanner, Gallagher PRL 2005

Resonant d-d to van der Waals

Förster resonance

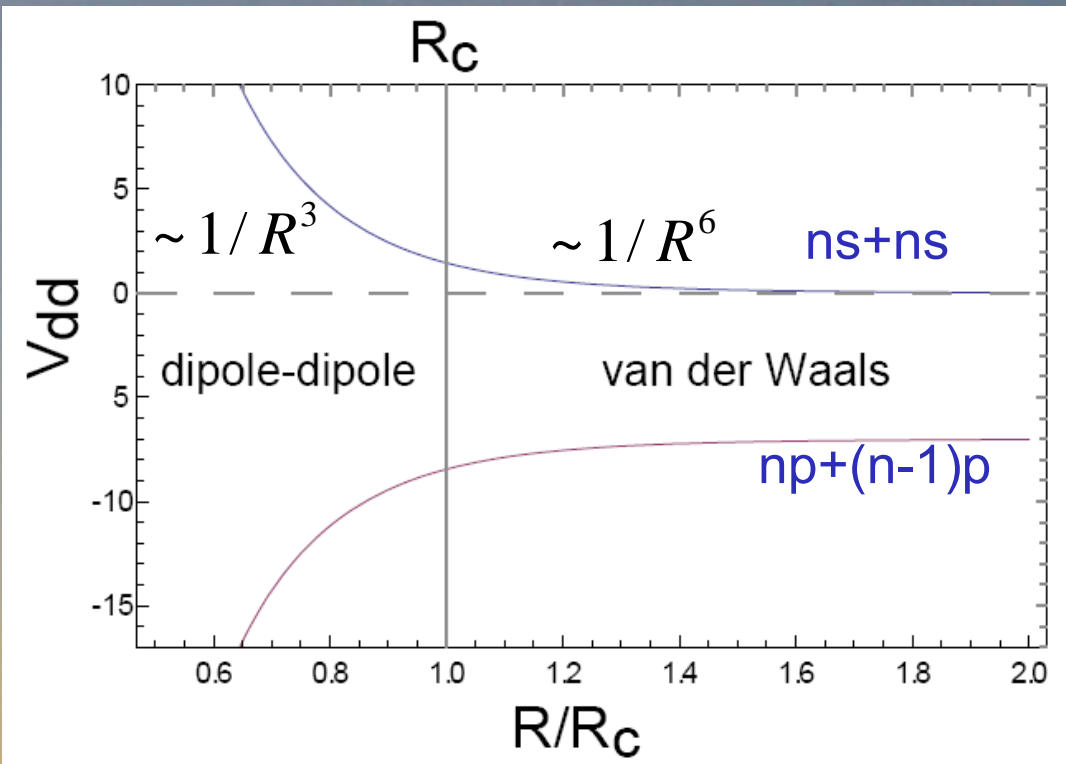


The resonant interaction strength is

$$V_{dd} \sim C_3/R^3 \quad C_3 \sim d_1 d_2$$

With energy defect δ we get

$$V_{vdW} \sim C_6/R^6 \quad C_6 = C_3^2/h\delta$$



Molecular potentials

Dipole-dipole operator in spherical basis

$$\hat{V}_{\text{dd}} = \frac{-e^2}{4\pi\epsilon_0 r^3} \sqrt{6} \sum_p C_{1p1-p}^{20} r_{A p} r_{B -p}$$

$M=m_A+m_B$ is conserved

Symmetrized states

$$\begin{aligned} |1\rangle &= |n_0 0; n_0 0\rangle & |3\rangle &= |n_1 1 1; n_2 1 - 1\rangle \\ |2\rangle &= |n_1 1 0; n_2 1 0\rangle & |4\rangle &= |n_1 1 - 1; n_2 1 1\rangle \end{aligned}$$

Hamiltonian

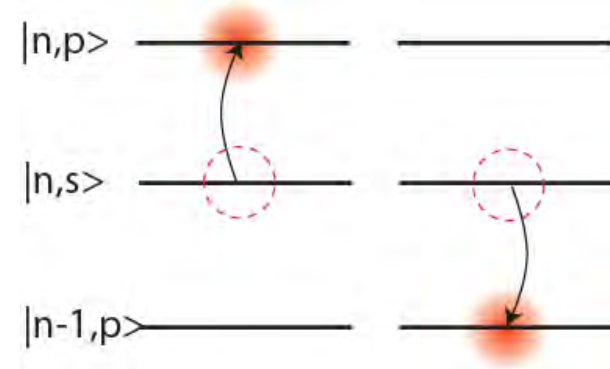
$$\mathcal{H}_0 = \hbar \begin{pmatrix} 0 & 0 & 0 & 0 \\ 0 & \delta & 0 & 0 \\ 0 & 0 & \delta & 0 \\ 0 & 0 & 0 & \delta \end{pmatrix} \quad \mathcal{H}_1 = -\frac{\sqrt{2}}{3} U_3 \begin{pmatrix} 0 & 2 & 1 & 1 \\ 2 & 0 & 0 & 0 \\ 1 & 0 & 0 & 0 \\ 1 & 0 & 0 & 0 \end{pmatrix}$$

energy defect

$$\hbar\delta = E(n_1 p) + \bar{E}(n_2 p) - 2E(ns)$$

long range interaction

$$U_3(r) = \frac{e^2}{4\pi\epsilon_0 r^3} \langle n_1 1 || r || n_0 \rangle \langle n_2 1 || r || n_0 \rangle$$



Eigenvalues - van der Waals limit

$$U_{\pm}(r) = \frac{\hbar\delta}{2} \pm \sqrt{\frac{(\hbar\delta)^2}{4} + \frac{4U_3^2(r)}{3}}$$

$$\hbar\delta = E(n_1p) + \bar{E}(n_2p) - 2E(ns)$$

$$U_3(r) = \frac{e^2}{4\pi\epsilon_0 r^3} \langle n_3 1 || r || n_0 \rangle \langle n_4 1 || r || n_0 \rangle$$

When the energy defect is large $\hbar\delta \gg U_3$.

$$U_{\pm}(r) \simeq \frac{\hbar\delta}{2} \pm \frac{4U_3^2(r)}{3\hbar\delta}$$

We recover the short range van der Waals interaction

$$U_{vdW} = \frac{C_6}{r^6} = \frac{4U_3^2(r)}{3\hbar\delta}$$

$$C_6 \sim n^{11}$$

For Rb, Cs large n , $v_s - v_p \sim 0.5$.

This implies $\delta \sim 1/n^4$ so

$$C_6 \sim n^{12}$$

heavy alkali
ns states

Eigenvalues - dipole-dipole limit

$$U_{\pm}(r) = \frac{\hbar\delta}{2} \pm \sqrt{\frac{(\hbar\delta)^2}{4} + \frac{4U_3^2(r)}{3}}$$

$$\hbar\delta = E(n_1p) + \bar{E}(n_2p) - 2E(ns)$$

$$U_3(r) = \frac{e^2}{4\pi\epsilon_0 r^3} \langle n_3 1 || r || n_0 \rangle \langle n_4 1 || r || n_0 \rangle$$

When the energy defect is small $\hbar\delta \ll U_3$ we obtain a long range $1/r^3$ interaction

$$U_{\pm}(r) \cong \frac{\hbar\delta}{2} \pm \frac{2}{\sqrt{3}} U_3(r) \quad \frac{C_3}{r^3} = \frac{2}{\sqrt{3}} U_3(r) \quad C_3 \sim n^4$$

The effective dipole-dipole interaction is isotropic (for s states).

Discussion

This simplest case $ns+ns \rightarrow n'p + n''p$ is easily solved by hand.

There are many more cases “channels”.

Walker & MS PRA (2008)

TABLE I. Relative interaction strengths for van der Waals interactions of Rydberg atoms, for various collision channels. The potential energy at distance R is the product $C_6 D_\psi / R^6$, which contains the effects of Zeeman degeneracy, with the overall C_6 coefficient [Eq. (37)] for a particular channel that depends only on the energy level structure and radial matrix elements. Cases where the j quantum number is not included in the channel description are the sum over fine-structure components of the final state.

Channel	$ M \{D_\psi\}$	Channel	$ M \{D_\psi\}$
$s_{1/2} + s_{1/2} \rightarrow$	1 {1.33}	$s_{1/2} + s_{1/2} \rightarrow$	1 {0.0988}
$p + p$	0 {1.33, 1.33}	$p_{1/2} + p_{1/2}$	0 {0.395, 0}
$s_{1/2} + s_{1/2} \rightarrow$	1 {0.346}	$s_{1/2} + s_{1/2} \rightarrow$	1 {0.543}
$p_{1/2} + p_{3/2}$	0 {0.444, 0.0494}	$p_{3/2} + p_{3/2}$	0 {0.84, 0.444}
$p_{1/2} + p_{1/2} \rightarrow$	1 {0.0988}	$p_{1/2} + p_{1/2} \rightarrow$	1 {0.346}
$s_{1/2} + s_{1/2}$	0 {0.395, 0}	$s_{1/2} + d_{3/2}$	0 {0.444, 0.0494}
$p_{1/2} + p_{1/2} \rightarrow$	1 {0.543}	$p_{3/2} + p_{3/2} \rightarrow$	3 {0}
$d_{3/2} + d_{3/2}$	0 {0.84, 0.444}	$s_{1/2} + s_{1/2}$	2 {0, 0}
			1 {0.543, 0, 0}
			0 {0.84, 0.444, 0, 0}
$p_{3/2} + p_{3/2} \rightarrow$	3 {0}	$p_{3/2} + p_{3/2} \rightarrow$	3 {0.267}
$s_{1/2} + d_{3/2}$	2 {0.08, 0.00889}	$s_{1/2} + d_{5/2}$	2 {0.48, 0.0533}
	1 {0.0622, 0.0491, 0.00322}		1 {0.64, 0.0533, 0.16}
	0 {0.0494, 0.0178, 0, 0}		0 {0.693, 0.267, 0, 0}

etc...

Discussion

The higher angular momentum channels are generally anisotropic, and can have zero or small eigenvalues.

Walker & MS PRA (2008)

TABLE I. Relative interaction strengths for van der Waals interactions of Rydberg atoms, for various collision channels. The potential energy at distance R is the product $C_6 D_\psi / R^6$, which contains the effects of Zeeman degeneracy, with the overall C_6 coefficient [Eq. (37)] for a particular channel that depends only on the energy level structure and radial matrix elements. Cases where the j quantum number is not included in the channel description are the sum over fine-structure components of the final state.

Channel	$ M \{D_\psi\}$	Channel	$ M \{D_\psi\}$
$s_{1/2} + s_{1/2} \rightarrow$	1 {1.33}	$s_{1/2} + s_{1/2} \rightarrow$	1 {0.0988}
$p + p$	0 {1.33, 1.33}	$p_{1/2} + p_{1/2}$	0 {0.395, 0}
$s_{1/2} + s_{1/2} \rightarrow$	1 {0.346}	$s_{1/2} + s_{1/2} \rightarrow$	1 {0.543}
$p_{1/2} + p_{3/2}$	0 {0.444, 0.0494}	$p_{3/2} + p_{3/2}$	0 {0.84, 0.444}
$p_{1/2} + p_{1/2} \rightarrow$	1 {0.0988}	$p_{1/2} + p_{1/2} \rightarrow$	1 {0.346}
$s_{1/2} + s_{1/2}$	0 {0.395, 0}	$s_{1/2} + d_{3/2}$	0 {0.444, 0.0494}
$p_{1/2} + p_{1/2} \rightarrow$	1 {0.543}	$p_{3/2} + p_{3/2} \rightarrow$	3 {0}
$d_{3/2} + d_{3/2}$	0 {0.84, 0.444}	$s_{1/2} + s_{1/2}$	2 {0, 0}
			1 {0.543, 0, 0}
			0 {0.84, 0.444, 0, 0}
$p_{3/2} + p_{3/2} \rightarrow$	3 {0}	$p_{3/2} + p_{3/2} \rightarrow$	3 {0.267}
$s_{1/2} + d_{3/2}$	2 {0.08, 0.00889}	$s_{1/2} + d_{5/2}$	2 {0.48, 0.0533}
	1 {0.0622, 0.0491, 0.00322}		1 {0.64, 0.0533, 0.16}
	0 {0.0494, 0.0178, 0, 0}		0 {0.693, 0.267, 0, 0}

etc...

Förster zero states are linear combinations of Zeeman levels with zero coupling.

Consider $M=m_A+m_B=0$. Say initial states have angular momentum j , there are $2j+1$ states with $M=0$.

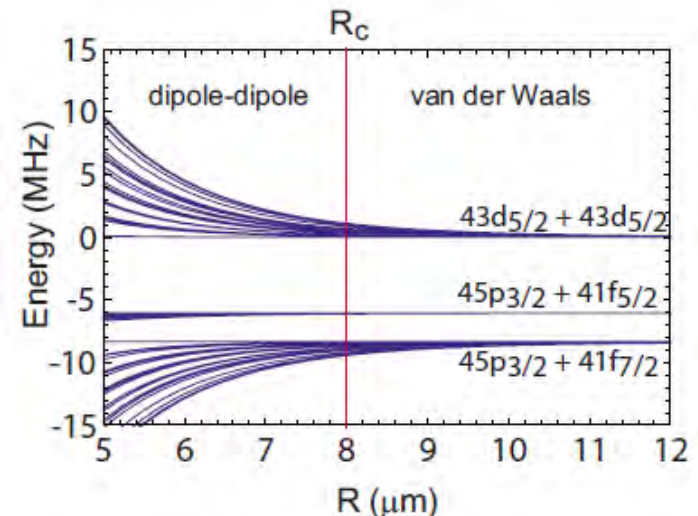
These couple to j_s, j_t with $j_s \leq j_t$, giving $2j_s + 1$ $M=0$ intermediate states

We get zero vdW coupling to the Förster zero state $|\psi_F\rangle$ when

$$\langle st|V_{dd}|\psi_F\rangle = \sum_{J=0}^{2j} \langle st|V_{dd}|J\rangle \langle J|\psi_F\rangle = 0 \quad \text{for all } 2j_s + 1 \text{ coupled states}$$

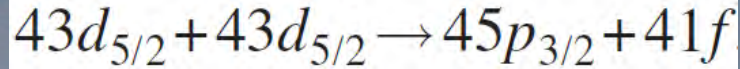
This is $2j_s + 1$ equations for $2j+1$ unknowns. A Förster zero solution typically exists when $j_s < j$.

When $j_s = j$, no exact zero, but we always find very small eigenvalues.



Angular structure examples

The $43d_{5/2}$ state has a small defect and very strong interaction.



Energy defect 7.5 MHz.

There are Förster zero states, so strong angular dependence.

We need to go to 55s to get a comparable strength isotropic interaction.

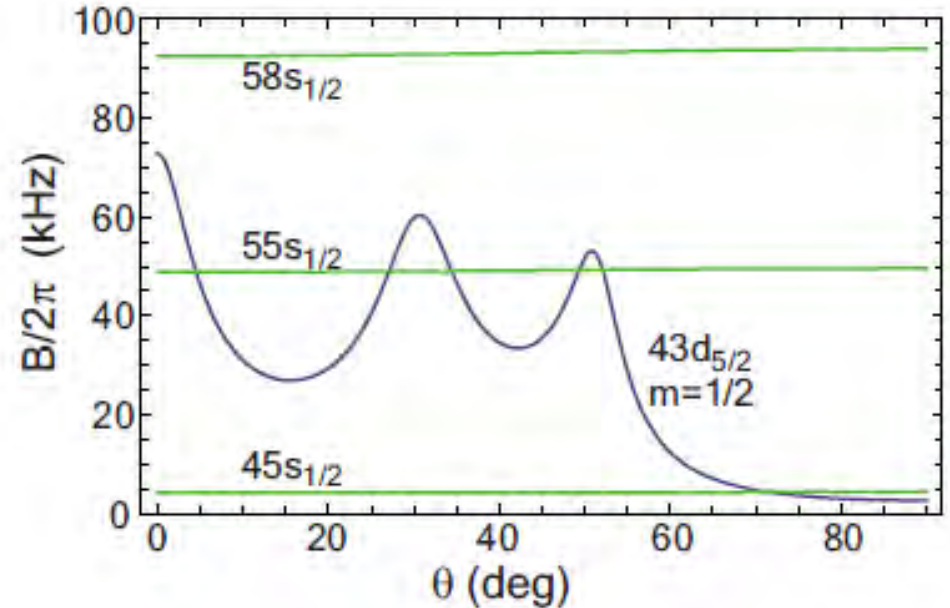
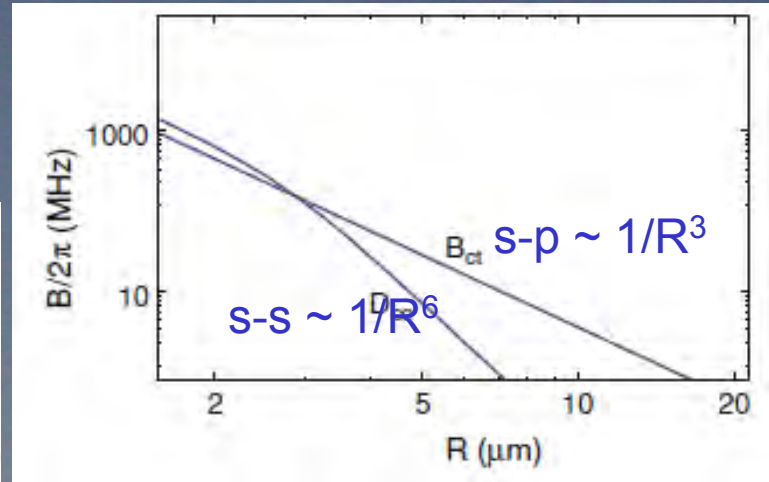


FIG. 10. (Color online) Angular dependence of blockade shift for $43d_{5/2}, m=1/2, 45s_{1/2}, 55s_{1/2},$ and $58s_{1/2}$ at $R=10 \mu\text{m}$ with θ the angle between the molecular axis and \hat{z} .

Angular structure examples

States with $||l-l'|=1$ have a strong resonant interaction. If one of them is an s state the interaction is largely isotropic.

Fig. 6 The blockade B_{cf} and interaction D_{cc} strengths for control atom in $|s\rangle = |60p_{3/2}, m = 1/2\rangle$ and target atom in $|r\rangle = |60s_{1/2}, m = 1/2\rangle$ states



We can also have large asymmetries between s-s, s-p and p-p, interaction strengths. Very useful for various quantum gate protocols.

L. Isenhower, M. Saffman, and K. Mølmer, *Quant. Inf. Proc.* **10**, 755 (2011).

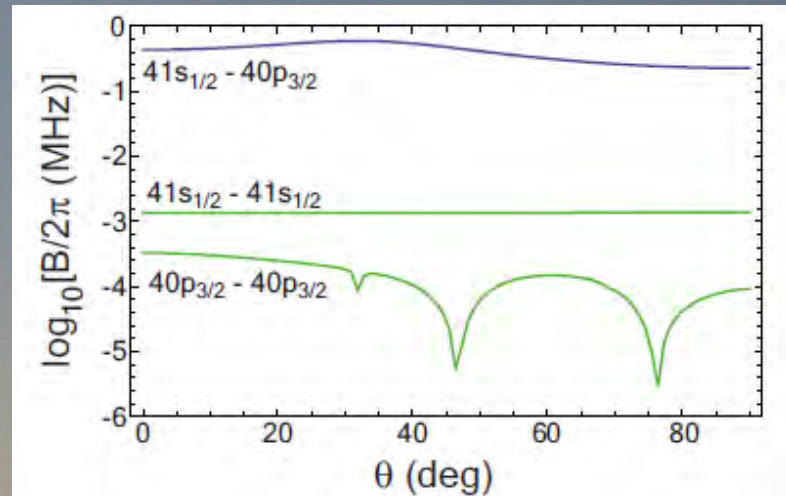
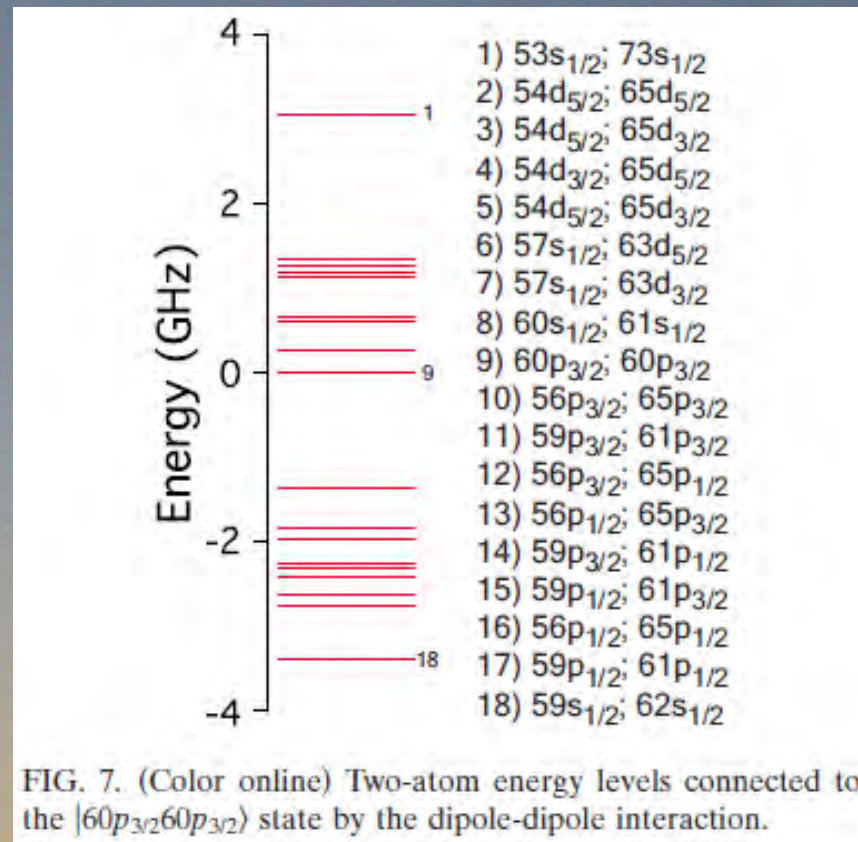


FIG. 11. (Color online) Comparison of the blockade shift B at $R = 10 \mu\text{m}$ for interacting Rb $41s_{1/2} - 40p_{3/2}$ atoms as compared to van der Waals blockade for two $41s_{1/2}$ or $40p_{3/2}$ atoms. All atoms have magnetic quantum number $m = 1/2$.

Discussion

This analysis assumes a single channel dominates. At high n and small separation this is not a good approximation.

There are 18 dipole coupled pairs of states within ± 4 GHz of $60p_{3/2}+60p_{3/2}$.



Discussion

However, not all near resonant states play a role since the dipole matrix elements are concentrated at neighboring n, n' .

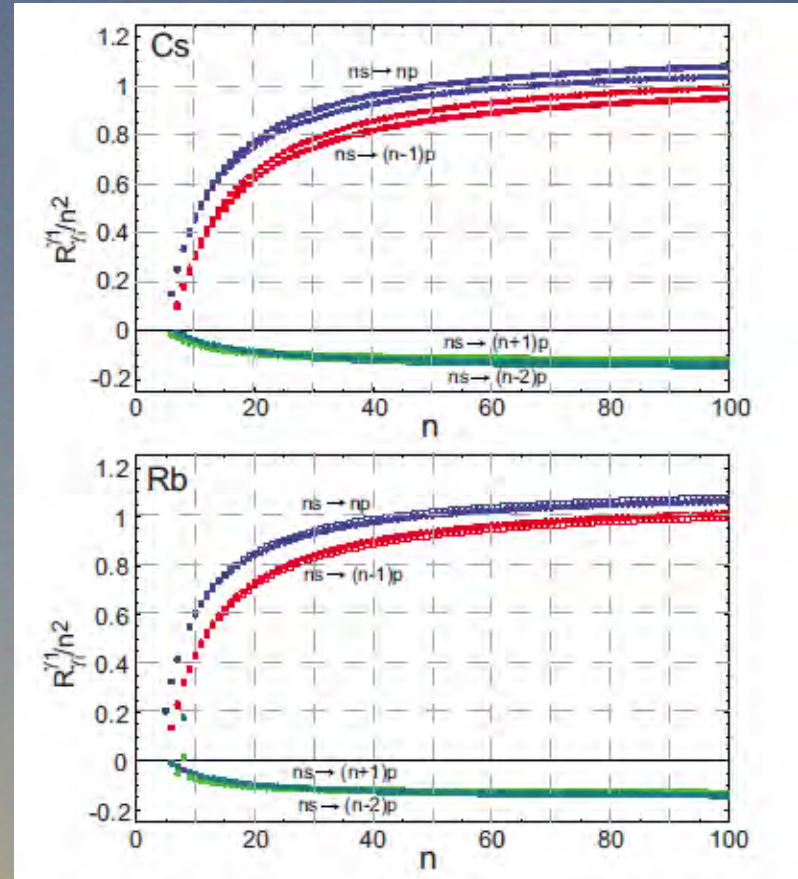
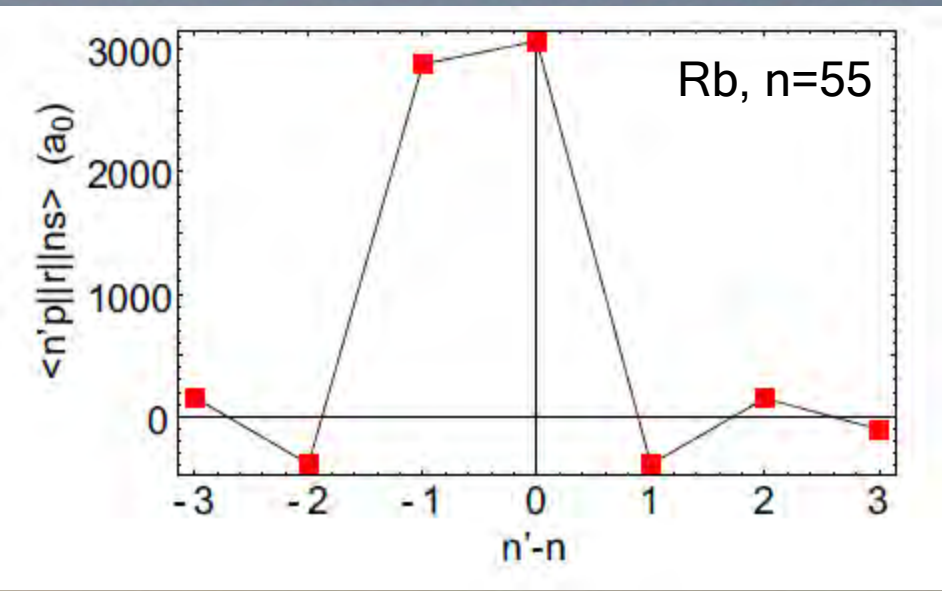


FIG. 4. (Color online) Radial matrix elements divided by n^2 for transitions $ns_{1/2} \rightarrow n_p p_{3/2}$ (filled circles) and $ns_{1/2} \rightarrow n_p p_{1/2}$ (filled boxes) in Cs and Rb, in atomic units.

Discussion

When multiple channels play a role it is easiest to use direct numerical diagonalization of the Hamiltonian. Easy to include Zeeman, Stark effects.

$$H = H_{\text{atomic}} + H_{\text{dd}} + H_{\text{Stark}} + H_{\text{Zeeman}}$$

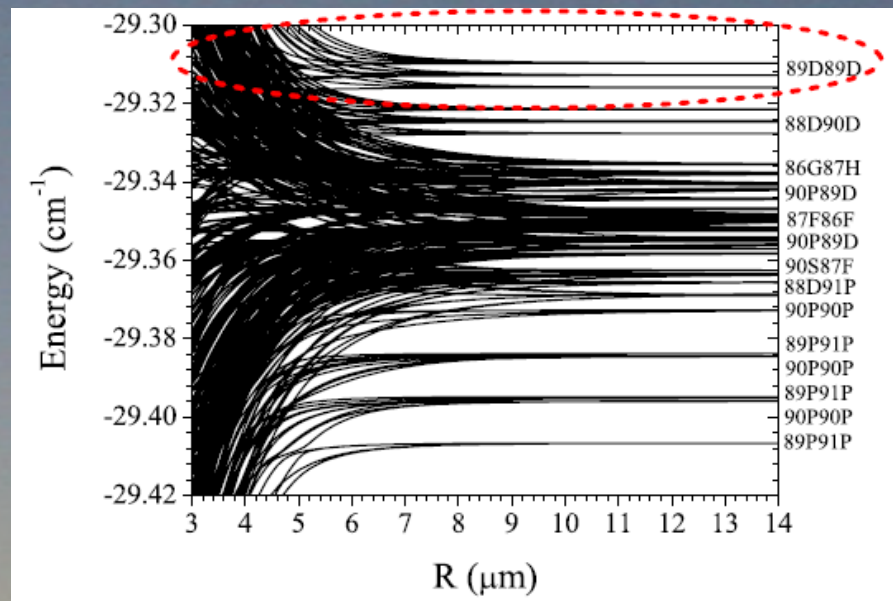
Spaghetti physics ensues. It appears highly unlikely that Förster zero interactions persist.

PHYSICAL REVIEW A 74, 020701(R) (2006)

Cold Cs Rydberg-gas interactions

Arne Schwettmann, Jeff Crawford, K. Richard Overstreet, and James P. Shaffer

FIG. 1. (Color online) Overview of the pair potentials of the $89D89D$ and surrounding states for zero background E field. Labels are zero-field labels. The $89D89D$ potentials are circled.



Including enough states to ensure convergence is an open problem (I. Deutsch).

Calculating matrix elements

As for optical excitation there are several calculation methods available.

Semi-classical (WKB) (my favorite Kaulakys, J. Phys. B, 28, 4963 (1995))
Coulomb wave functions (Seaton)
Model potentials

Review: D.P. Dewangan, Physics Reports 511 (2012) 1-142

Numerics are more challenging than for excitation from ground state since both wavefunctions are spatially extended.

For excitation from ground state we had x2 discrepancy.

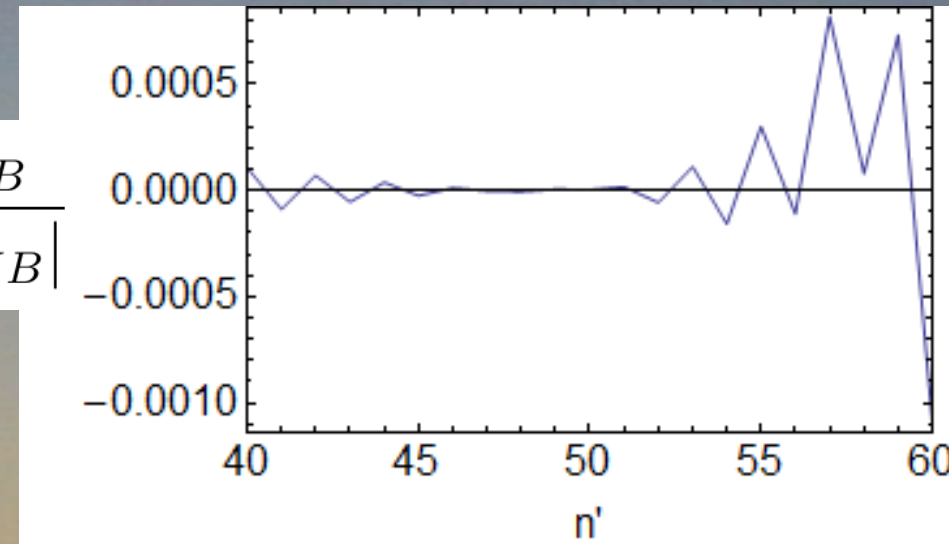
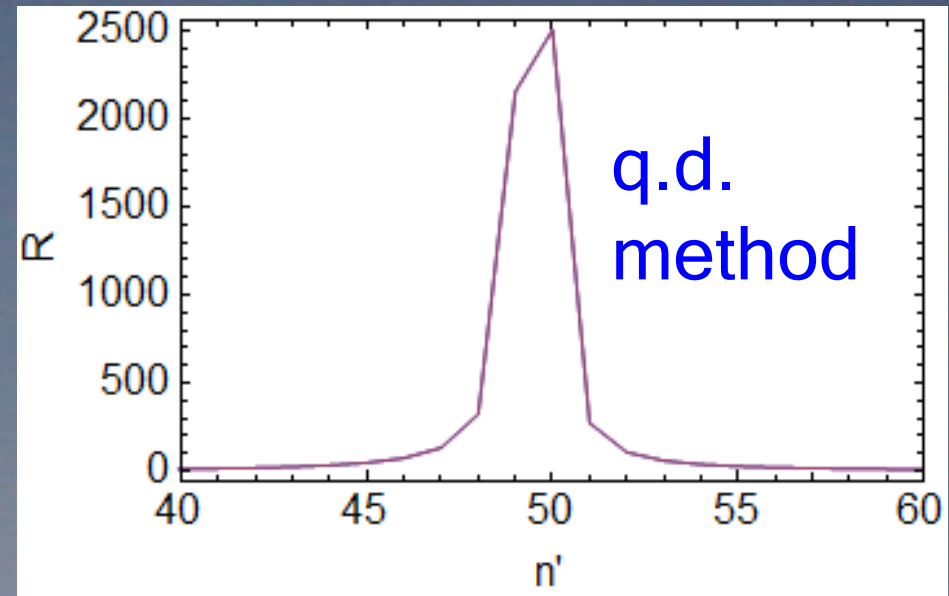
In this case WKB agrees very well with Coulomb wavefunctions.

Coulomb – WKB comparison

Radial matrix element
50s - n' p_{1/2}

Error :

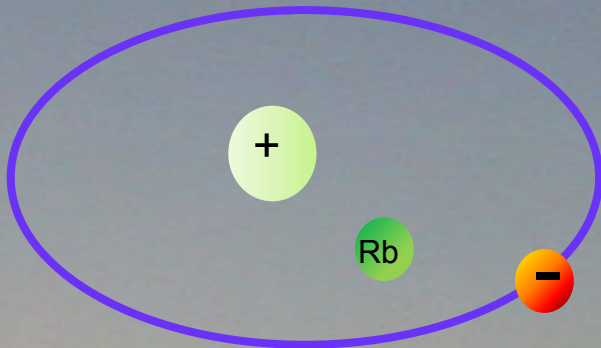
$$\frac{R_C - R_{WKB}}{|R_C| + |R_{WKB}|}$$



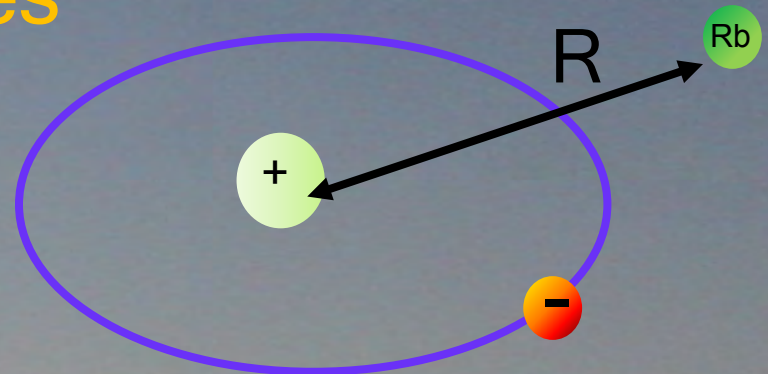
Ground-Rydberg interactions

- For $n \sim 100$ Rydberg-Rydberg interaction is stronger than ground-ground mag. dip. by 10^{12} , ground-ground vdW by 10^{17} at $1 \mu\text{m}$.
- What about Rydberg-ground? Guess 3×10^8 stronger than ground-ground vdW.

Two cases



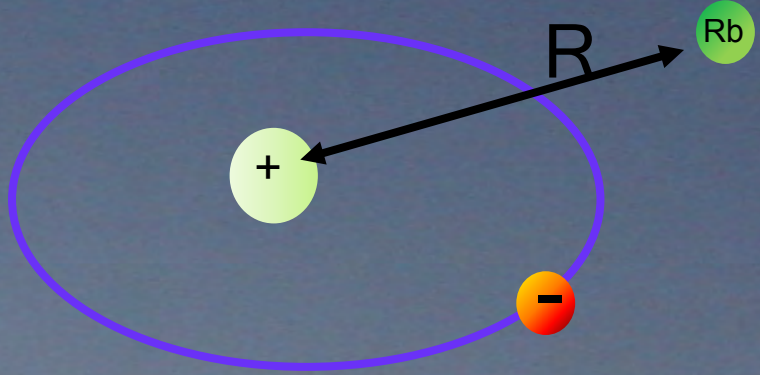
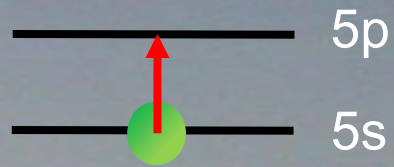
Ground perturber inside
Rydberg wavefunction -
molecular binding
(T. Pfau lectures)



perturber outside,
 $R > a_0 n^2$
Van der Waals interaction

Ground-Rydberg interactions

We can calculate using same method as for Rydberg-Rydberg



Förster defect is essentially the 5s-5p splitting 12820 cm^{-1}

Putting in the matrix elements we find

$$C_6(100s-5s) \sim 17 \text{ (Hz } \mu\text{m}^6)$$

The ground-ground vdW is

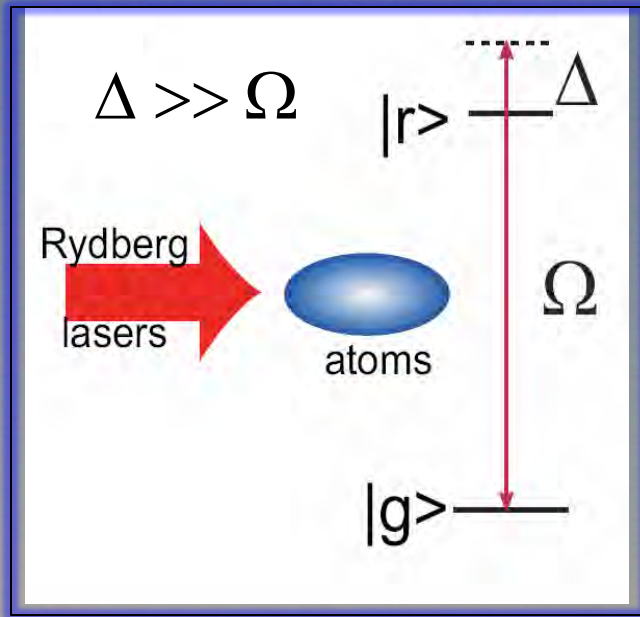
$$C_6(5s-5s) \sim 0.64 \times 10^{-6} \text{ (Hz } \mu\text{m}^6)$$

The ratio is 0.27×10^8

This interaction is of relevance to high density/high precision experiments.

Rydberg dressing of ground state interactions

If the excitation is off-resonant the ground state atoms will be “dressed” by the Rydberg interaction.



original proposal:

VOLUME 85, NUMBER 9

PHYSICAL REVIEW LETTERS

28 AUGUST 2000

Bose-Einstein Condensation in Trapped Dipolar Gases

L. Santos,¹ G. V. Shlyapnikov,^{1,2,3} P. Zoller,^{1,4} and M. Lewenstein¹

details for few atoms:

PHYSICAL REVIEW A **82**, 033412 (2010)

Interactions between Rydberg-dressed atoms

J. E. Johnson and S. L. Rolston

Relevant for nonlinear optics, atom-optics, Quantum simulation of spin models

Effective interaction

- To find the effective nonlocal interaction consider two-atoms in the basis

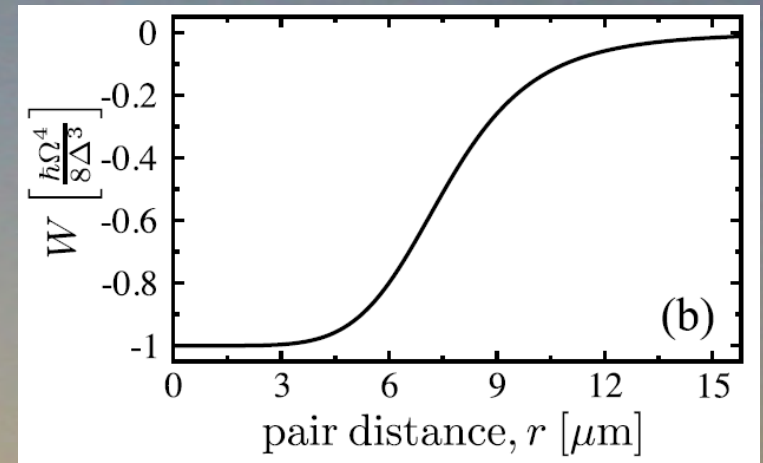
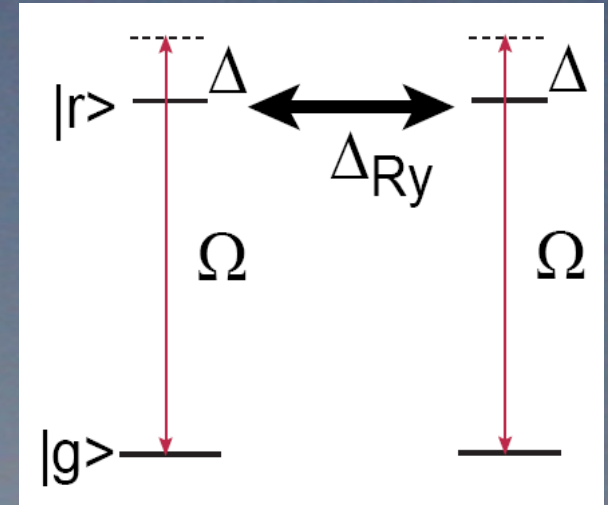
$$\{|gg\rangle, |gr\rangle, |rg\rangle, |rr\rangle\}$$

Interaction picture Hamiltonian

$$\hat{\mathcal{H}} = \frac{\hbar}{2} \begin{pmatrix} 0 & \Omega^* & \Omega^* & 0 \\ \Omega & -2\Delta & 0 & \Omega^* \\ \Omega & 0 & -2\Delta & \Omega^* \\ 0 & \Omega & \Omega & 2(-2\Delta + \Delta_{Ry}) \end{pmatrix}$$

Eigenvalues give the effective interaction potential.

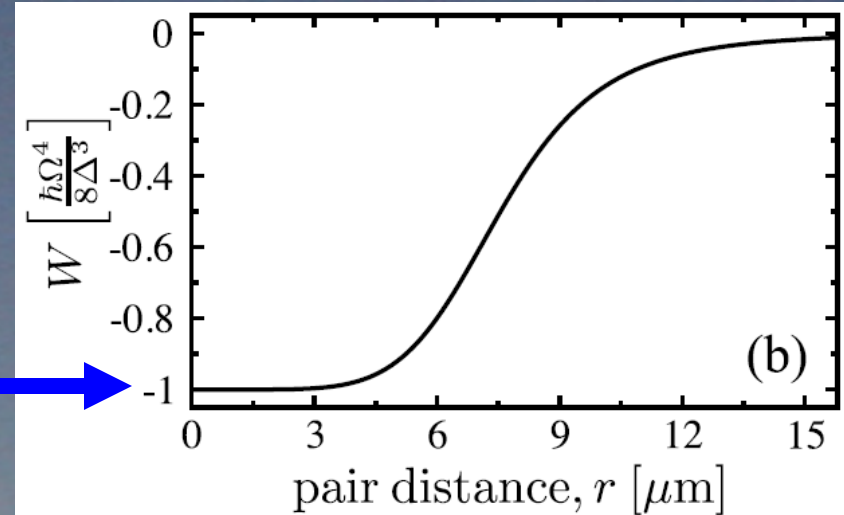
Soft core form due to blockade.



Effective interaction

We can find the soft core interaction strength without solving the Hamiltonian

$$-\frac{|\Omega|^4}{8\Delta^3}$$



Two noninteracting atoms have

$$\Delta_{\text{LS}2} = 2\frac{|\Omega|^2}{4\Delta}$$

Due to blockade only get

$$\Delta_{\text{LS}1} = \frac{|\Omega|^2}{4\Delta}$$

Interaction effect

$$\Delta_{\text{LS}1} - \Delta_{\text{LS}2} = -\frac{|\Omega|^2}{4\Delta}$$

Admixture of Rydberg in ground state

$$\frac{|\Omega|^2}{2\Delta^2}$$

Multiply

$$-\frac{|\Omega|^4}{8\Delta^3}$$

Summary

- Rydberg states have extraordinarily strong interactions.
- The interaction can be transferred to the ground states by dressing
- When one channel is dominant the problem can be solved more or less analytically
- For multiple channels numerics are best suited
- The Rydberg dipole-dipole interaction has been observed in experiments with many atoms: frozen Rydberg gas, line broadening, blockade (T. Gallagher lectures)
- The interaction is crucial for quantum gate experiments (O. Morsch lectures) and recent single photon experiments
- A quantitative observation of the dipole-dipole shift at the level of two atoms remains an outstanding challenge.

III: Coherence properties of ground and Rydberg traps

- Optical traps and ground state (qubit) coherence
- Ramsey spectroscopy
- magic traps
- traps for Rydberg atoms
- 3D Rydberg atom trapping

Traps and coherence

Long coherence times compared to gate times or other dynamical times are important for studies of quantum dynamics

Several decoherence mechanisms:

collisional loss - about 50 s. lifetime at 10^{-10} mbar

radiative decay

light scattering

magnetic noise

electric fields

AC electric field in optical traps

motional dephasing

Types of traps:

Electric

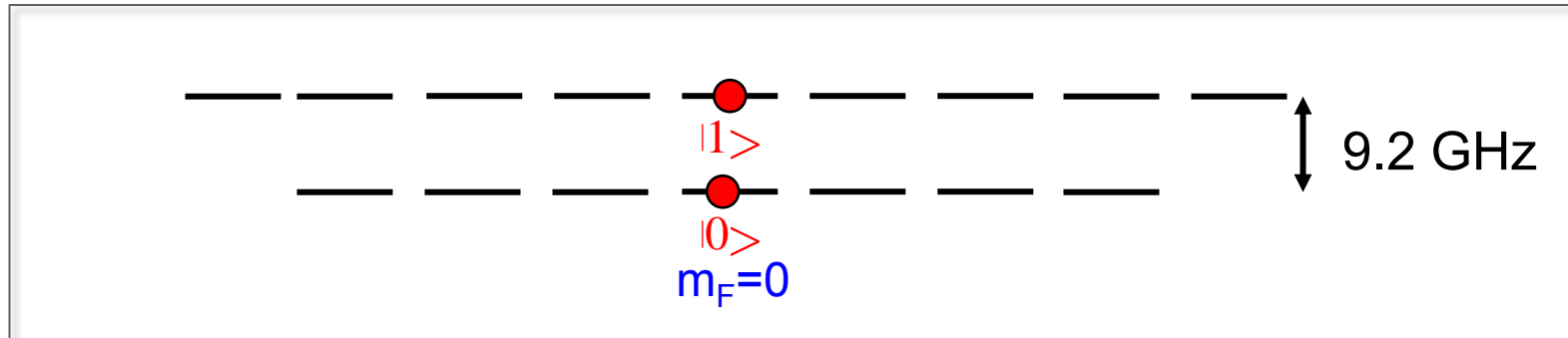
Magnetic

Optical

Optical in cavities
or near surfaces

Radiative decay

For optical qubits metastable upper level has a finite radiative lifetime,
e.g. 160 s for Sr 3P_0

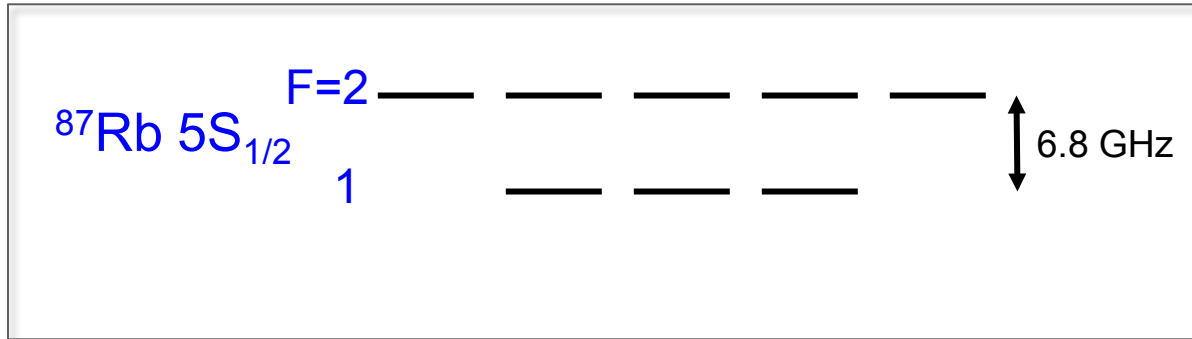
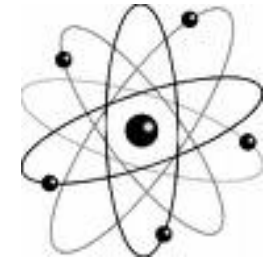


For hyperfine qubits the radiative lifetime is not of concern.
For Cs the lifetime is

T=0	23,300 years
T=300 K	34 years

In a giga-qubit room temperature Cs computer 1 decay per second
(QEC is needed!)

Magnetic decoherence



$$\Delta U_{F=2} = \frac{3A}{4}$$

$$\Delta U_{F=1} = -\frac{5A}{4}$$

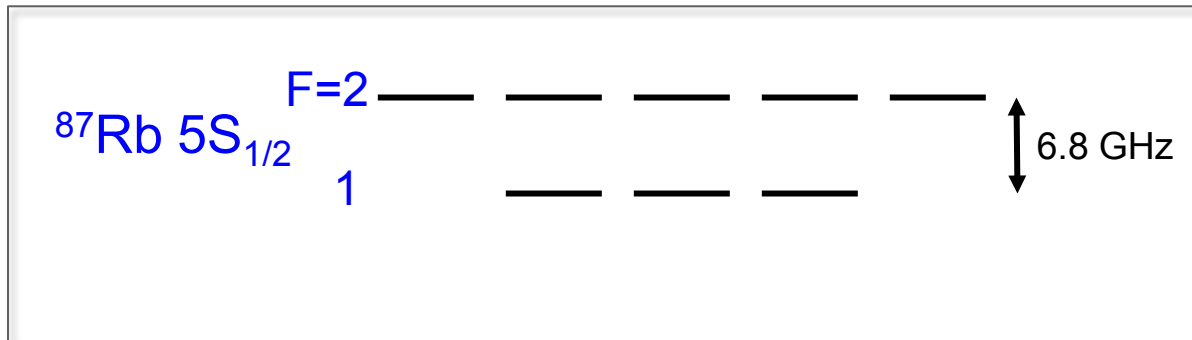
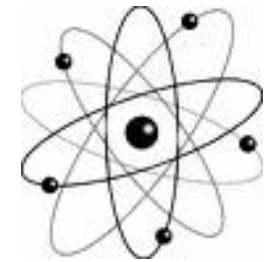
$$A = 3.417 \text{ GHz}$$

Ground state, single unpaired electron, $L=0$, $S=1/2$, $J=1/2$

Nucleus, ^{87}Rb $I=3/2$, so total angular momentum $F=1,2$.

$$\hat{H} = A\hat{\mathbf{I}} \cdot \hat{\mathbf{J}} \quad \Delta U_{\text{hf}} = \frac{A}{2} [F(F+1) - I(I+1) - J(J+1)]$$

Breit-Rabi plot

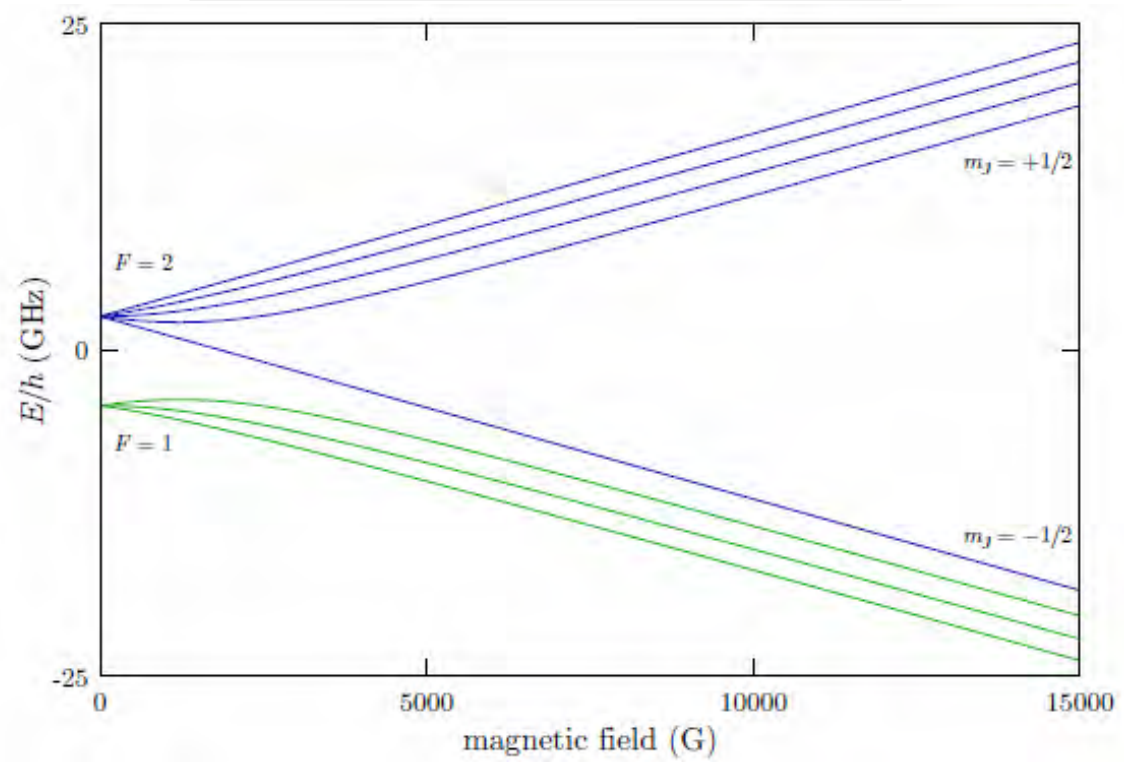


$$\Delta U_{F=2} = \frac{3A}{4}$$

$$\Delta U_{F=1} = -\frac{5A}{4}$$

$$A = 3.417 \text{ GHz}$$

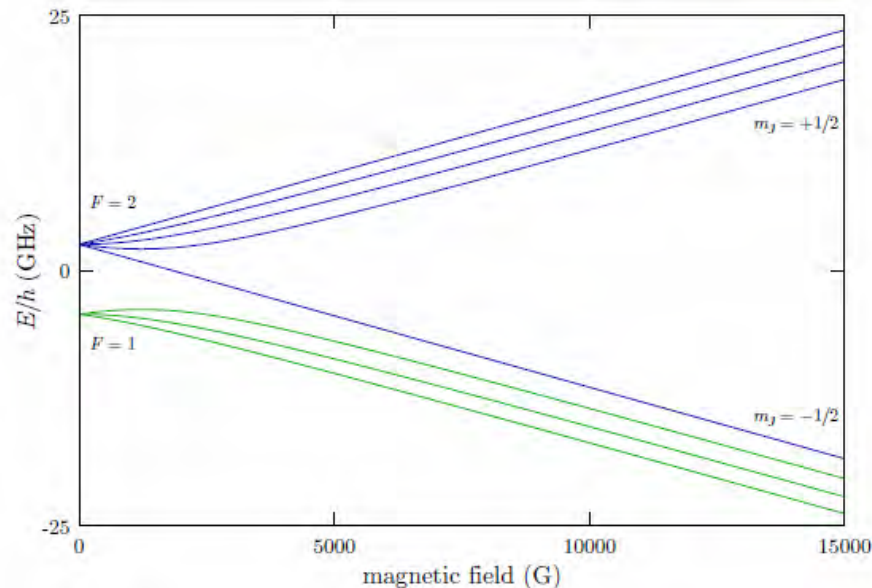
$$\hat{H} = A\hat{\mathbf{I}} \cdot \hat{\mathbf{J}} + \frac{\mu_B}{\hbar} (g_s\hat{\mathbf{S}} + g_l\hat{\mathbf{L}} + g_I\hat{\mathbf{I}}) \cdot \mathbf{B}$$



Magnetostatic traps

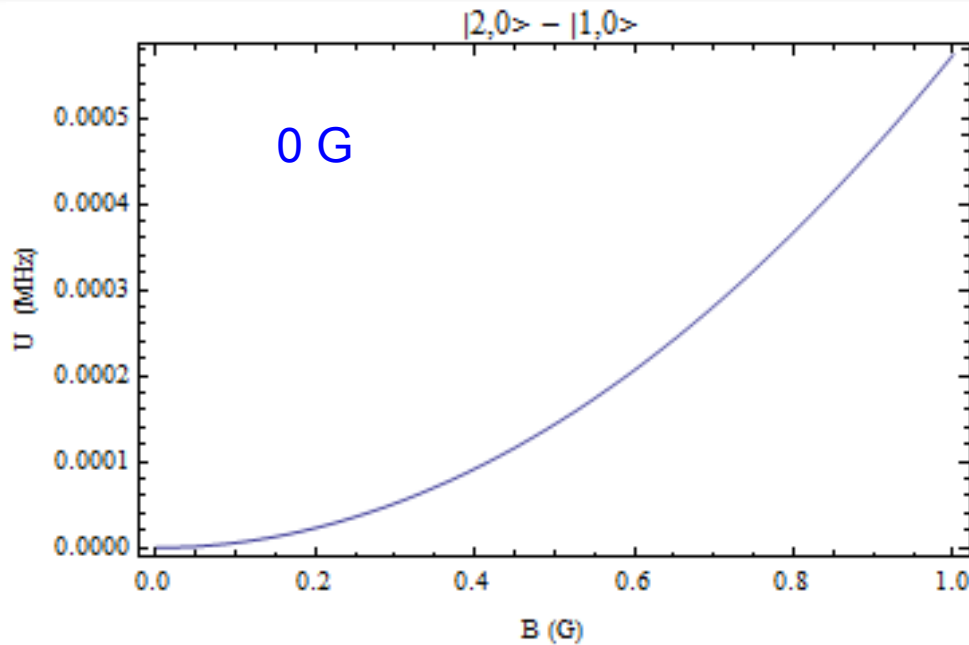
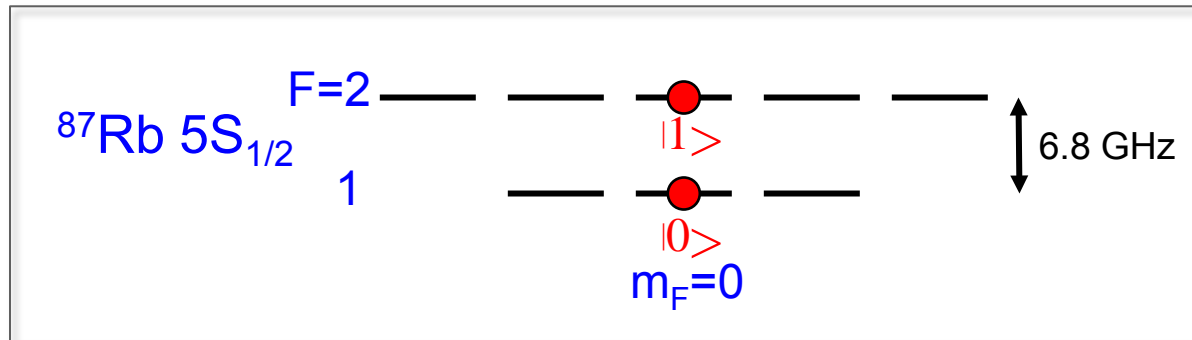
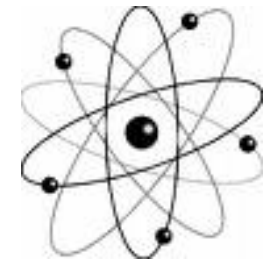
There are weak (magnetic) field seeking ground states.

^{87}Rb $|1,-1\rangle$, $|2,1\rangle$, $|2,2\rangle$



This is widely used for experiments with degenerate quantum gases, BEC and Fermi systems.

Fluctuation insensitive qubit trapping



$$\omega_{ba} = \omega_{\text{hf}} \left[1 + \left(\frac{(g_S - g_I)\mu_B \delta B}{\hbar \omega_{\text{hf}}} \right)^2 \right]^{1/2}$$

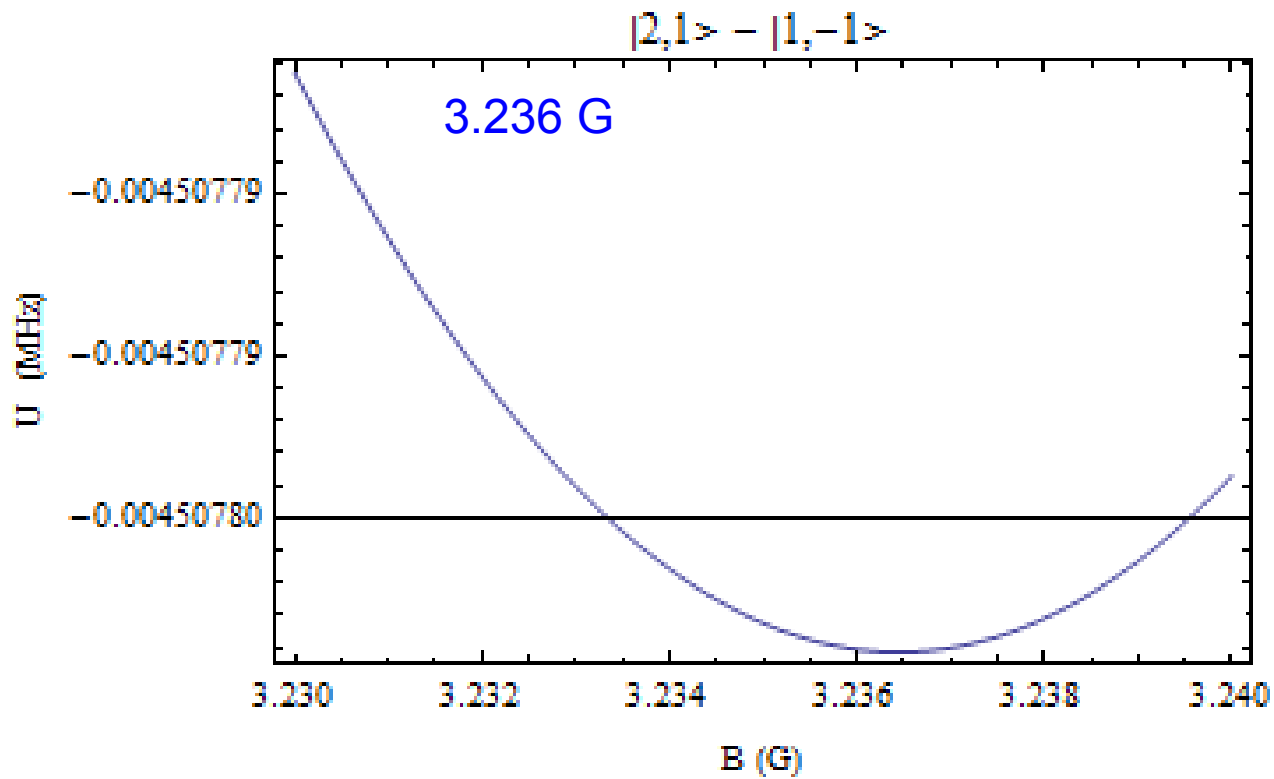
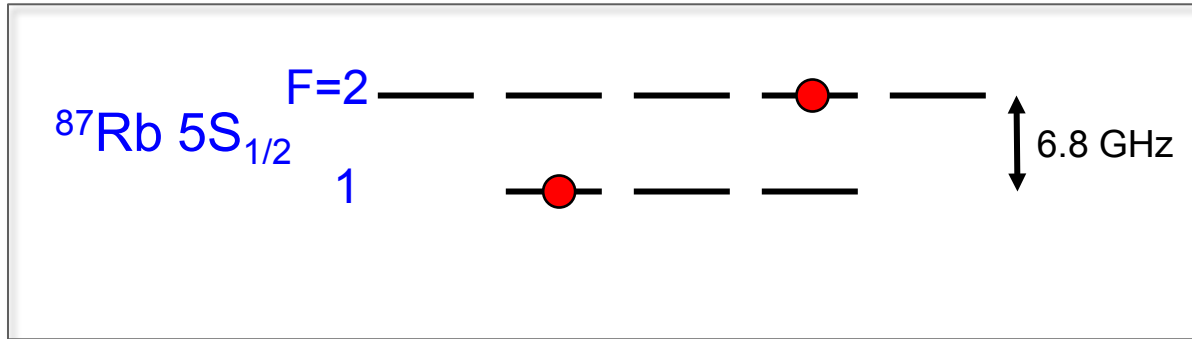
$$\frac{1}{\pi^2} \frac{\mu_B^2 B_0}{\hbar^2 \nu_{\text{hf}}} \quad \text{Hz/T.}$$

1.14 Hz/mG at 1 G bias field

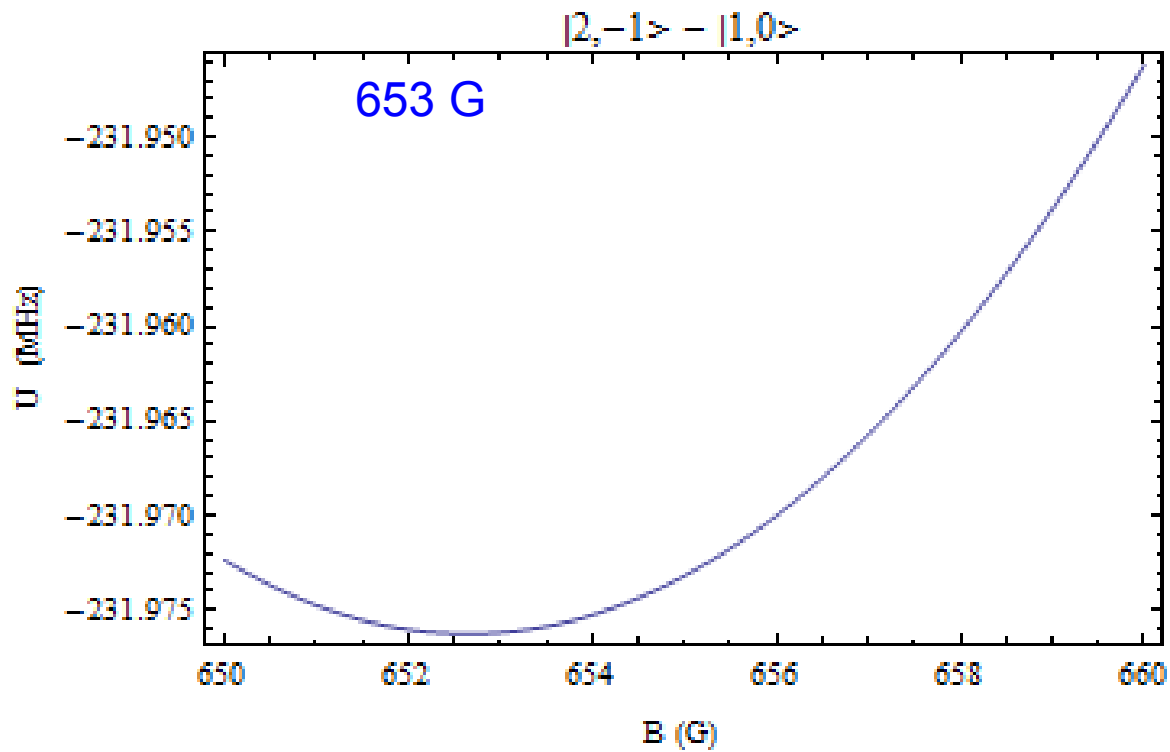
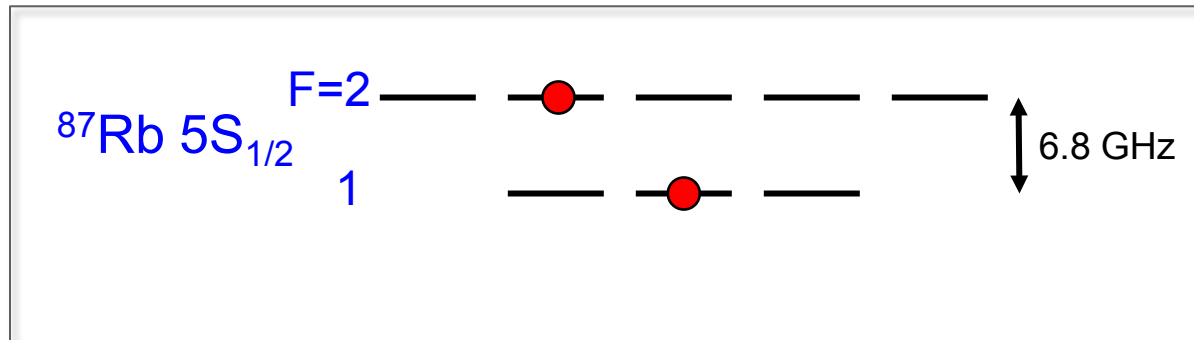
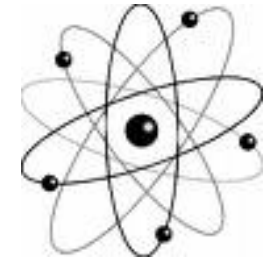
At zero B field $m=0$ Zeeman states are ideal qubits.

Bias field needed to define quantization axis.

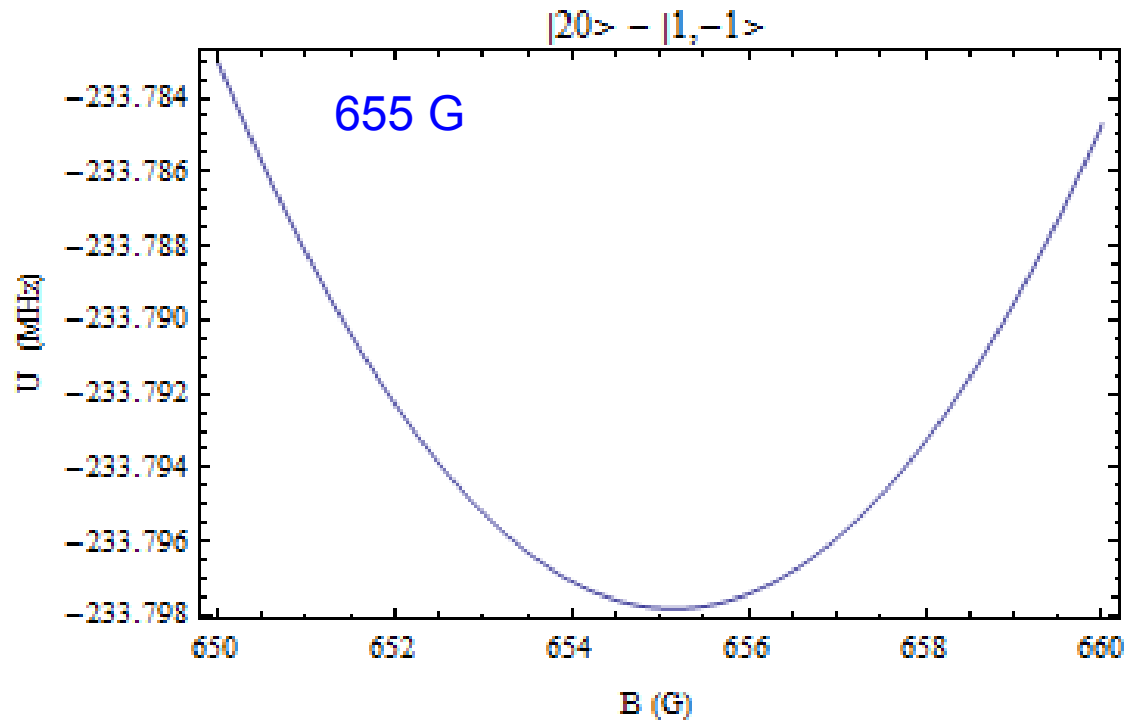
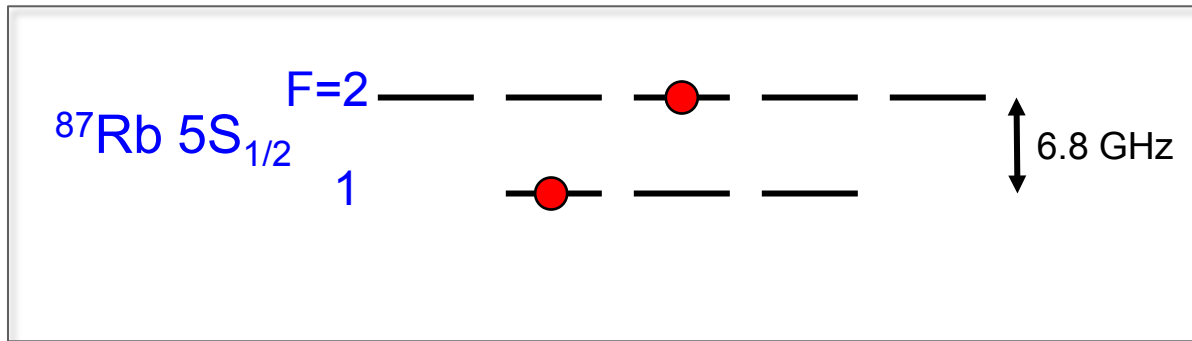
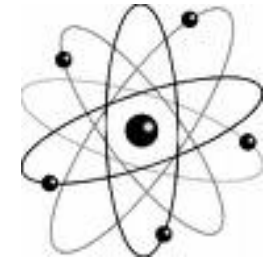
Fluctuation insensitive qubit trapping



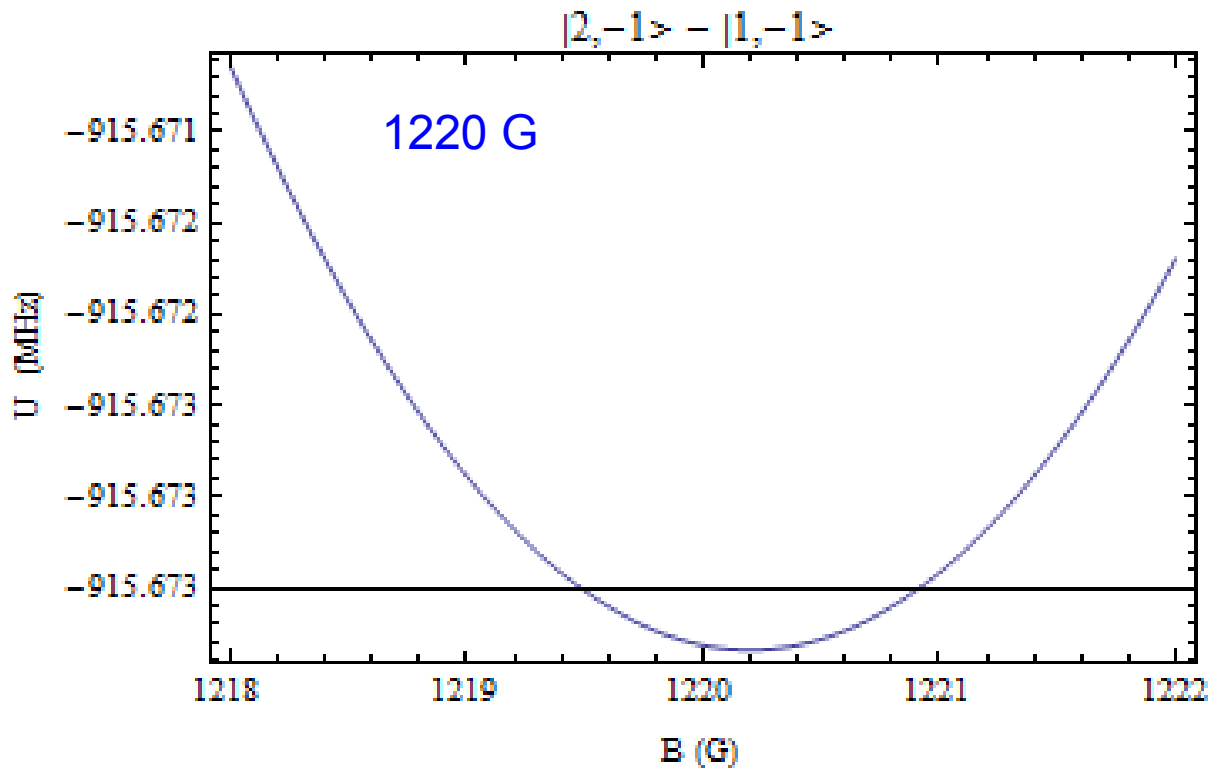
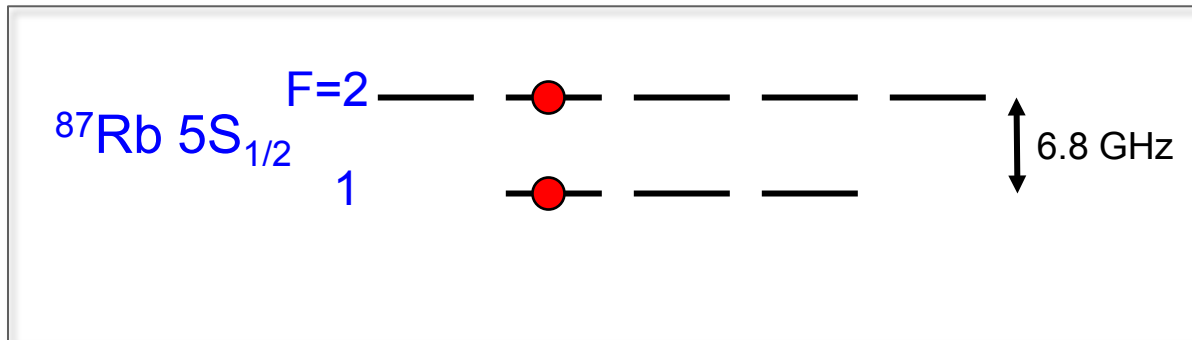
Fluctuation insensitive qubit trapping



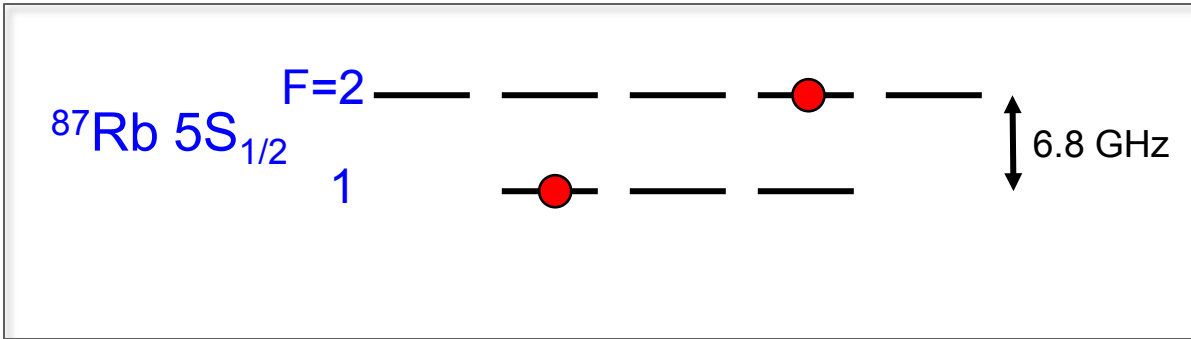
Fluctuation insensitive qubit trapping



Fluctuation insensitive qubit trapping



Long coherence time magnetically trapped atoms



3.236 G bias field

Coherence in Microchip Traps

Philipp Treutlein,^{*} Peter Hommelhoff,[†] Tilo Steinmetz, Theodor W. Hänsch, and Jakob Reichel

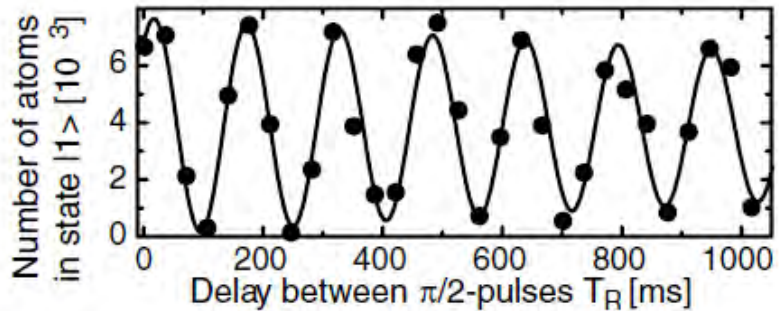
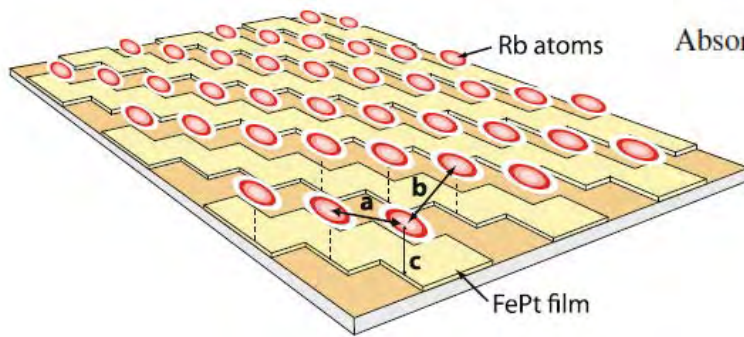
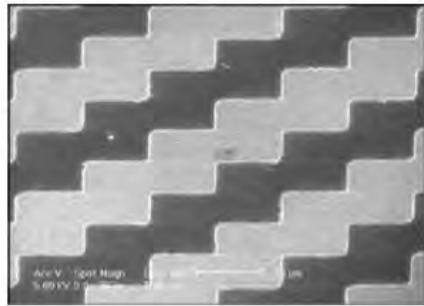


FIG. 1. Ramsey spectroscopy of the $|0\rangle \leftrightarrow |1\rangle$ transition with atoms held at a distance $d = 9 \mu\text{m}$ from the chip surface. An exponentially damped sine fit to the Ramsey fringes yields a $1/e$ coherence lifetime of $\tau_c = 2.8 \pm 1.6 \text{ s}$. Each data point corresponds to a single shot of the experiment.

Magnetostatic trap arrays



Absorption image of the loaded lattice, showing ~ 500 traps loaded with 200–2500 atoms each

Periodicity about $20 \mu\text{m}$

**Microtrap arrays on magnetic film atom chips
for quantum information science**

V. Y. F. Leung · A. Tauschinsky ·
N. J. van Druten · R. J. C. Spreeuw

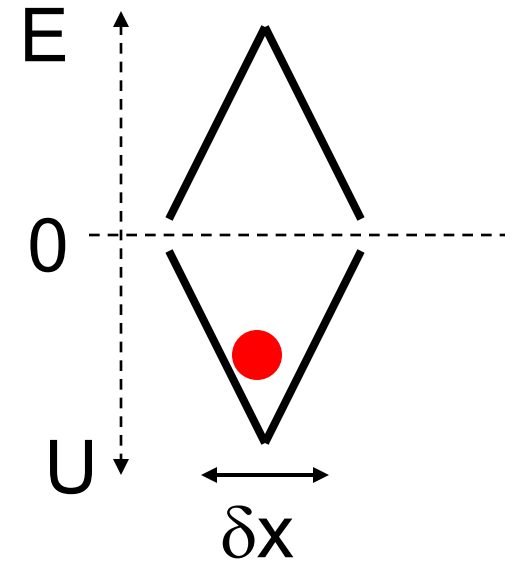
Quantum Inf Process (2011) 10:955–974

also, Hannaford, Hinds

Electrostatic traps

Cs has a dc polarizability $\alpha = +1.0 \times 10^{-5} \text{ Hz}/(\text{V}/\text{m})^2$
giving a potential

$$U = -\frac{1}{2}\alpha E^2$$



Potential minimum at field maximum.

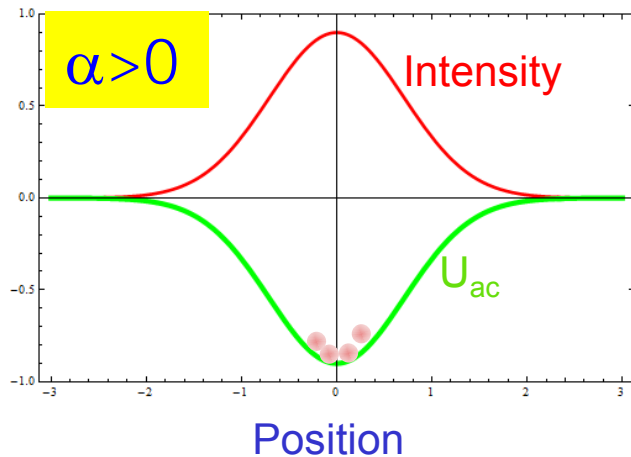
General property of harmonic functions – no maximum inside simply connected domain. (Earnshaw theorem)

No electrostatic traps for atomic ground states.

Optical traps for atoms

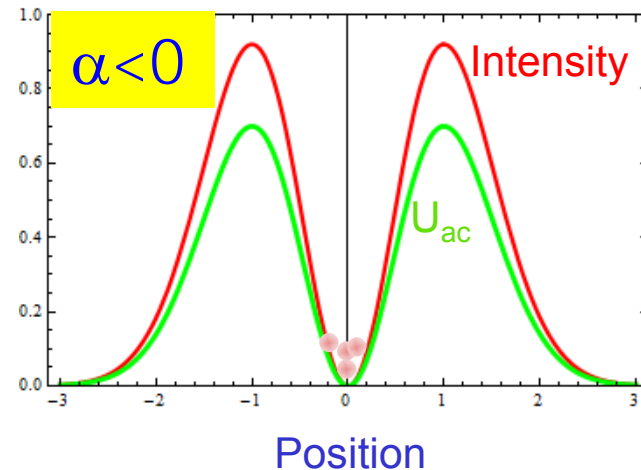
- Far off-resonance traps (FORTs): sub-micron localization, long coherence times.

- red detuned
 $\Delta = \omega - \omega_a < 0$



- + simple optics
- more light scattering and differential light shifts

- blue detuned
 $\Delta = \omega - \omega_a > 0$



- more complex optics
- + less light scattering and differential light shifts
- + Rydberg trapping

Light shifts – AC Stark effect

An off-resonant optical field shifts the energy of atomic levels. This is important for optical traps, Z gates, and decoherence.

Electric dipole interaction $\hat{H} = -\hat{\mathbf{d}} \cdot \mathbf{E}$

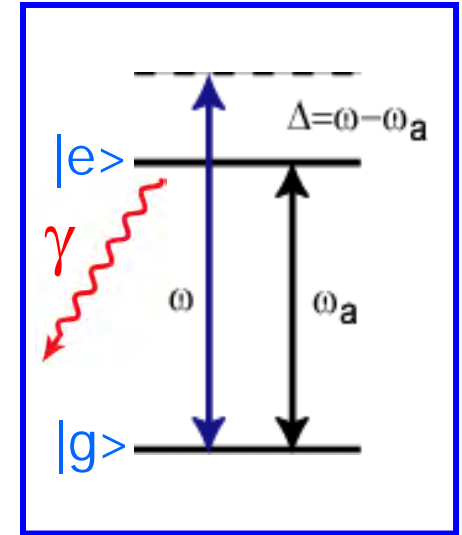
To first order $d_{gg} = \langle g | \hat{\mathbf{d}} | g \rangle = 0$

However, if we go to second order in the field we get a nonzero d_{gg} . Write this as $d_{gg} \equiv \mathbf{d} = \alpha \mathbf{E}$

Then

$$U_{\text{ac}} = \langle \hat{H} \rangle = -\langle \hat{\mathbf{d}} \cdot \mathbf{E} \rangle = -\langle \hat{\alpha} \cdot \mathbf{E}^2 \rangle = \boxed{-\frac{1}{4} \alpha \mathcal{E}^2}$$

with α the polarizability.

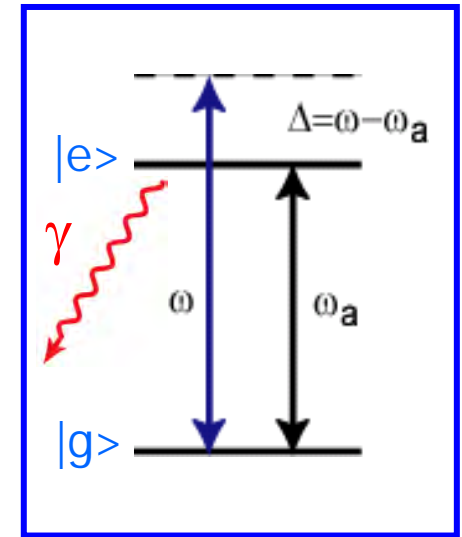


Calculation of α

Use second order perturbation theory:

$$U_{ac} = \sum_e \frac{\langle e | \hat{H} | g \rangle|^2}{U_g - U_e}$$

$$= \sum_e \frac{\mathbf{E} \cdot \langle g | \hat{\mathbf{d}} | e \rangle \langle e | \hat{\mathbf{d}} | g \rangle \cdot \mathbf{E}}{(\hbar\omega_g + \hbar\omega) - \hbar\omega_e}$$



The interaction involves two powers of the vector \mathbf{d} , so in general α is a 2nd rank tensor with scalar, vector, and tensor parts.

Let's just consider the scalar polarizability. Two-level model, RWA

$$U_{ac} = \frac{\hbar^2 |\Omega|^2}{4(\hbar\omega_g + \hbar\omega) - \hbar\omega_e} = \frac{\hbar |\Omega|^2}{4\Delta}$$

$$\langle e | \hat{\mathbf{d}} | g \rangle \cdot \mathbf{E} = \frac{\hbar\Omega}{2}$$

The polarizability is

$$U_{ac} = -\frac{1}{4} \alpha \mathcal{E}^2 \quad d^2 = \frac{3\pi\epsilon_0 c^3 \hbar \gamma}{\omega_a^3}$$

$$\alpha_{\text{two-level}} = -\frac{3\pi\epsilon_0 c^3}{\omega_a^3} \frac{\gamma}{\Delta}$$

Light scattering

Photon scattering rate is

$$r = \rho_{ee}\gamma$$

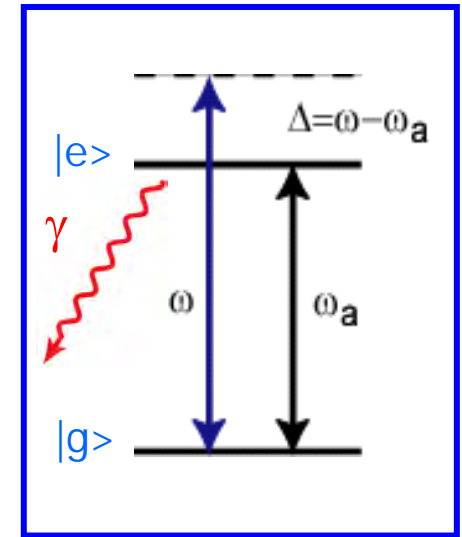
Excited state population

$$\rho_{ee} = \frac{1}{2} \frac{I/I_s}{1 + 4\frac{\Delta^2}{\gamma^2} + \frac{I}{I_s}}$$

so

$$r = \frac{\gamma}{2} \frac{I/I_s}{1 + 4\frac{\Delta^2}{\gamma^2} + \frac{I}{I_s}} \rightarrow \frac{\gamma}{8(\Delta^2/\gamma^2)} \frac{I}{I_s}$$

(large detuning)



We see that

trap depth $\sim \boxed{1/\Delta}$ scattering rate $\sim \boxed{1/\Delta^2}$

At large detunings we have near ideal conservative traps.

Light scattering and spin relaxation

If we store a hyperfine qubit in an optical trap
Rayleigh scattering gives heating but largely
preserves the quantum state.

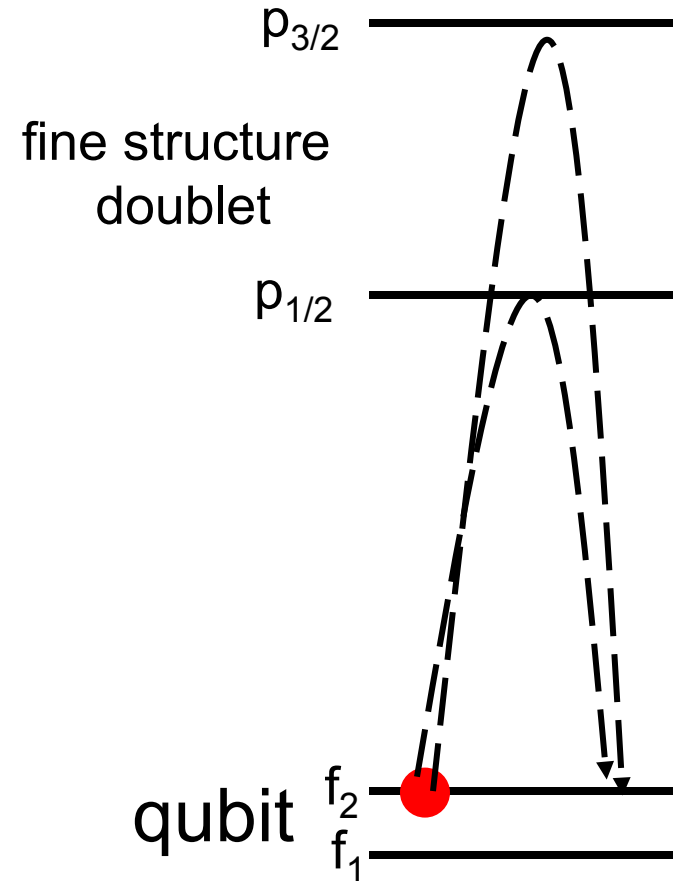
Raman scattering changes the quantum state.

The amplitudes for Rayleigh scattering add.
Rayleigh rate $\sim 1/\Delta^2$.

For Raman scattering (f_1 to f_2) they cancel
giving Raman rate $\sim 1/\Delta^4$.

Qualitative explanation. At large detuning
compared to the fine structure splitting the alkali
atom looks like a spin $1/2$ particle, no tensor
polarizability quantum state is preserved.

Also require linear light polarization to suppress
vector polarizability.



Spin relaxation of optically trapped atoms by light scattering

R. A. Cline, J. D. Miller, M. R. Matthews, and D. J. Heinzen

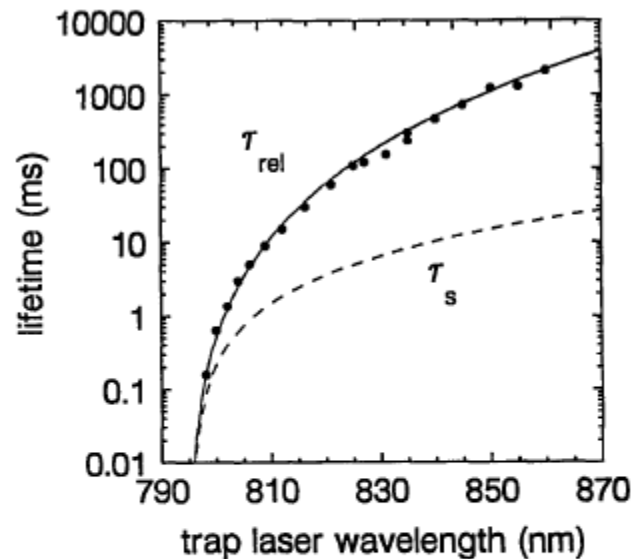


Fig. 2. Hyperfine population relaxation time as a function of trap laser wavelength. Experimental measurements are shown as filled circles. Calculated relaxation times are shown by the solid curve. The calculated mean time between spontaneous photon scattering events is shown by the dashed curve.

This was accepted truth for 15 years. However the Bollinger group showed that also Rayleigh scattering can lead to decoherence scaling as $1/\Delta^2$ in some cases.

PRL **105**, 200401 (2010)

Experimental Observation of Optically Trapped Atoms

Steven Chu, J. E. Bjorkholm, A. Ashkin, and A. Cable

AT&T Bell Laboratories, Holmdel, New Jersey 07733

We report the first observation of optically trapped atoms. Sodium atoms cooled below 10^{-3} K in "optical molasses" are captured by a dipole-force optical trap created by a single, strongly focused, Gaussian laser beam tuned several hundred gigahertz below the D_1 resonance transition. We estimate that about 500 atoms are confined in a volume of about $10^3 \mu\text{m}^3$ at a density of 10^{11} – 10^{12}cm^{-3} . Trap lifetimes are limited by background pressure to several seconds. The observed trapping behavior is in good quantitative agreement with theoretical expectations.

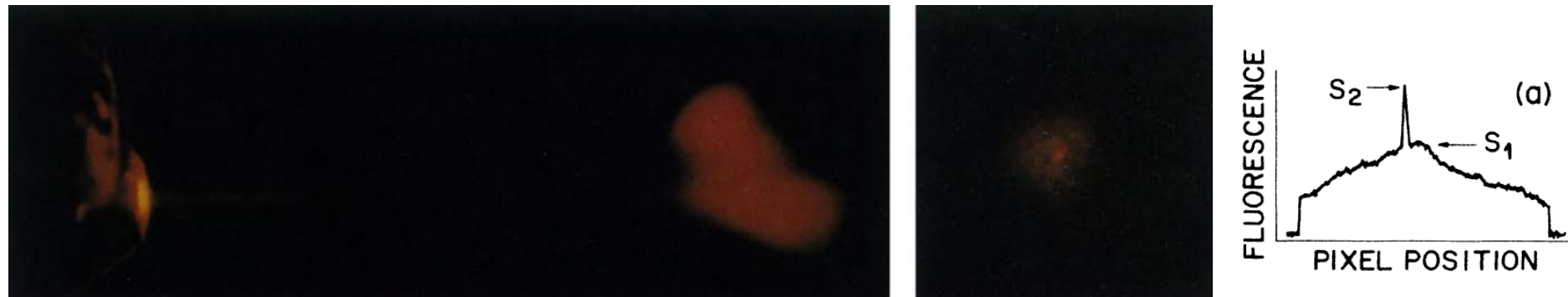


FIG. 2. (a) Photo showing the collimating nozzle, atomic beam, and atoms confined in OM. The distance from the nozzle to the OM region is 5 cm. (b) Photo taken after the atomic source and the slowing laser beam have been turned off, showing trapped atoms.

Optical trapping – single atoms

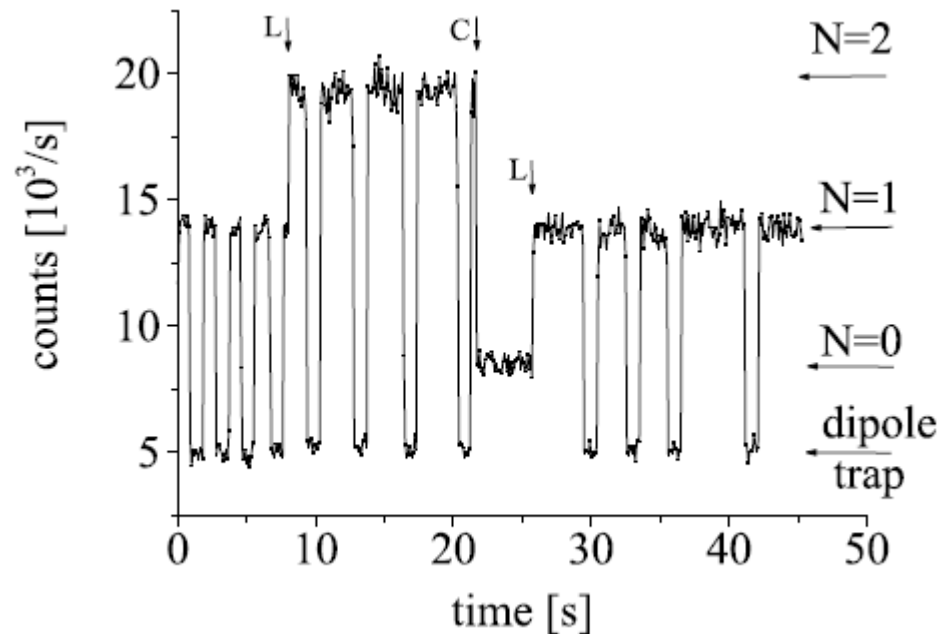
VOLUME 85, NUMBER 18

PHYSICAL REVIEW LETTERS

30 OCTOBER 2000

Single Atoms in an Optical Dipole Trap: Towards a Deterministic Source of Cold Atoms

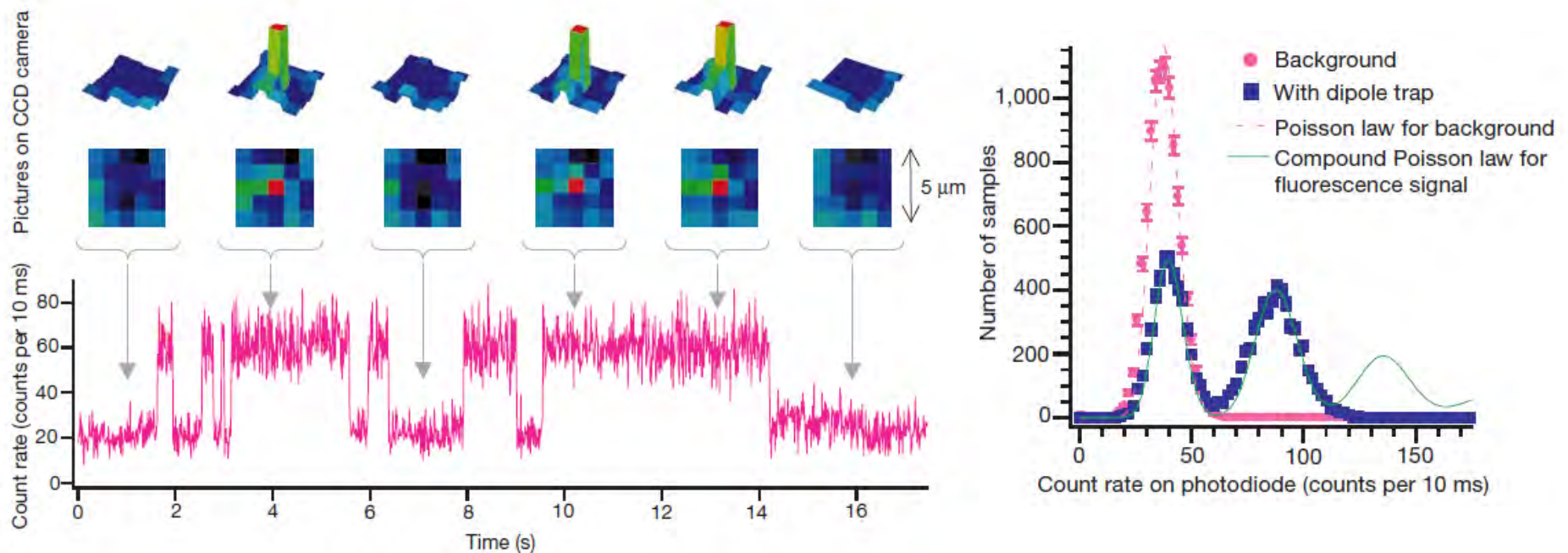
D. Frese, B. Ueberholz, S. Kuhr, W. Alt, D. Schrader, V. Gomer, and D. Meschede



Sub-poissonian loading of single atoms in a microscopic dipole trap

Nicolas Schlosser, Georges Reymond, Igor Protsenko
& Philippe Grangier

NATURE | VOL 411 | 28 JUNE 2001

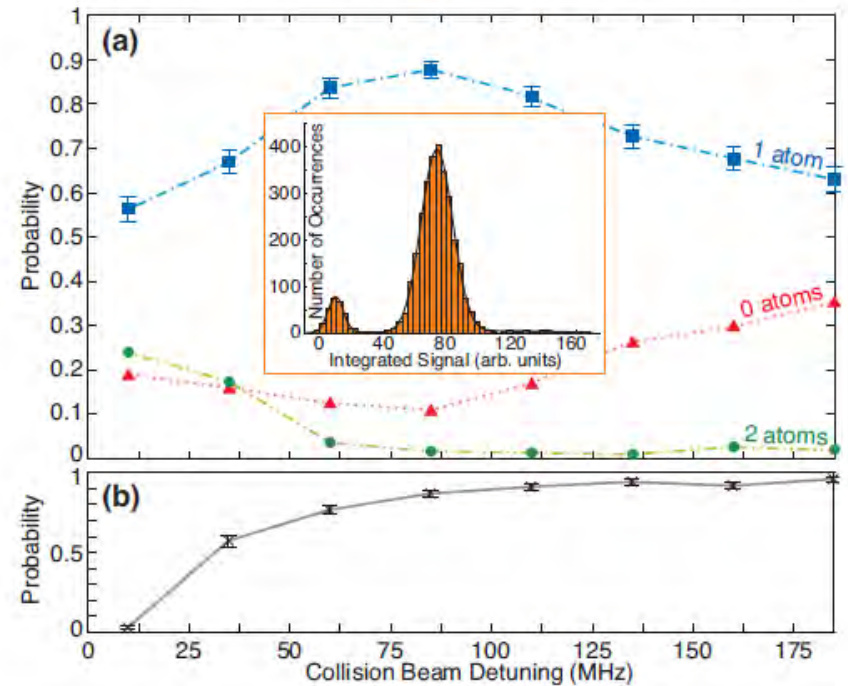
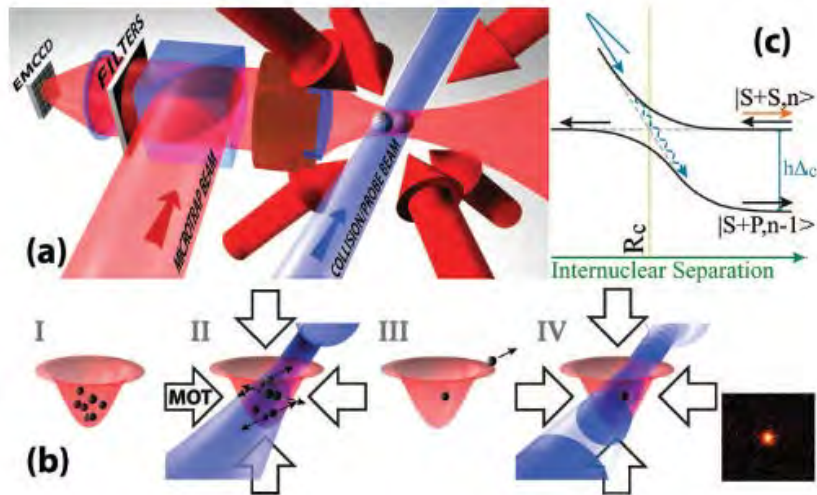


Optical trapping – 91% atom loading

arXiv:1208.0707v1

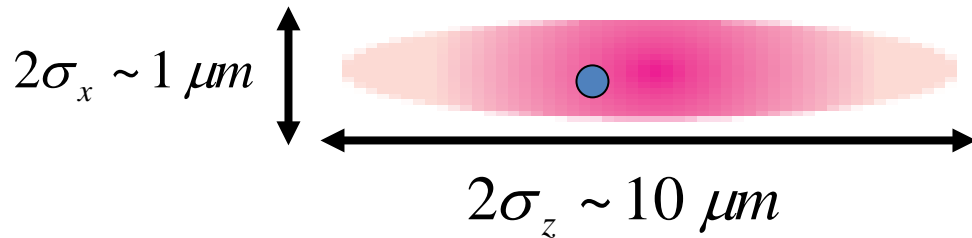
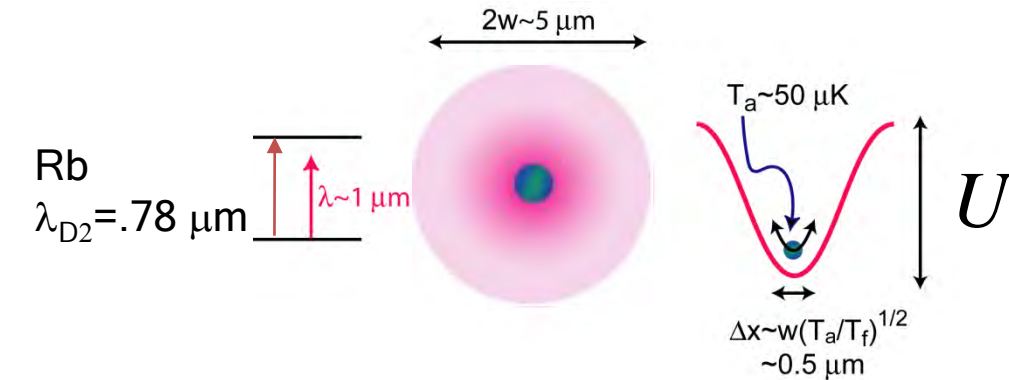
High efficiency preparation of single trapped atoms using blue detuned light assisted collisions

A. V. Carpentier,¹ Y. H. Fung,¹ P. Sompet,¹ A. J. Hilliard,¹ T. G. Walker,² and M. F. Andersen¹



Spatial Localization

- With a single focused laser beam:



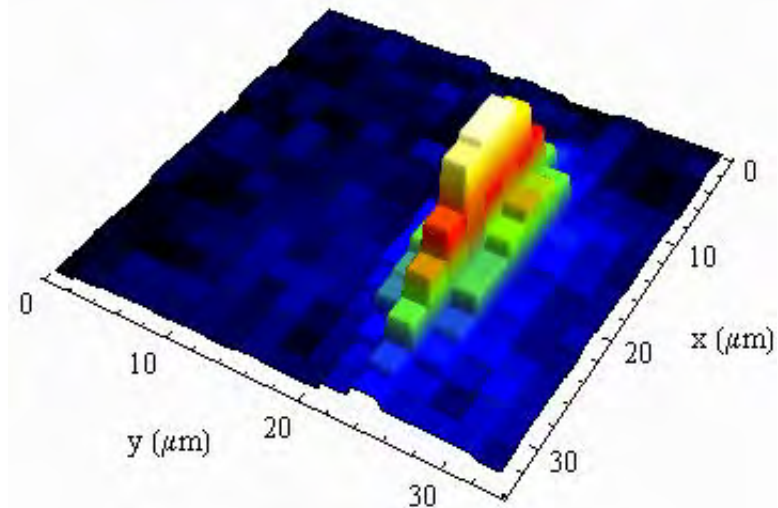
$w = 3.0 \mu\text{m}, \quad \lambda = 1.06 \mu\text{m}, \quad P = 300 \text{ mW}$
 $T_a = 0.1 - 0.5 \text{ mK}, \quad U_f / k_B = 5 \text{ mK}$

Spatial variance

$$\langle x_a^2 \rangle = \langle y_a^2 \rangle = \frac{w_{f0}^2 T_a}{4 |U_m|}$$

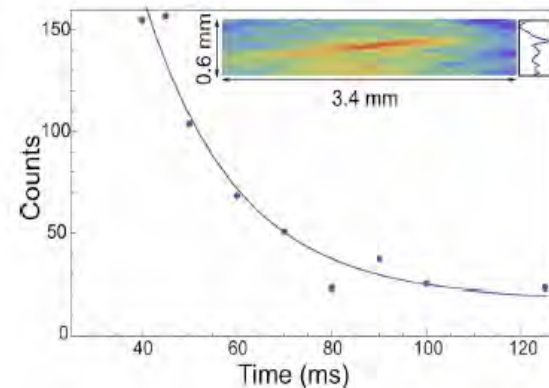
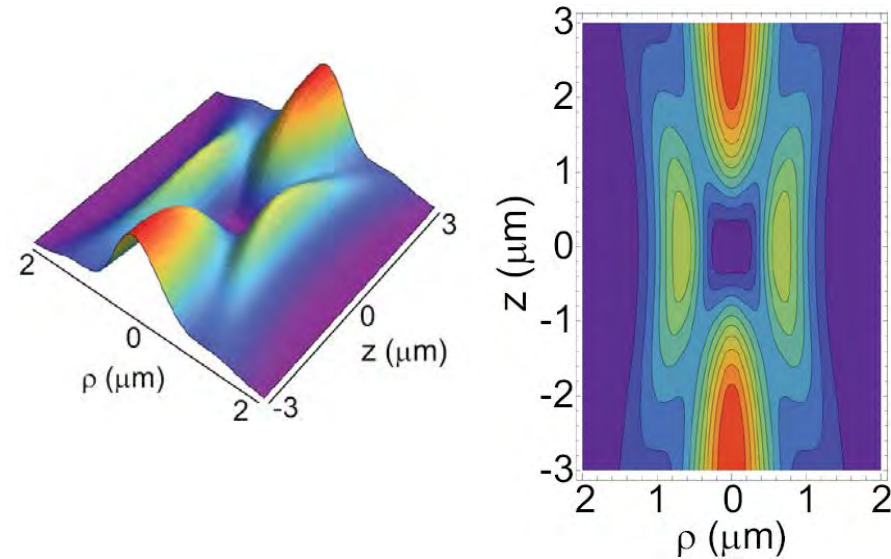
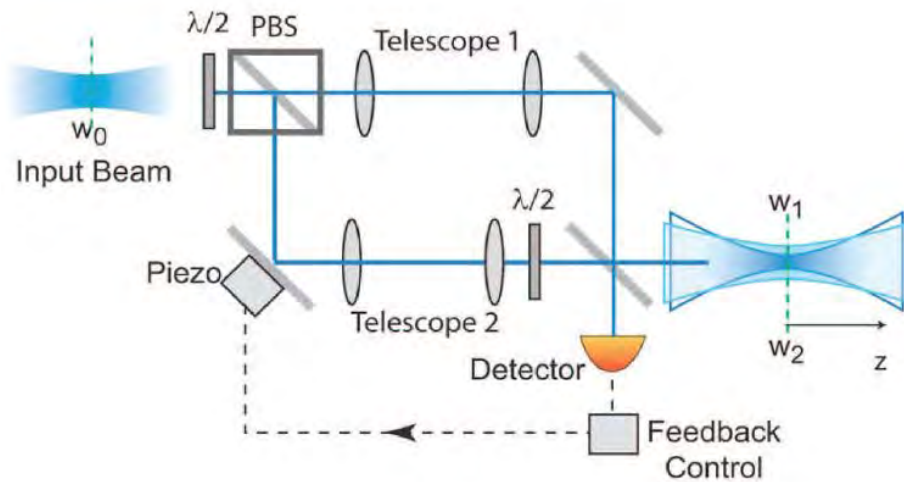
$$\langle z_a^2 \rangle = \frac{\pi^2 w_{f0}^4 T_a}{2 \lambda_f^2 |U_m|}$$

Fluorescence image



Blue detuned traps

- A large range of optical configurations have been used
- 3D optical lattices trap atoms at nodes of the field.
- Bottle Beam traps (BBT) only require access from a single side



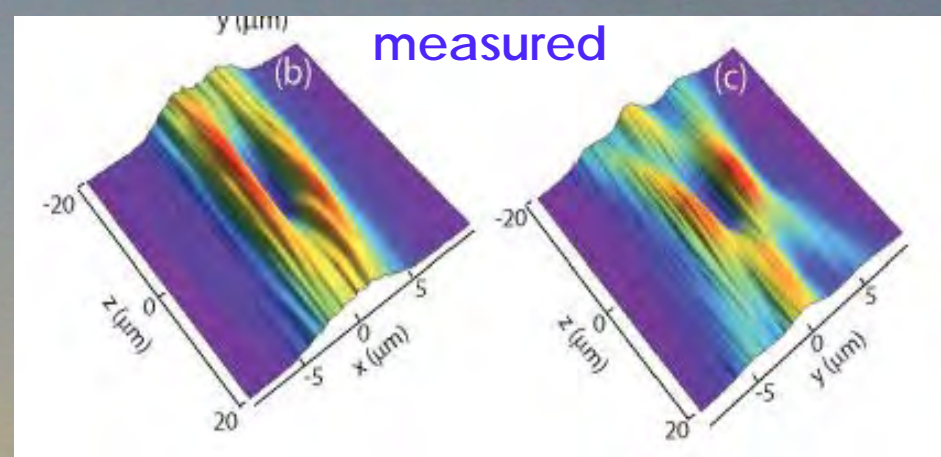
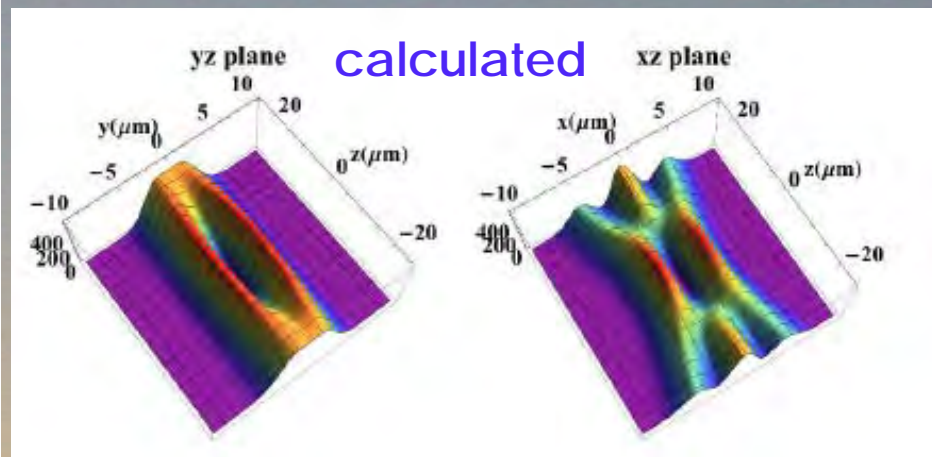
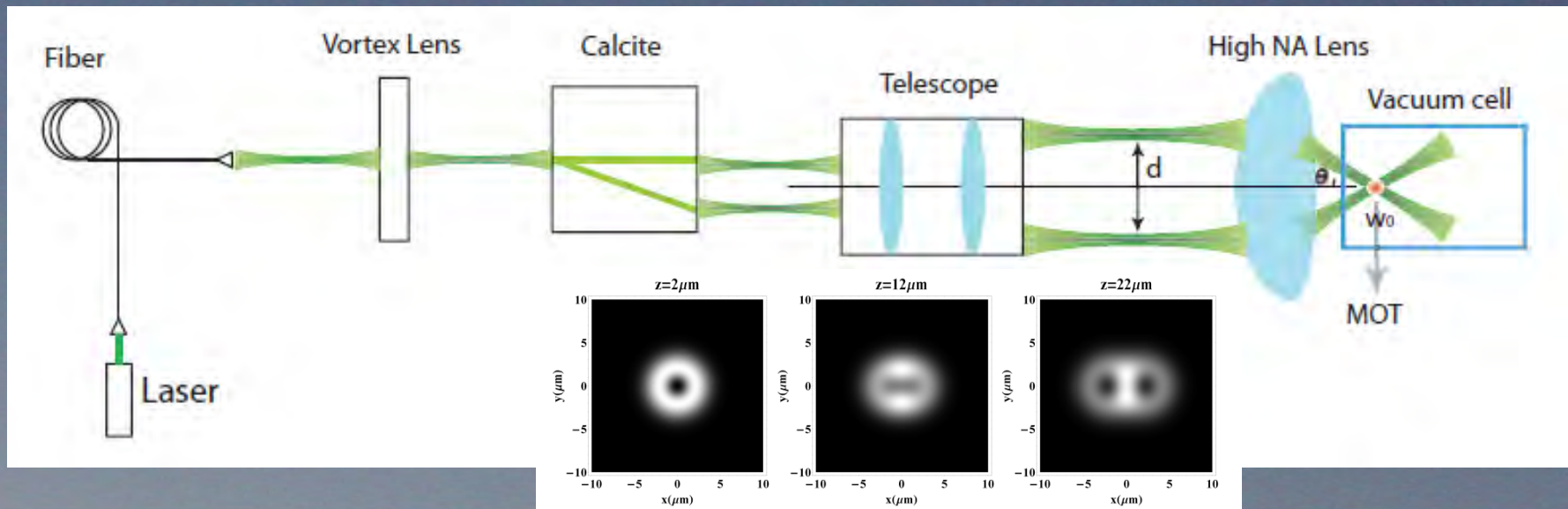
trapped atoms

April 15, 2009 / Vol. 34, No. 8 / OPTICS LETTERS

Atom trapping in an interferometrically generated bottle beam trap

L. Isenhower, W. Williams, A. Dally, and M. Saffman*

Crossed vortex Bottle Beam Trap (BBT)

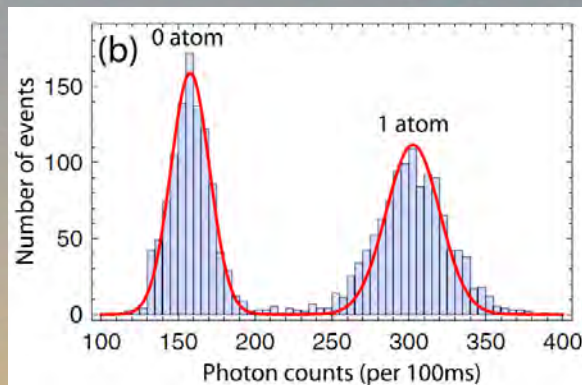
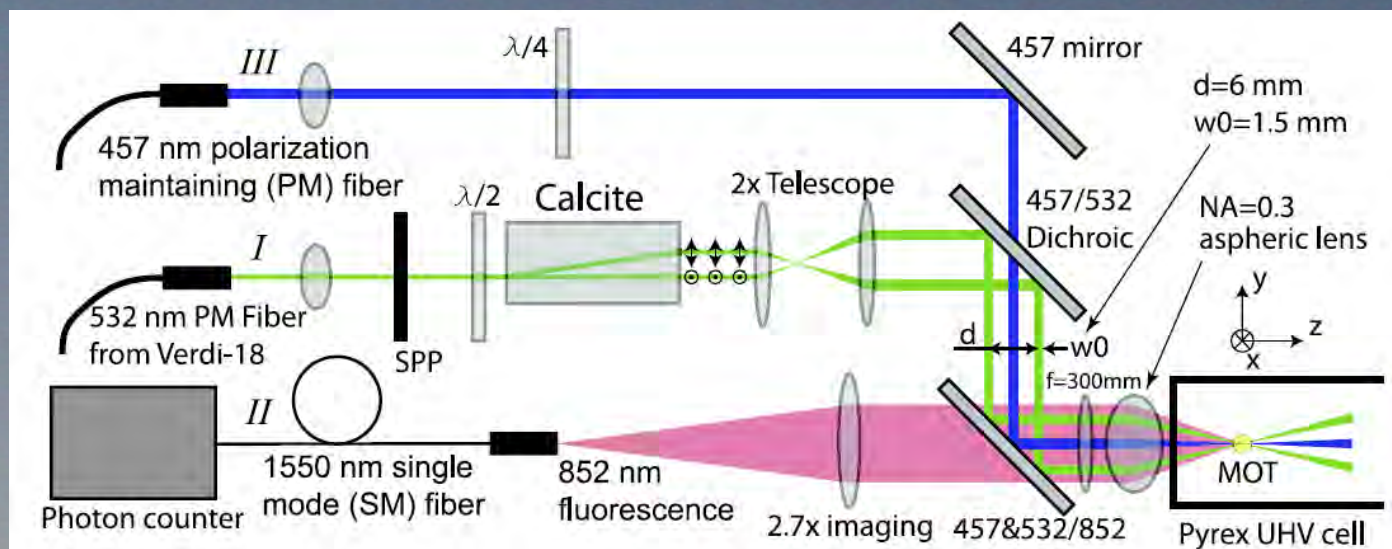


Atomic qubits in a BBT

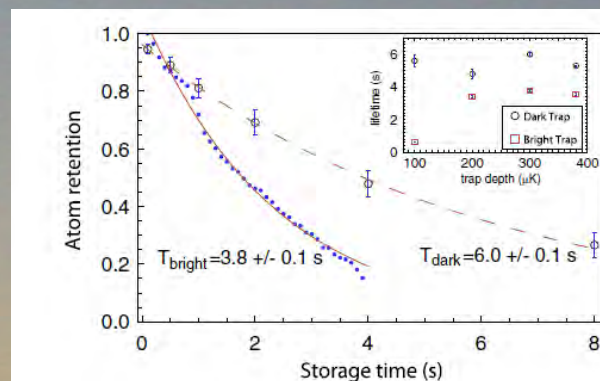
March 1, 2012 / Vol. 37, No. 5 / OPTICS LETTERS

Crossed vortex bottle beam trap for single-atom qubits

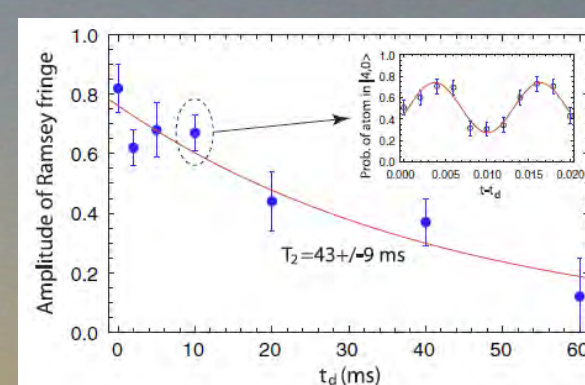
G. Li, S. Zhang, L. Isenhower, K. Maller, and M. Saffman*



Single atom detection



Lifetime 6s.



Coherence time 43 ms.

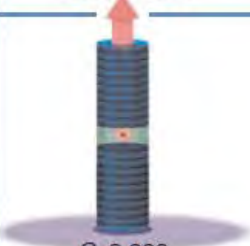
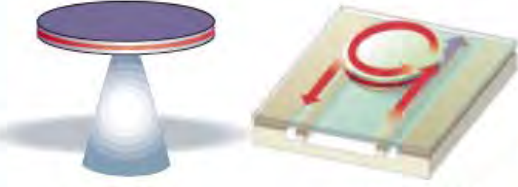

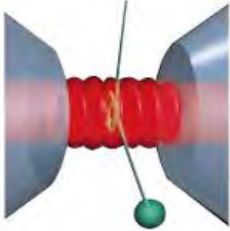
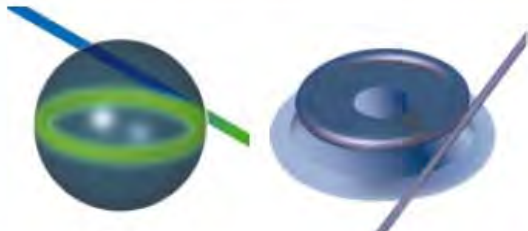
Traps near surfaces

Optical resonators can serve as buildup cavities to enhance the field strength giving strong trapping with low optical power.

Evanescent fields at surfaces have large gradients giving good localization.

Optical microcavities

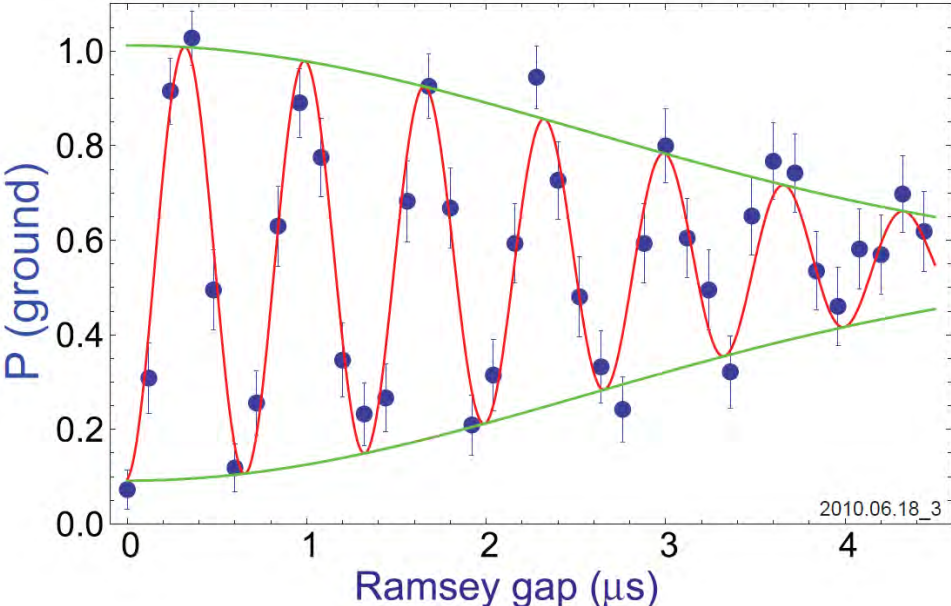
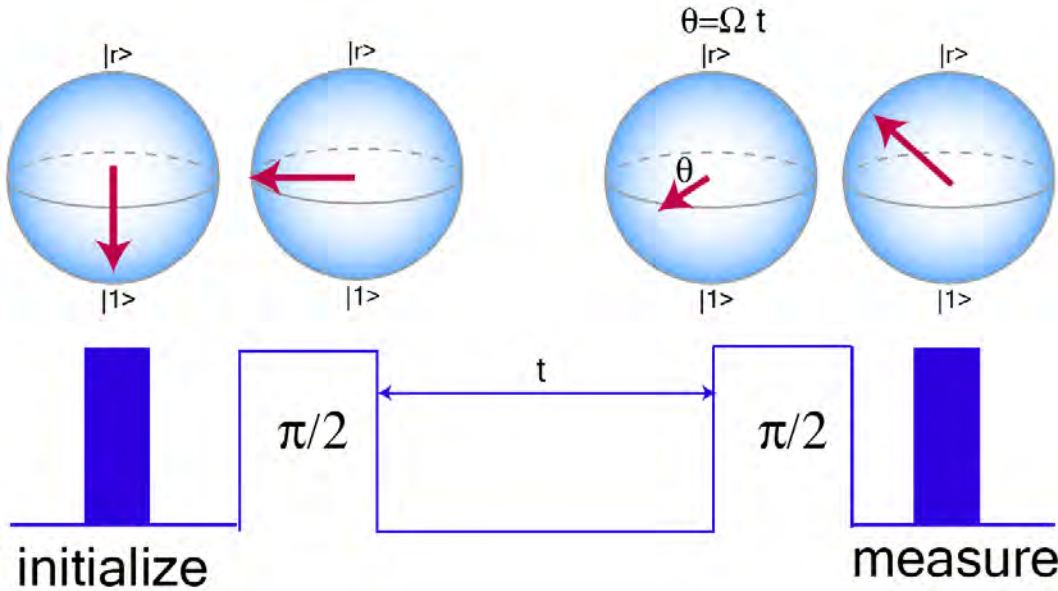
Kerry J. Vahala | NATURE | VOL 424 | 14 AUGUST 2003 |

	Fabry-Perot	Whispering gallery	Photonic crystal
High Q	 $Q: 2,000$ $V: 5 (\lambda/n)^3$	 $Q: 12,000$ $V: 6 (\lambda/n)^3$ $Q_{\text{III-V}}: 7,000$ $Q_{\text{Poly}}: 1.3 \times 10^5$	 $Q: 13,000$ $V: 1.2 (\lambda/n)^3$
Ultra-high Q	 $F: 4.8 \times 10^5$ $V: 1,690 \mu\text{m}^3$	 $Q: 8 \times 10^9$ $V: 3,000 \mu\text{m}^3$ $Q: 10^8$	

III: Coherence properties of ground and Rydberg traps

- Optical traps and ground state (qubit) coherence
- Ramsey spectroscopy
- magic traps
- traps for Rydberg atoms
- 3D Rydberg atom trapping

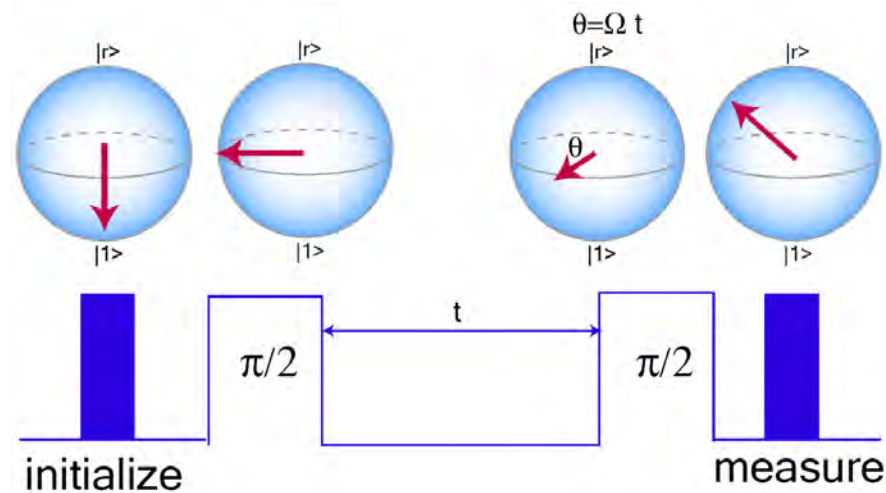
Qubit coherence – Ramsey measurement



The envelope of the Ramsey fringes is related to the coherence time T_2 .

Simply define T_2 as the $1/e$ time.

Ramsey measurement of decoherence



Start in $|1\rangle$, $\pi/2$ pulse

$$|\psi\rangle = \frac{1}{\sqrt{2}}(|1\rangle + i|r\rangle)$$

wait time t

$|r\rangle$ picks up a phase of $\varphi = \varphi_R + \varphi_{st}$

$\pi/2$ pulse

$$|\psi\rangle = \frac{1}{2}(|1\rangle + i|r\rangle) + \frac{e^{i\varphi}}{2}(i|r\rangle - |1\rangle)$$

Probability of measuring $|1\rangle$

$$P_1 = |\langle 1|\psi\rangle|^2 = \frac{1}{4}|1 - e^{i\varphi}|^2 = \frac{1}{2}(1 - \cos \varphi)$$

Oscillation amplitude

$$\frac{1}{2}(1 - \cos(\pi + \varphi_{st})) - \frac{1}{2}(1 - \cos(\varphi_{st})) = \cos(\varphi_{st})$$

Zero mean random process

$$\langle \cos(\varphi_{st}) \rangle = \langle e^{i\varphi_{st}} \rangle$$

Magnetic decoherence

Magnetic phase $\varphi_{\text{st}} = \nu_{B,g} \delta B t$ $\nu_{B,g} = \frac{1}{\pi^2} \frac{\mu_B^2 B_0}{\hbar^2 \nu_{\text{hf}}} \text{ Hz/T.}$

For ^{87}Rb at $B_0 = 0.5(3.5) \text{ G}$ we find $\nu_{B,g} = 0.57(4.0) \text{ Hz/mG.}$

assume Gaussian fluctuations $P(\delta B) = \left(\frac{1}{2\pi\sigma^2} \right)^{1/2} e^{-\delta B^2/2\sigma^2}$

average $\langle e^{i\varphi_{\text{st}}} \rangle = e^{-\nu_{B,g}^2 \sigma^2 t^2 / 2} = e^{-t^2 / T_{2,gB}^2}$

1/e time is

$$T_{2,gB} = \frac{2^{1/2}}{\nu_{B,g}\sigma}$$

Motional decoherence

This is due to the different trap depths seen by the two hyperfine states.

The effect scales with the ratio of the differential light shift to the average shift.

The analysis is more complicated than for magnetic decoherence. Need to average over the motional states in the harmonic trap.

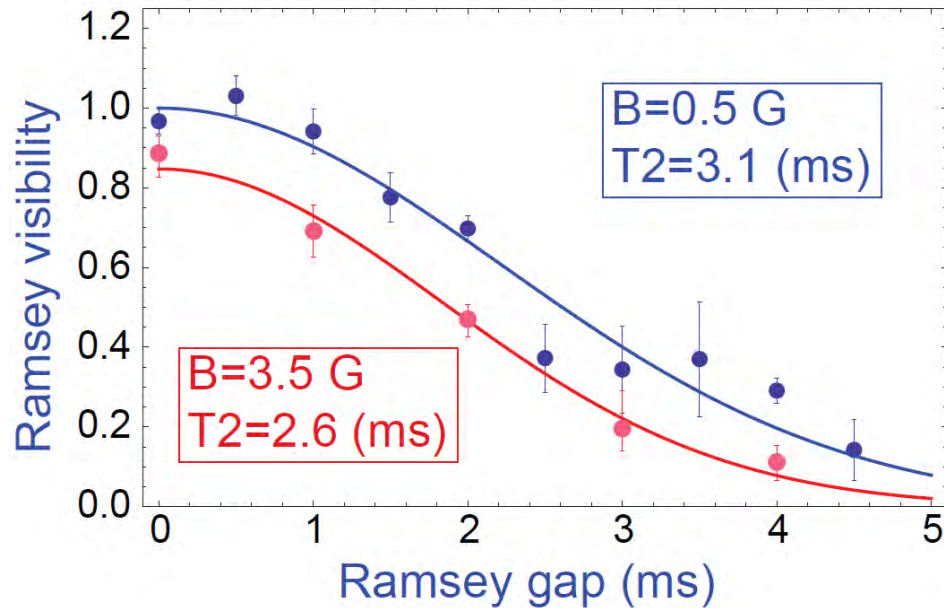
Find Ramsey envelope $\alpha(t) = \frac{1}{[1 + 0.95 \left(\frac{t}{T_{2,L}}\right)^2]^{3/2}}$ Kuhr, et al. PRA **72**, 023406 (2005)

$$T_{2,L} = 0.97 \frac{2\hbar}{\eta k_B T}$$

This more complicated behavior is well approximated by a Gaussian

$$e^{-t^2/T_{2,L}^2}$$

Extracting T2



two sources of decoherence

$$T_2 = \frac{T_{2,a}T_{2,b}}{(T_{2,a}^2 + T_{2,b}^2)^{1/2}}$$

Decoherence due to magnetic field and differential light shift

model as: e^{-t^2/T_2^2}

extract:

$$T_2_{B=3.5\text{ G}} = 7.1\text{ ms}$$

$$T_2_{B=0.5\text{ G}} = 50\text{ ms}$$

$$T_2_{\text{optical trap}} = 2.6\text{ ms}$$

Matching to theory for T2 implies $\delta B_{\text{rms}} = 50\text{ mG}$
 $T_a = 85\text{ }\mu\text{K}$

III: Coherence properties of ground and Rydberg traps

- Optical traps and ground state (qubit) coherence
- Ramsey spectroscopy
- magic traps
- traps for Rydberg atoms
- 3D Rydberg atom trapping

Quantum State Engineering and Precision Metrology Using State-Insensitive Light Traps

Jun Ye,^{1*} H. J. Kimble,² Hidetoshi Katori³

27 JUNE 2008 VOL 320 SCIENCE

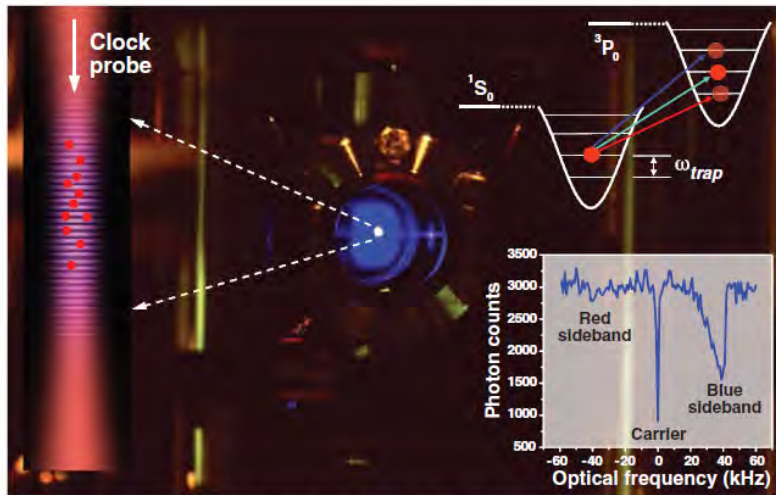
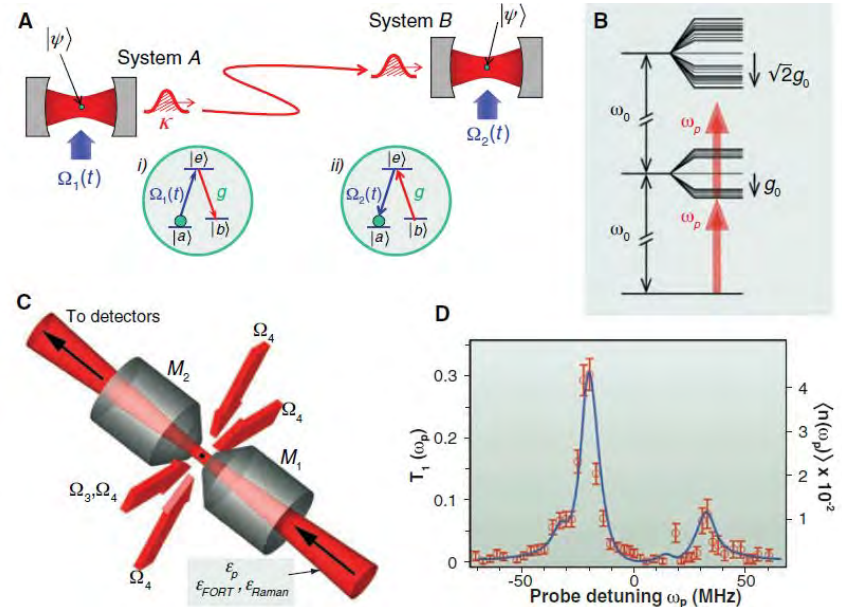
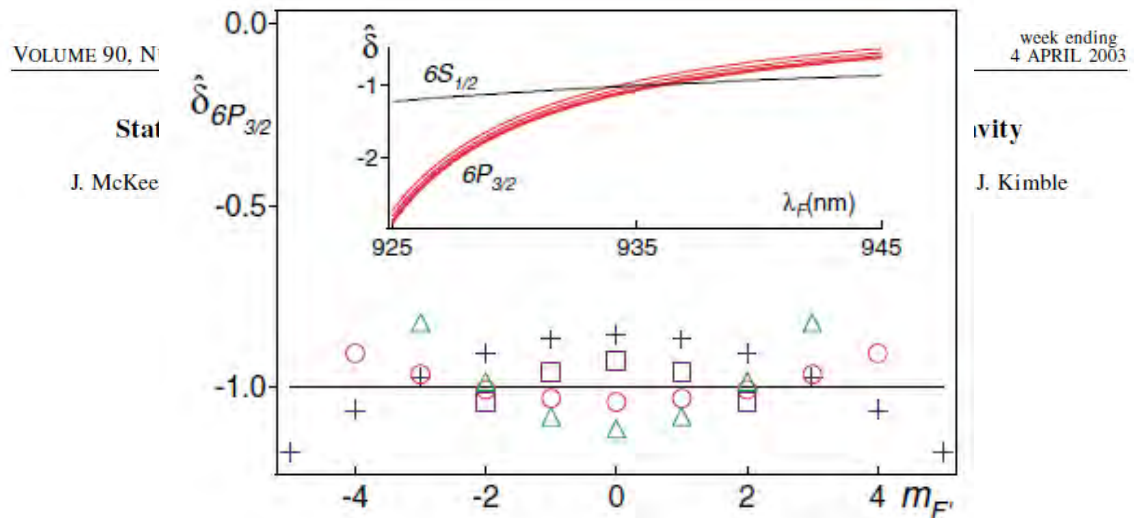
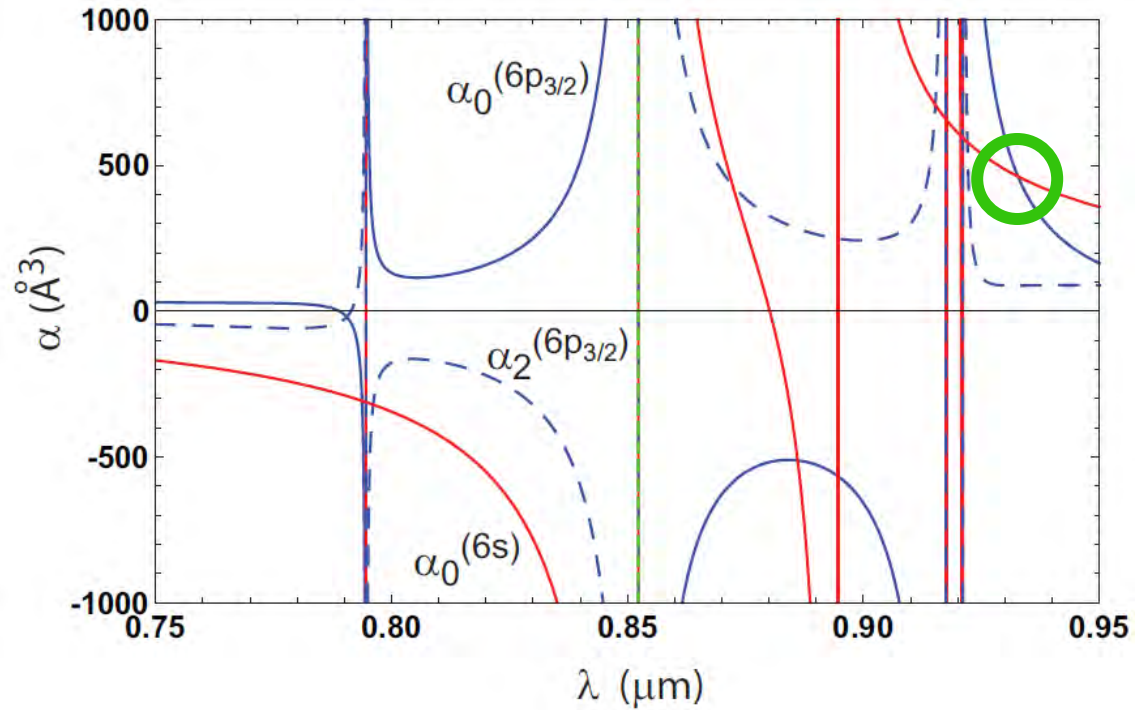
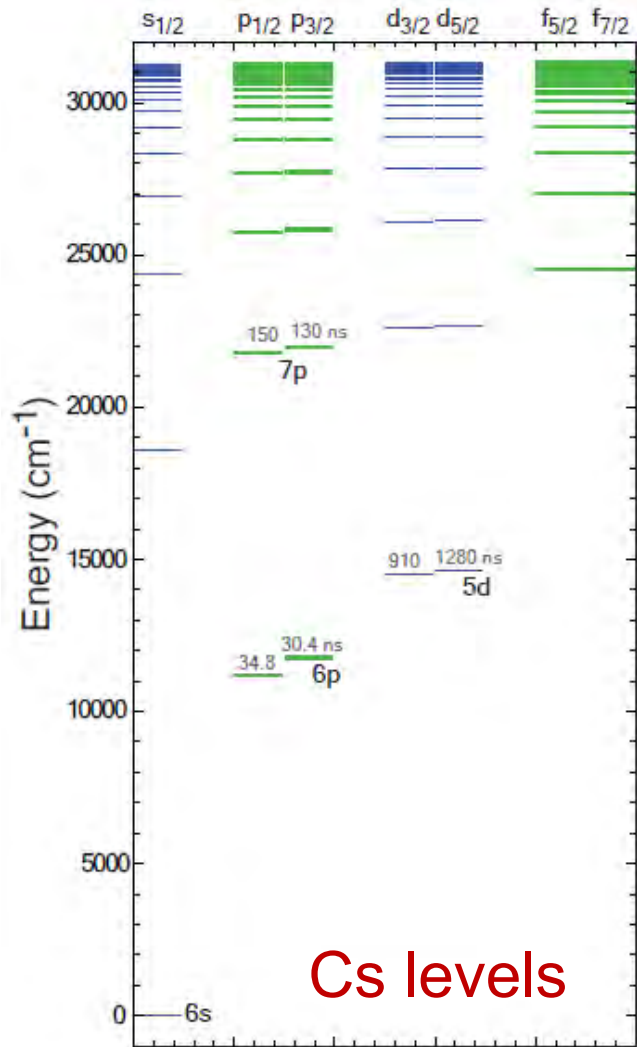


Fig. 2. ⁸⁷Sr lattice clock. Blue laser light (¹S₀ to ¹P₁) is used to cool and trap Sr atoms at the center of the vacuum chamber. Atoms are further cooled with red light (¹S₀ to ³P₁) in the second stage. Atoms are then loaded into a state-insensitive, vertical 1D optical lattice made of near-infrared light. (Top Right) Schematic levels for lattice spectroscopy, where the two electronic states are convolved with the quantized motional states. (Bottom Right) Line shape of a saturated ¹S₀ to ³P₀ electronic transition and the motional sidebands.

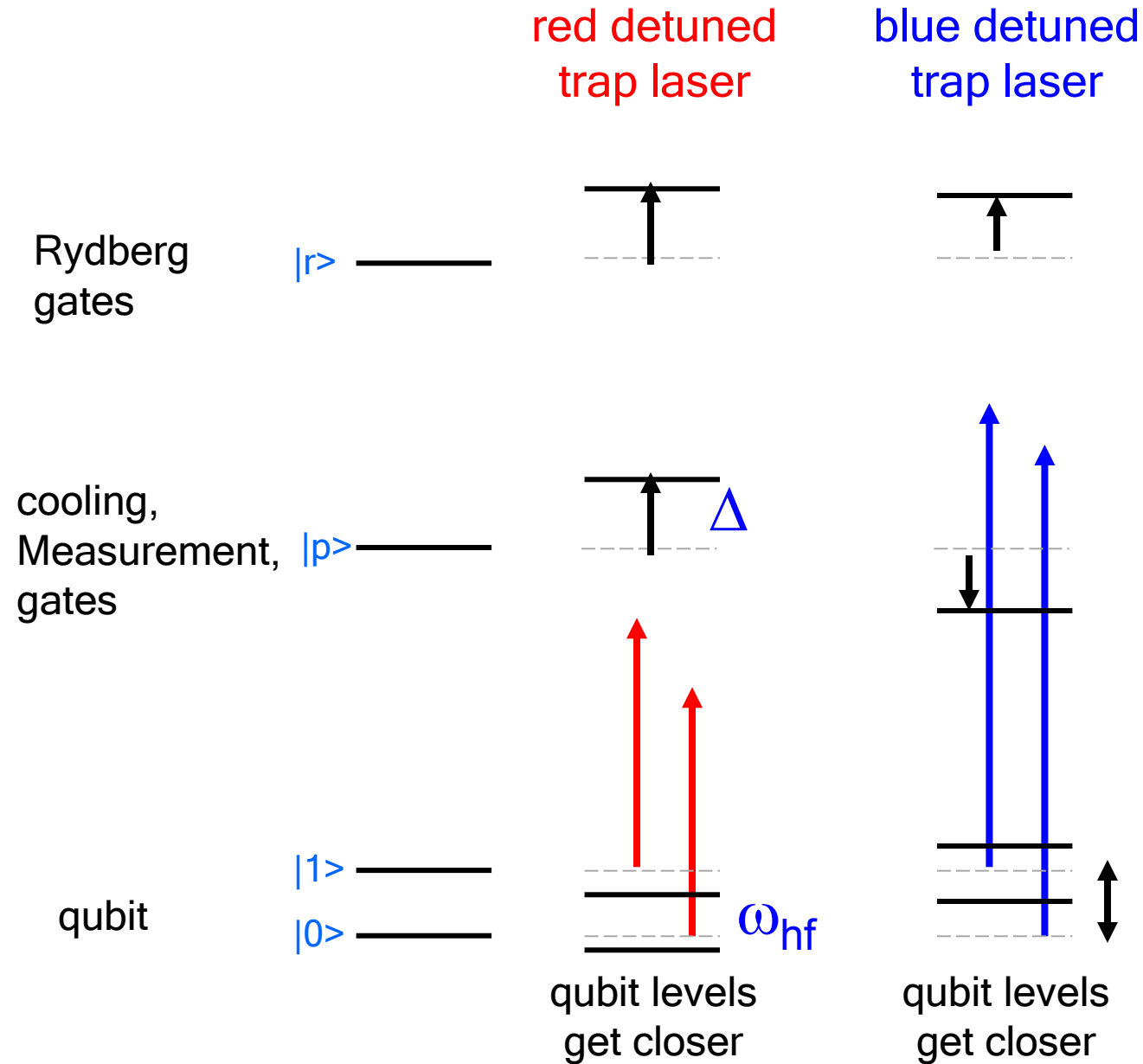


Rempe, Kimble,...

Magic trapping for s and p states

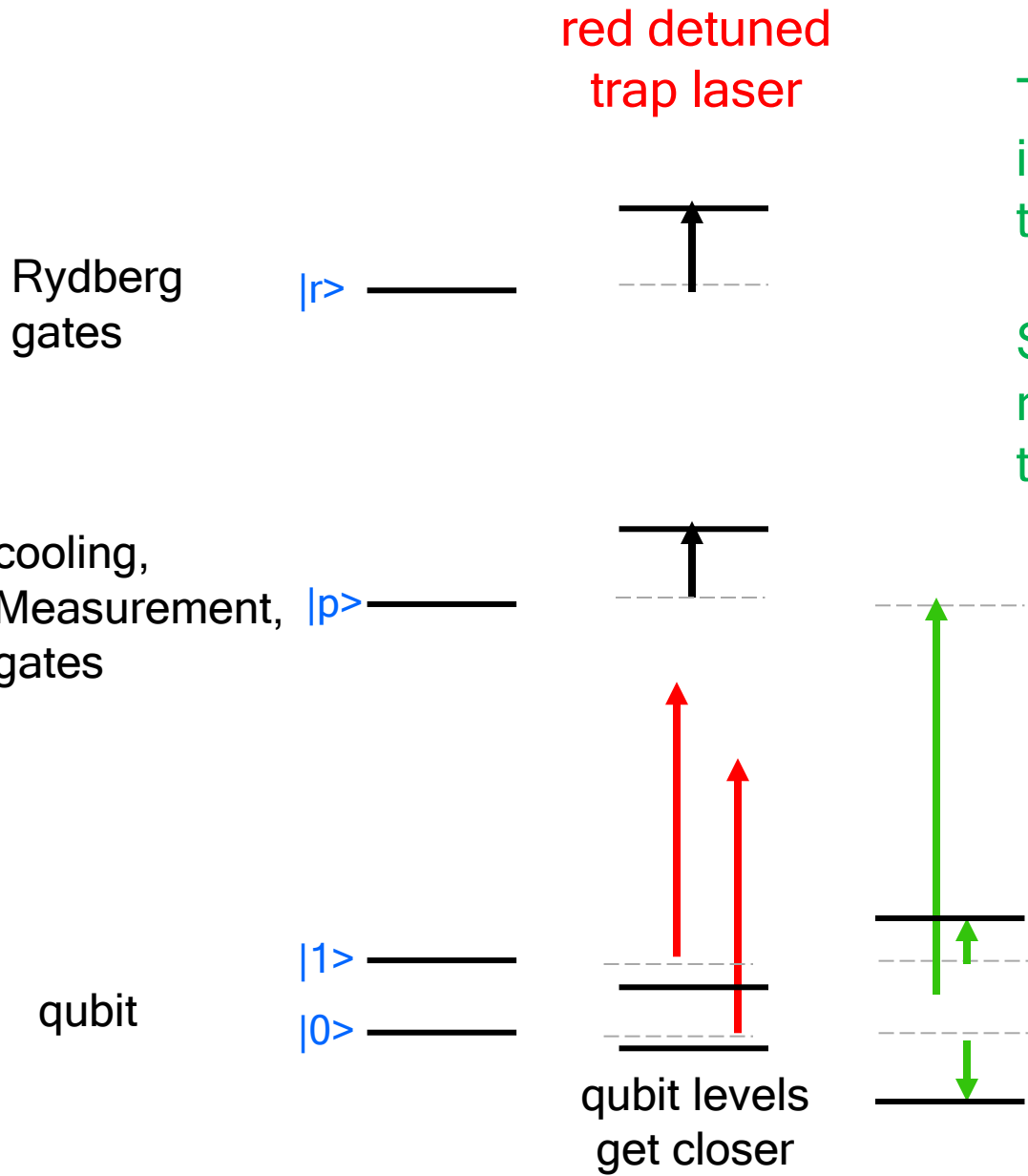


Magic qubit trapping



$$\delta\omega_{hf} \sim U_{\text{trap}} \frac{\omega_{hf}}{\Delta}$$

Magic qubit trapping



To make the qubit frequency independent of trap intensity tune in between the levels.

Small detuning - large scattering rate, but only need small intensity to compensate trap.

Suppression of inhomogeneous broadening in rf spectroscopy of optically trapped atoms

Ariel Kaplan, Mikkel Fredslund Andersen, and Nir Davidson

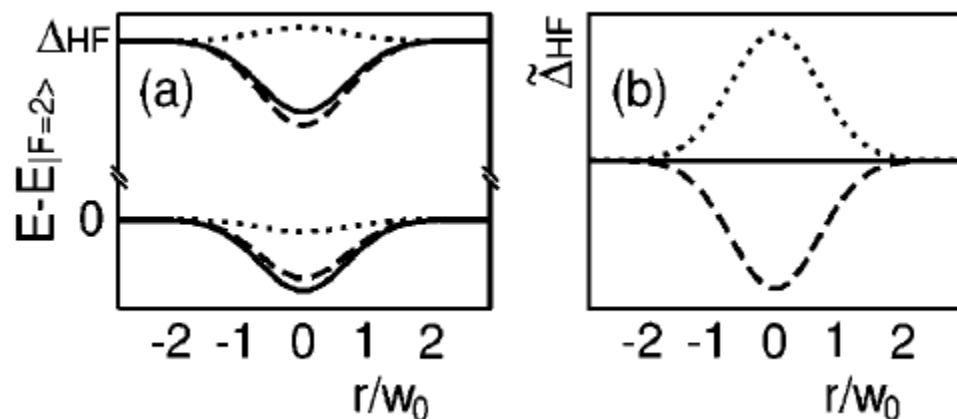
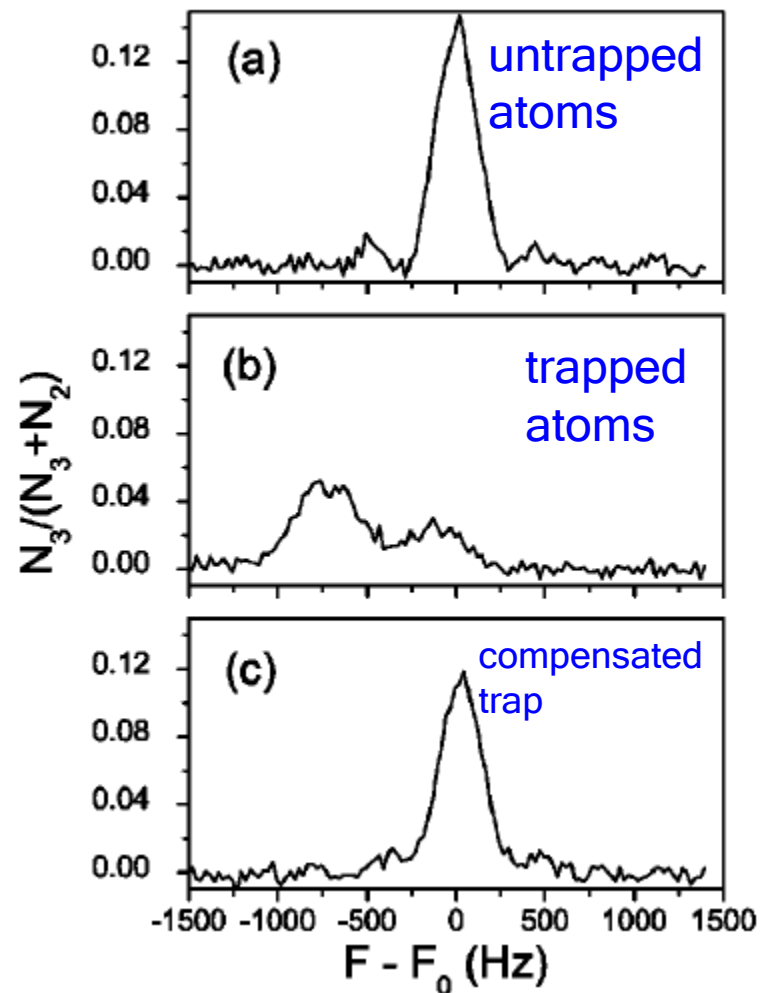


FIG. 1. Ground-level energies (a) and energy difference (b) of atoms trapped in a focused Gaussian beam. When exposed to the trapping laser, the two hyperfine levels have a different ac Stark shift (dashed line). An additional weak laser, detuned to the middle of the hyperfine splitting, creates an ac Stark shift (dotted line) such that the total amount of light shift (full line) is identical for both hyperfine levels.



Rabi spectroscopy

Doubly magic qubit trapping

PRL **105**, 033002 (2010)

PHYSICAL REVIEW LETTERS

week ending
16 JULY 2010

“Doubly Magic” Conditions in Magic-Wavelength Trapping of Ultracold Alkali-Metal Atoms

Andrei Derevianko*

Qubit hyperfine transition insensitive to both magnetic and intensity fluctuations !

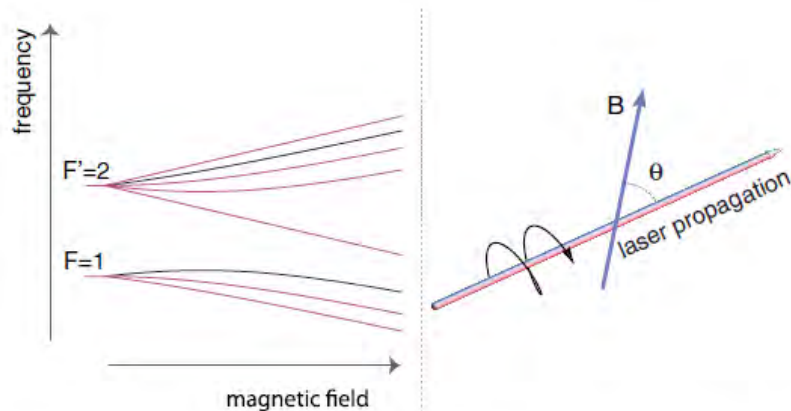


FIG. 1 (color online). Left panel: Zeeman effect for the hyperfine manifold in the ground state of $I = 3/2$ isotopes of alkali-metal atoms. Two clock or qubit levels $|F' = 2, M'_F = +1\rangle$ and $|F = 1, M_F = -1\rangle$ are shown in black. The right panel illustrates the geometry of laser-atom interaction: the degree of circular polarization, angle θ , and laser wavelength may be varied.

TABLE I. Values of magic B fields and magic wavelengths.

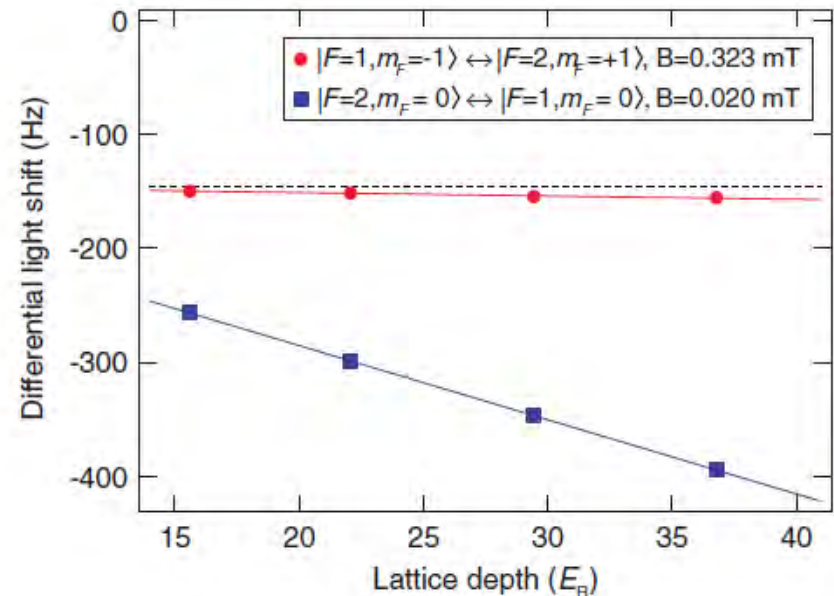
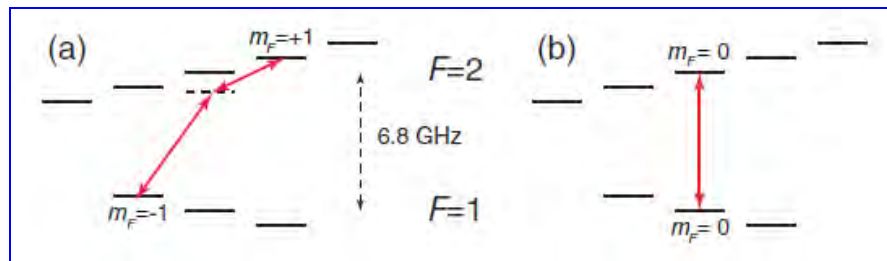
Transition	B_m , Gauss	λ_m
		$^{87}\text{Rb}, I = 3/2, \nu_{\text{clock}} = 6.83 \text{ GHz}$
$ 2, 1\rangle \rightarrow 1, -1\rangle$	3.25	806 nm ^a
		$^{85}\text{Rb}, I = 5/2, \nu_{\text{clock}} = 3.04 \text{ GHz}$
$ 3, 1\rangle \rightarrow 2, -1\rangle$	0.359	
$ 3, 2\rangle \rightarrow 2, -2\rangle$	1.15	479–658; 797–878
		$^{133}\text{Cs}, I = 7/2, \nu_{\text{clock}} = 9.19 \text{ GHz}$
$ 4, 1\rangle \rightarrow 3, -1\rangle$	1.41	
$ 4, 2\rangle \rightarrow 3, -2\rangle$	3.51	906–1067; 560–677
$ 4, 3\rangle \rightarrow 3, -3\rangle$	9.04	898–1591; 863–880; 512–796

^aNearly doubly magic.

Differential Light-Shift Cancellation in a Magnetic-Field-Insensitve Transition of ^{87}Rb

R. Chicireanu,^{1,*} K. D. Nelson,¹ S. Olmschenk,¹ N. Lundblad,² A. Derevianko,³ and J. V. Porto¹

The precise measurement of transition frequencies of trapped atomic samples is susceptible to inaccuracy arising from the inhomogeneous differential shift of the relevant energy levels in the presence of the trapping fields. We demonstrate near-complete cancellation of the differential ac Stark shift (“light shift”) of a two-photon magnetic-field-insensitve microwave hyperfine (clock) transition in ^{87}Rb atoms trapped in an optical lattice. Up to 95(2)% of the differential light shift is cancelled while maintaining magnetic-field insensitivity. This technique should have applications in quantum information and frequency metrology.



III: Coherence properties of ground and Rydberg traps

- Optical traps and ground state (qubit) coherence
- Ramsey spectroscopy
- magic traps
- traps for Rydberg atoms
- 3D Rydberg atom trapping

Traps for Rydberg atoms

- Many experiments with cold Rydberg atoms would be enhanced if we could trap Rydberg states:

Quantum gates, Rydberg-ground dressing, precision atomic measurements, Casimir-Polder studies,...

- Electrostatic and magnetostatic Rydberg trapping has been demonstrated.

Hogan, S. D., and F. Merkt, “Demonstration of three dimensional electrostatic trapping of state-selected Rydberg atoms,” *Phys. Rev. Lett.* **100**, 043001 (2008).

Choi, J.-H., J. R. Guest, A. P. Povilus, E. Hansis, and G. Raithel, “Magnetic trapping of long-lived cold Rydberg atoms,” *Phys. Rev. Lett.* **95**, 243001 (2005).

- We use light for excitation, so optical traps would be convenient

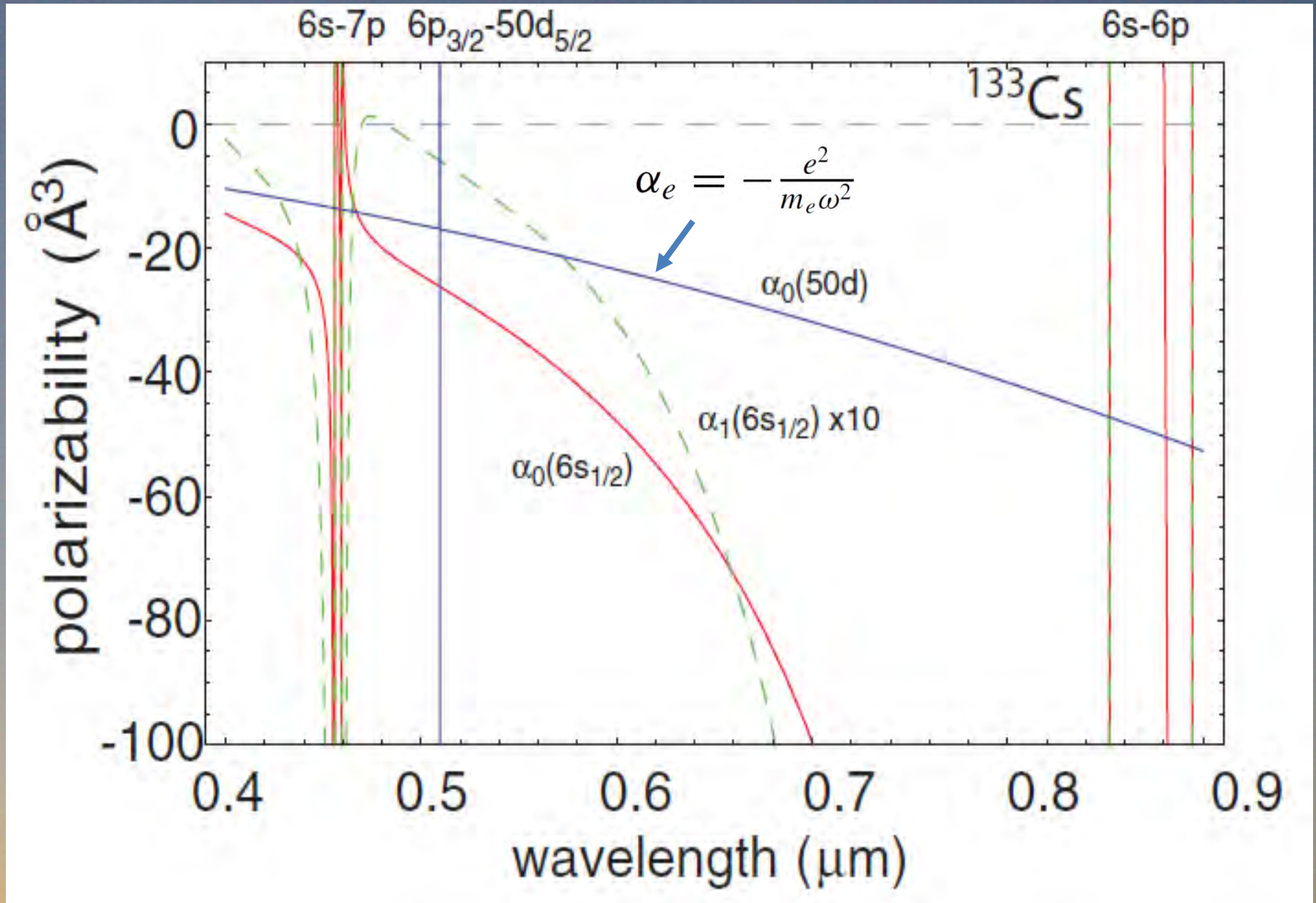
Optical Traps for Rydberg atoms

$$\alpha < 0$$

- Core polarizability is negligible.
- Rydberg polarizability is that of a free electron.
- To trap Rydberg atom need blue detuned trap.
- Choose wavelength and trap size so ground-Rydberg potentials are matched.

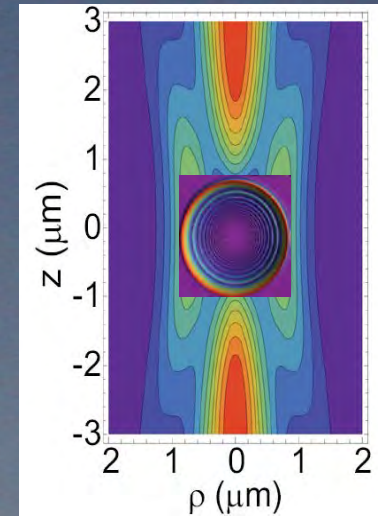
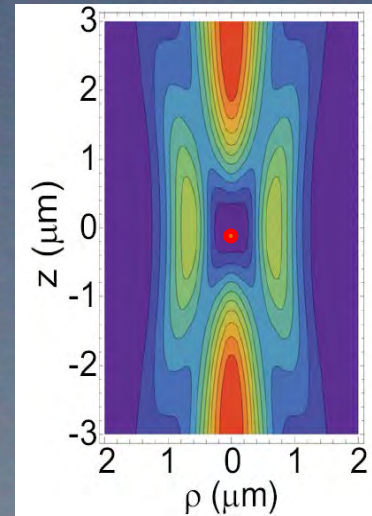


Ground-Rydberg magic trapping



Ground-Rydberg magic trapping

Delocalized Rydberg wavefunction sees different intensity than ground state atom.



Calculate effective light shift with $|\psi|^2$ weighting of optical intensity

VOLUME 85, NUMBER 26

PHYSICAL REVIEW LETTERS

25 DECEMBER 2000

Ponderomotive Optical Lattice for Rydberg Atoms

S. K. Dutta, J. R. Guest, D. Feldbaum, A. Walz-Flannigan, and G. Raithel

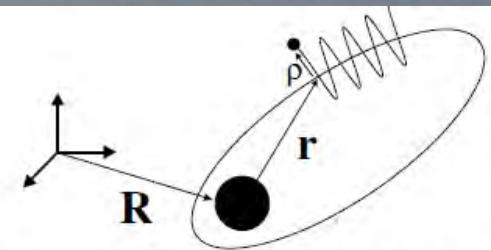
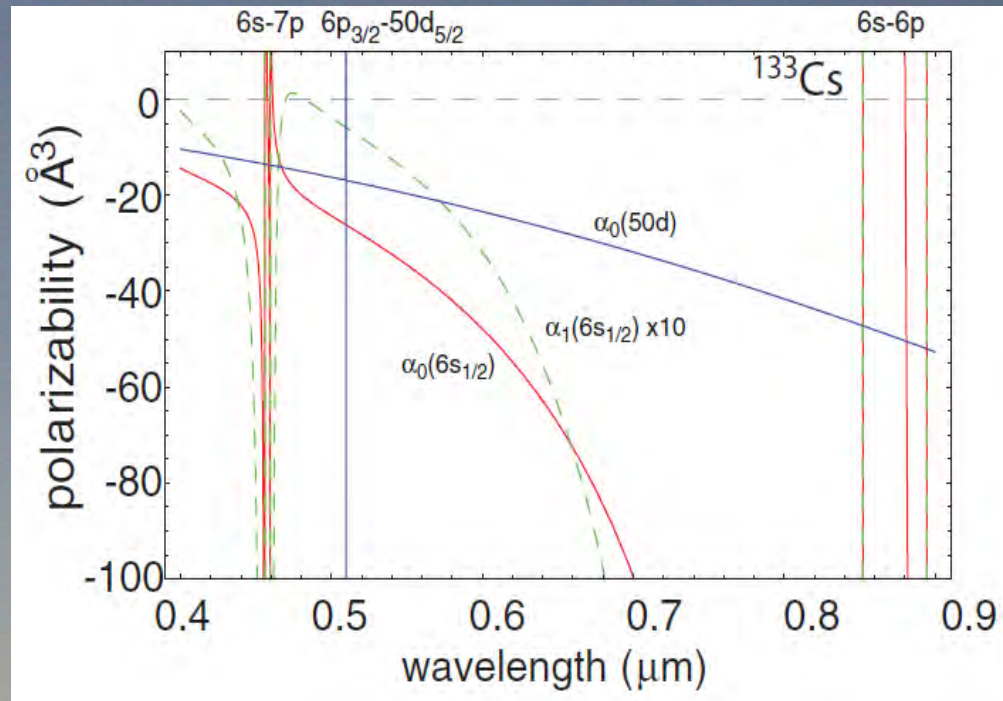


FIG. 1. The motion of a Rydberg atom in a laser field is characterized by a slowly evolving center-of-mass coordinate \mathbf{R} , a relative coordinate \mathbf{r} , and a quiver coordinate $\boldsymbol{\rho}$ evolving at the laser frequency.

Ground-Rydberg magic trapping

Any wavelength for which ground and Rydberg states have negative α and $|\alpha_g| > |\alpha_{Ryd}|$ can be used.



PHYSICAL REVIEW A **84**, 043408 (2011)

Magic-wavelength optical traps for Rydberg atoms

S. Zhang,¹ F. Robicheaux,² and M. Saffman^{1,*}

Ground-Rydberg magic trapping

We calculated light shifts for several BBT designs.

$$\begin{aligned} \Delta E_{R_j}(\vec{R}) &= \int d^3r U_P(\vec{R} + \vec{r}) |\psi_j^0(\vec{r}; \vec{R})|^2 \\ &= \frac{e^2}{2\epsilon_0 c m_e \omega^2} \int d^3r I(\vec{R} + \vec{r}) |\psi_j^0(\vec{r}; \vec{R})|^2. \end{aligned}$$

Adding a finite intensity at trap center gives ground – Rydberg matching

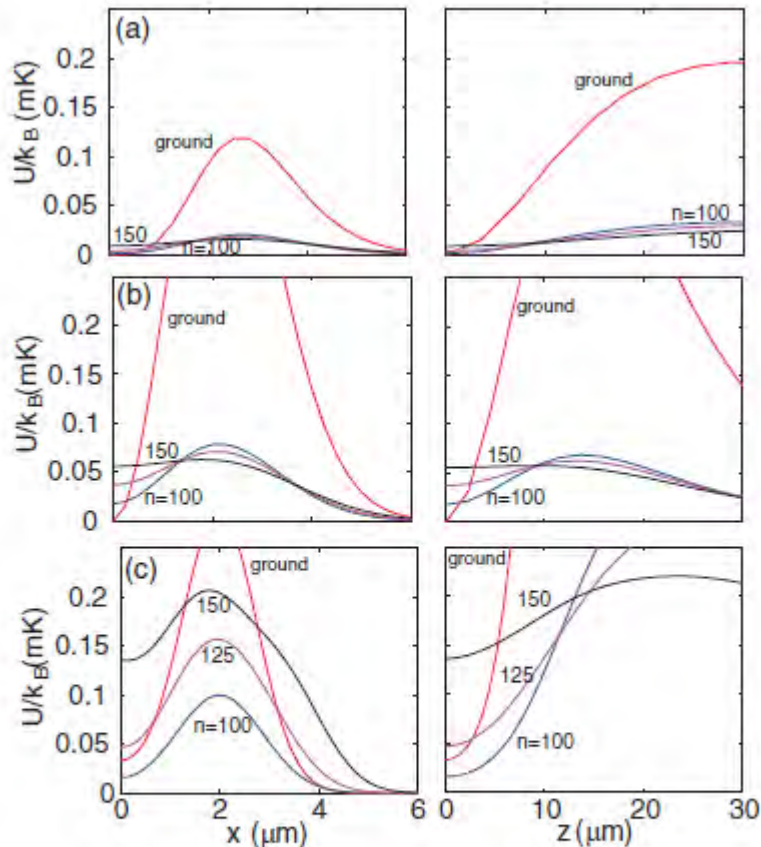


FIG. 4. (Color online) Potential energy of Cs ground-state and ns Rydberg states with $n = 100, 125, 150$ in (a) Gaussian interference BBT, (b) vortex BBT, and (c) Gaussian lattice BBT. Trap parameters the same as in Fig. 3.

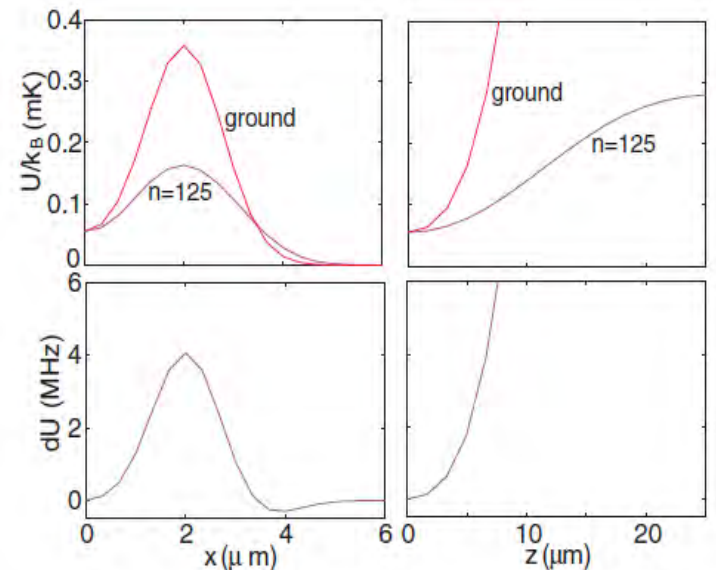


FIG. 6. (Color online) Trapping potential (top row) and shift difference (bottom row) between Cs $6s$ and $125s$ for a self-magic Gaussian lattice trap with $\lambda = 780$ nm, $d = 4$ μm , $w = 1.57$ μm , and $P = 50$ mW.

III: Coherence properties of ground and Rydberg traps

- Optical traps and ground state (qubit) coherence
- Ramsey spectroscopy
- magic traps
- traps for Rydberg atoms
- 3D Rydberg atom trapping

Observation of ponderomotive Rydberg potential

PRL 104, 173001 (2010)

PHYSICAL REVIEW LETTERS

week ending
30 APRIL 2010

State-Dependent Energy Shifts of Rydberg Atoms in a Ponderomotive Optical Lattice

K. C. Younge,* B. Knuffman,† S. E. Anderson, and G. Raithel

PRL 107, 263001 (2011)

PHYSICAL REVIEW LETTERS

week ending
23 DECEMBER 2011

Trapping Rydberg Atoms in an Optical Lattice

S. E. Anderson,* K. C. Younge, and G. Raithel

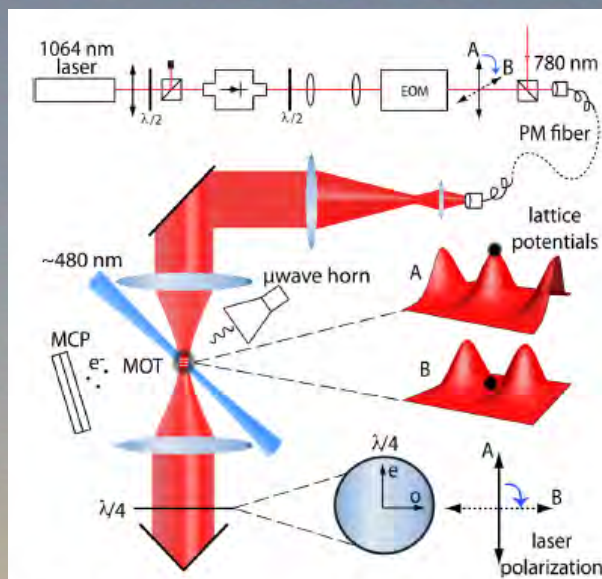


FIG. 1 (color online). Sketch of the experimental setup. Rydberg atoms are optically excited at potential maxima of a one-dimensional Rydberg-atom optical lattice. An electro-optic modulator (EOM) is used to switch the lattice polarization by 90° from A to B immediately after excitation, resulting in lattice inversion and efficient Rydberg-atom trapping.

Red detuned trap is inverted during excitation.

Lattice induced shift of μ wave spectra used to measure trapping.

This is a 2D trap.

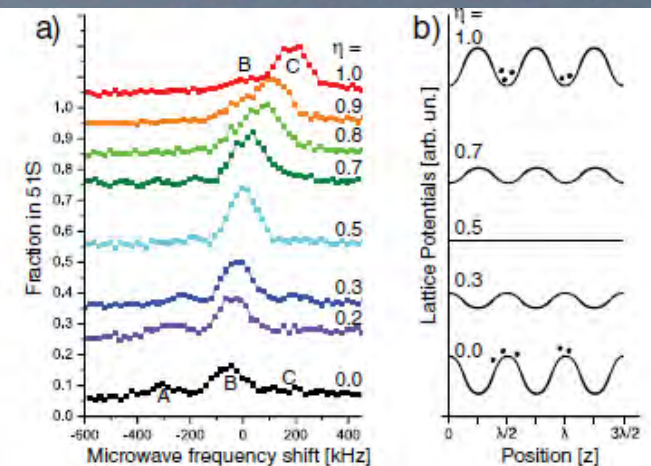
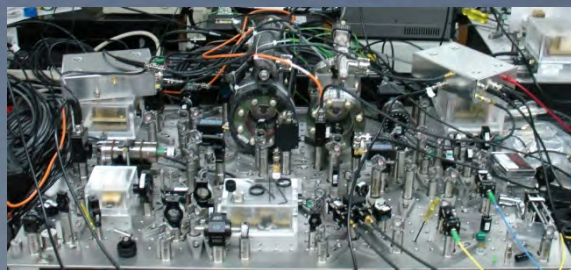


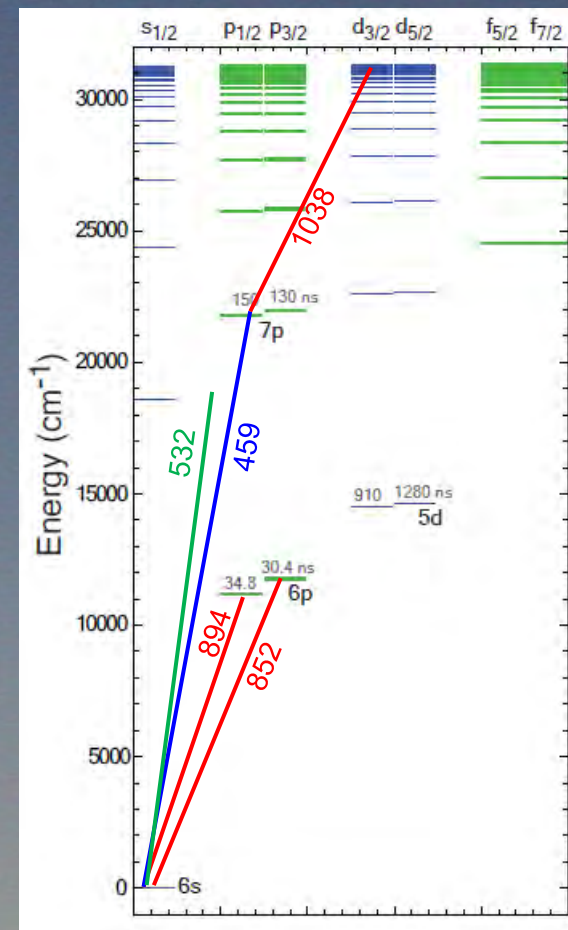
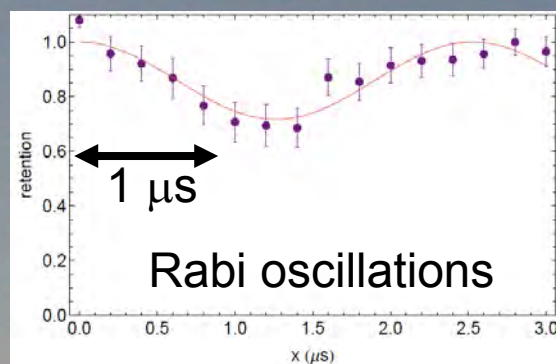
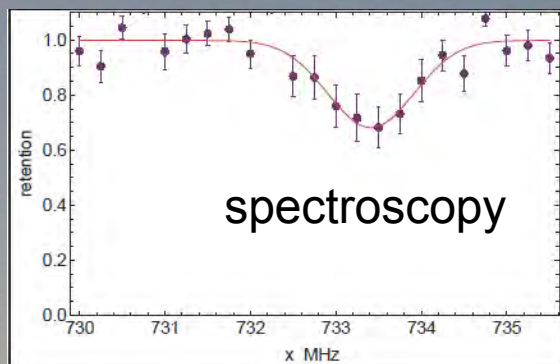
FIG. 2 (color online). (a) Experimental microwave spectra for $P = 0.8$ W and optical pulse length $\tau_{\text{ex}} = 0.5 \mu\text{s}$ for the indicated values of $\eta = P_{\text{trans}}/P$ (spectra offset for clarity). (b) Lattice potentials after inversion vs position for several of the η values used in panel (a). The fully inverted case, $\eta = 1$, leads to the strongest blueshifted signal component, indicative of most efficient Rydberg-atom trapping.

Rydberg excitation in a BBT

Two photon excitation via $7p_{1/2}$ using 459 and 1038 nm lasers. Highly stabilized and referenced to frequency comb.

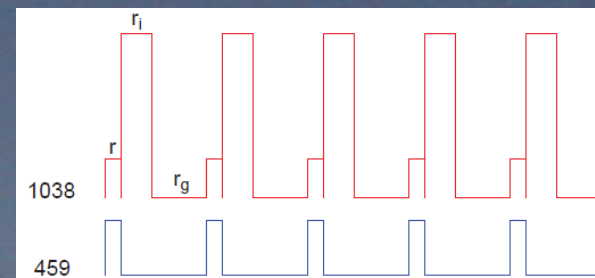
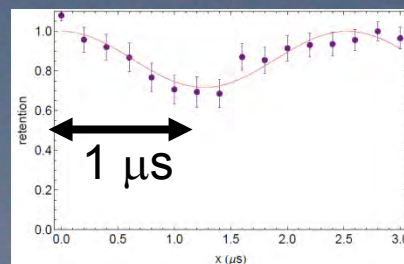
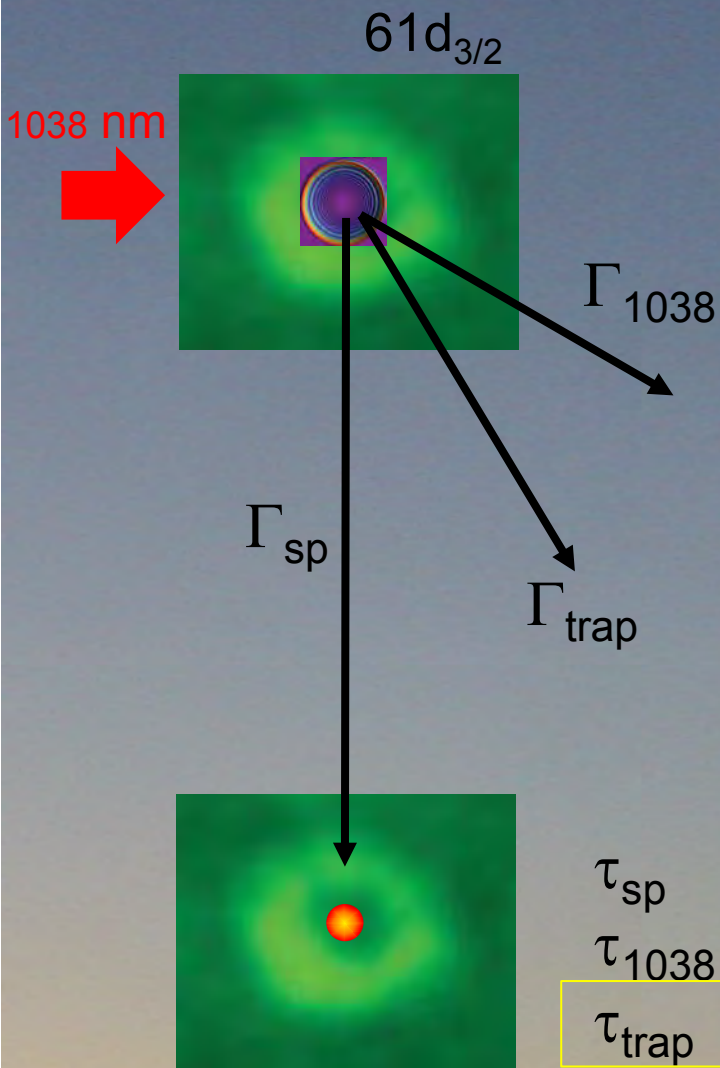


Data taken on $61d_{3/2}$ level.

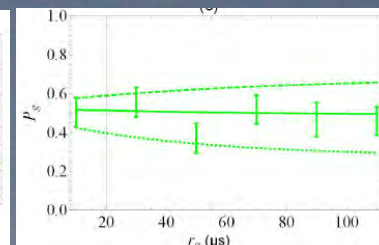
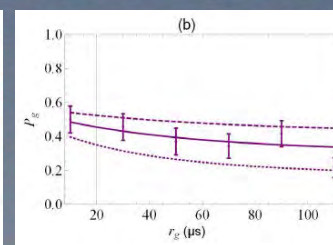
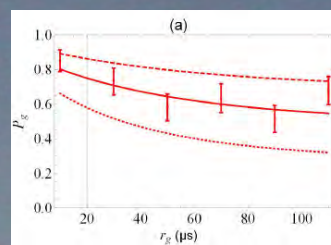


Rydberg data was taken while keeping the trap light on.

Rydberg trapping



P(ground)



Pulse time

Rate eq. model, global fit to three different pulse sequences gives

$$\tau_{sp} = 79 \mu\text{s} \text{ (calculated)}$$

$$\tau_{1038} = 16 \mu\text{s}$$

$$\tau_{trap} = 390 \mu\text{s}$$

Detection efficiency

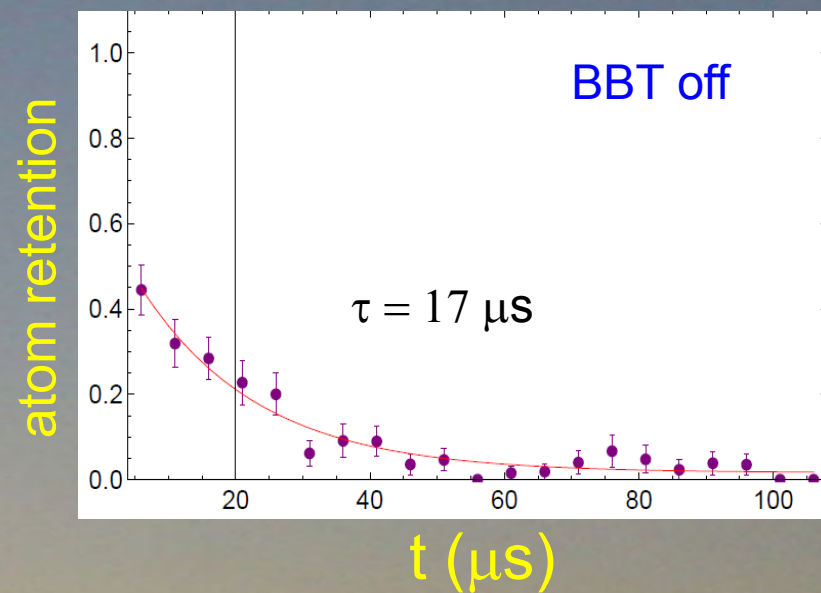
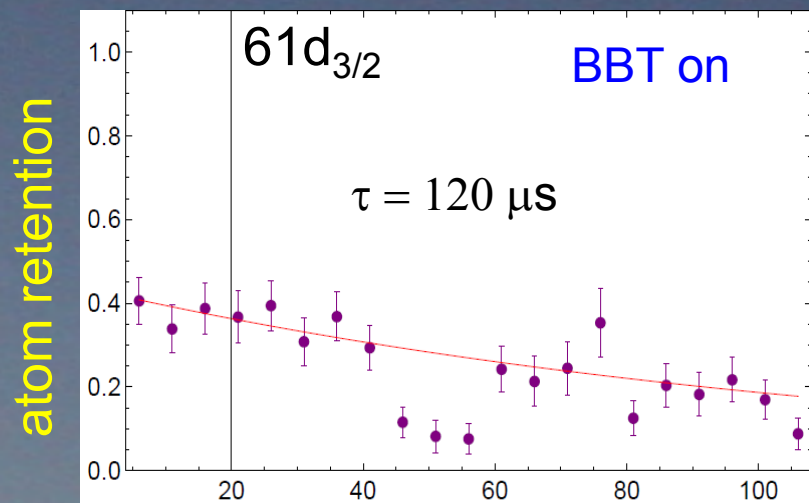
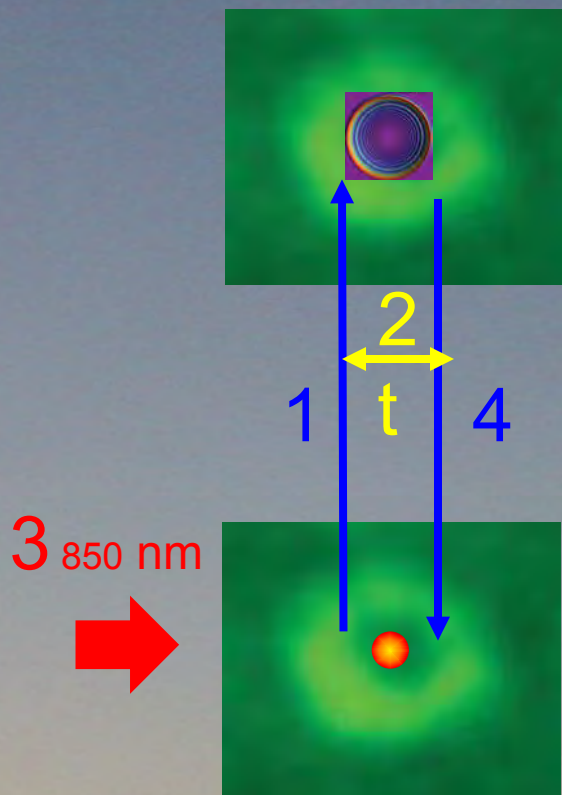
$$16/79=20\%$$

$$P(r) = 0.8$$

strong evidence
for Rydberg trapping

Rydberg trap lifetime

The trap lifetime is directly measured by blowing away non-Rydberg excited atoms.



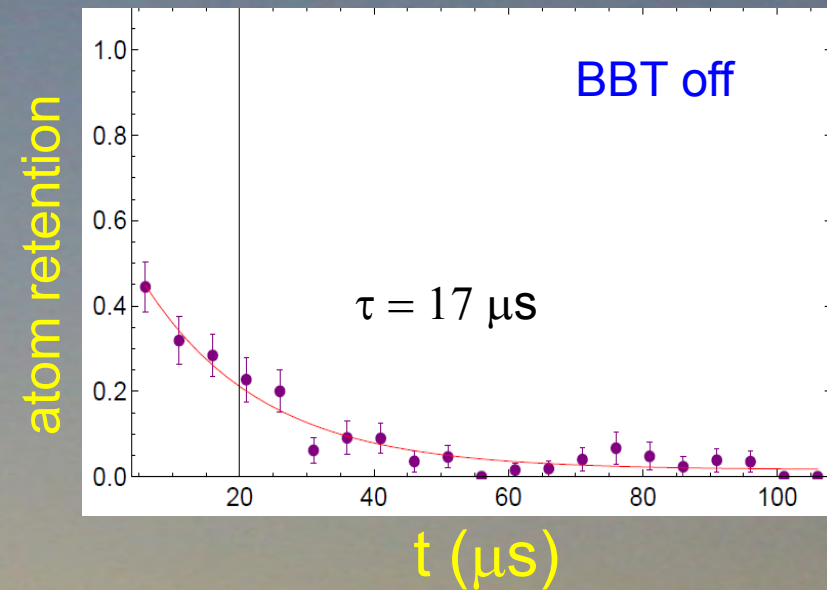
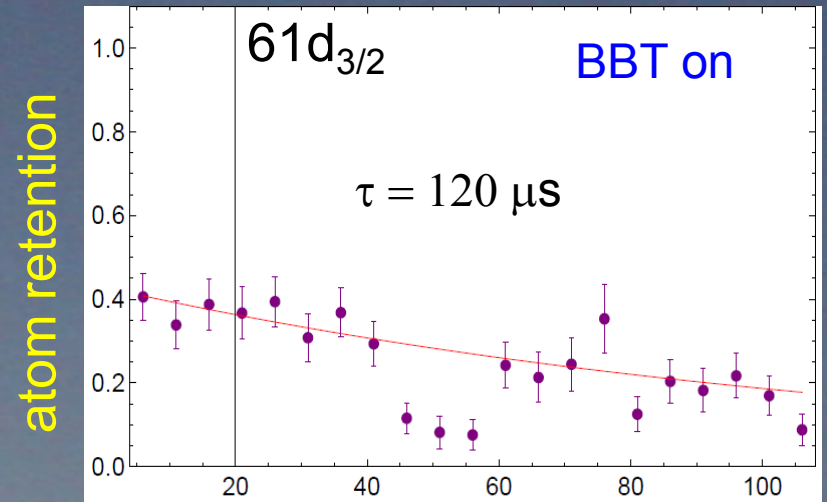
Rydberg trap lifetime

A Monte Carlo simulation including black body redistribution to other Rydberg levels (which are also trapped) gives a predicted lifetime before return to ground state of $143 \mu\text{s}$.

This implies a trap lifetime

$$\tau_{\text{BBT}} > 750 \mu\text{s}.$$

This data is preliminary.



Rydberg trap shift

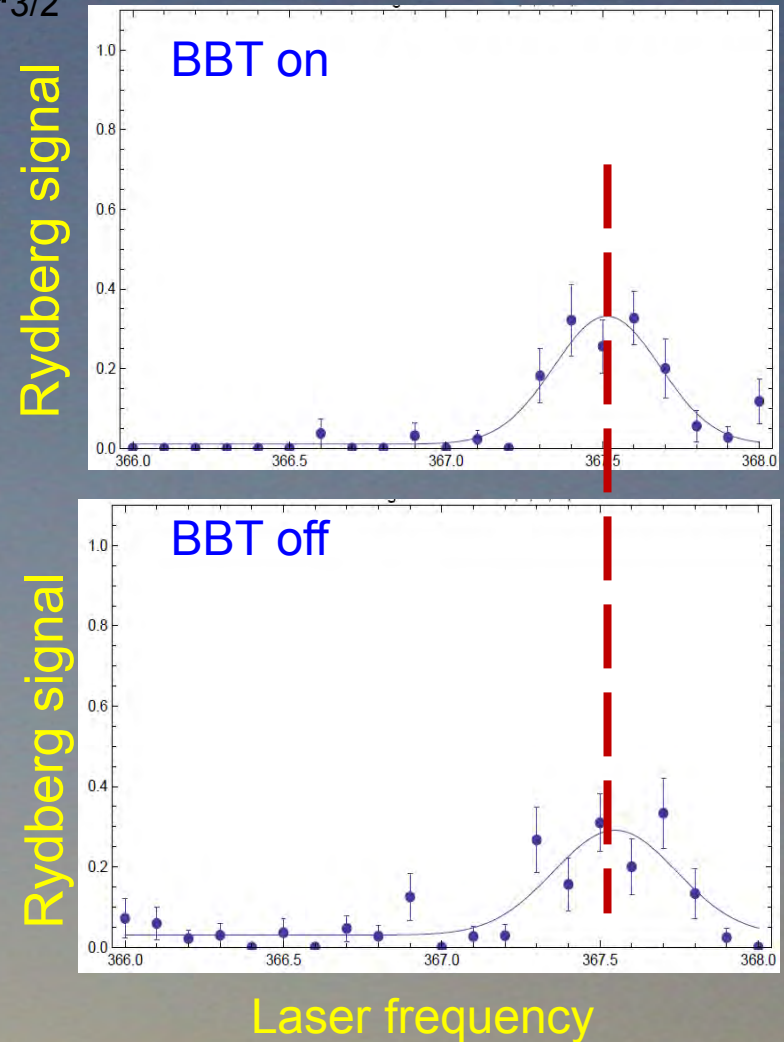
Line center is about 130 kHz higher with trap on.

About $6.5 \mu\text{K}$ in temperature units.

We did not expect perfect magic trapping with this trap.

It should be possible to tune the trap shift close to zero in the future.

$61d_{3/2}$



Summary

- Optical traps can hold neutral atoms with excellent coherence properties
- Rydberg atoms can be confined in bottle-beam type traps
- It is possible to design ground-Rydberg magic traps
- Experiments are showing clear evidence of Rydberg trapping

Rydberg atoms: excitation, interactions, trapping

I: Coherent excitation of Rydberg states

II: Rydberg atom interactions

III: Coherence properties of ground and
Rydberg atom traps